PLEASE TYPE

UNIVERSITY OF NEW SOUTH WALES

Thesis/Project Report Sheet

Surname or Family name: ZOPPOU

First name: CHRISTOPHER Other name/s:

Abbreviation for degree as given in the University calendar: ME

School: CIVIL ENGINEERING Faculty: UNIVERSITY COLLEGE

Title: ESTIMATING THE THICKNESS OF THE FRESHWATER LENS ON BONRIKI USING RELIABILITY ANALYSIS

Abstract 350 words maximum: (PLEASE TYPE)

ABSTRACT: Mathematical models are a valuable tool for predicting the behavior of aquatic systems. However, many of the parameters required by these models are not known with certainty. Reliability analysis provides a means of including uncertainties in the modelling process. Prediction limits of the model response can be established when the uncertainties involved in the analysis are taken into account. These prediction limits can have a significant influence on the decision making process.

A number of new reliability techniques for estimating the uncertainty of a hydraulic system are demonstrated. These include the point estimate method and an exact random field generator, which is used to produce realizations required in Monte Carlo simulation. Hypothetical examples and a case study are used to assess the performance of these techniques with other well known reliability methods. First-order analysis and the point estimate method were found to be suitable for simple problems. Monte Carlo simulation combined with the embedding circulant matrix approach, for generating spatially correlated random fields, is robust, efficient and provides results that are physically plausible for complicated multi-dimensional problems.

The behavior of the freshwater lens on Bonriki was chosen as the case study. A simple groundwater model was used to model the behavior of the freshwater lens. In the groundwater model, the permeability of the aquifer was considered as a spatially correlated model parameter with uncertainty. Measured data was used to establish the statistical properties of the permeability of the aquifer on Bonriki. The model was used to assess the impact of increasing the rate of freshwater extraction from the lens and reducing the amount of vegetation on Bonriki on the sustainability of the freshwater lens. Various reliability techniques were considered for estimating the prediction limit of the thickness of the freshwater lens for various management strategies. Only Monte Carlo simulation was suitable. The results for the case study show that managers who base their decisions on deterministic model results alone, may compromise the freshwater lens and jeopardize the survival of the inhabitants on the atoll. The stochastic-deterministic modelling approach also suggests that the removal of the vegetation may not provide the additional freshwater yield anticipated. There is a high probability that the freshwater lens could be compromised because of the uncertainty in the model parameters.

Declaration relating to disposition of project report/thesis

I am fully aware of the policy of the University relating to the retention and use of higher degree project reports and theses, namely that the University retains the copies submitted for examination and is free to allow them to be consulted or borrowed. Subject to the provisions of the Copyright Act 1968, the University may issue a project report or thesis in whole or in part, in photostate or microfilm or other copying medium.

I also authorise the publication by University Microfilms of a 350 word abstract in Dissertation Abstracts International (applicable to doctorates only).

9/6/95

Date

The University recognises that there may be exceptional circumstances requiring restrictions on copying or conditions on use. Requests for restriction for a period of up to 2 years must be made in writing to the Registrar. Requests for a longer period of restriction may be considered in exceptional circumstances if accompanied by a letter of support from the Supervisor or Head of School. Such requests must be submitted with the thesis/project report.

FOR OFFICE USE ONLY Date of completion of requirements for Award:

Registrar and Deputy Principal

THIS SHEET IS TO BE GLUED TO THE INSIDE FRONT COVER OF THE THESIS

ERRATA

Page 3.1, 2nd paragraph replace "100's" with "100s".
Page 3.1, 2nd and 3rd paragraphs replace "SULTRA" with "SUTRA".
Page 3.3, 4th line replace "net outflow" with "net inflow".
Page 3.5, 2nd paragraph replace "1000" with "10000".
Page 3.10, 3rd paragraph replace "Pliesocene" with "Pleistocene".
Page 3.17, in the title for Table 3.3 replace "Holocene" with "Holocene sediments".
Page 3.15, 3rd paragraph delete the sentence "Ghassemi (1994) suggests that for the large time steps used, the model results may be considered as steady over the interval Δt.".

Page 4.9, delete the first two lines.
Page 4.11, top of page insert "found that generating more than 2,00 samples produced very little improvement in the mean, variance and skewness of the sampled distribution. They concluded that sample sizes of 2,000 were appropriate in their problem containing six parameters".

Page 5.4, replace y-axis title in Figure 5.1 with "Correlation function".
Page 5.5, 2nd sentence replace "It is only necessary are" with "It is only necessary to".
Page 5.20, delete the first three lines.
Page 5.20, last line replace "required more" with "required eight times more computational effort than the matrix decomposition method and more than twice the computational effort than the circulant matrix approach. This is the most expensive means of generating the realizations. In addition, it is an approximate method and is restricted to certain covariance functions. Therefore, for this and similar problems, the matrix decomposition method is".

Page 6.1, last line 3rd paragraph replace "its'" with "its".
Page 6.1, 4th paragraph replace "the permeabilities K" with "the permeability K".
Page 6.2, in the title for Figure 6.2 replace "measures" with "measured".
Page 6.10, 2nd paragraph replace "that each storm" with "that the storm".
Page 6.12, 2nd line delete "along the channel".

Page 7.5, 4th paragraph replace "There figures show" with "These figures show".

Page 9.4, delete 4th reference.
Page 9.4, 6th reference replace "Propsed Well" with "Proposed Well".

Estimating the Thickness of the Freshwater Lens on Bonriki Using Reliability Analysis

by

Christopher Zoppou

Submitted for the degree of Master of Engineering

DEPARTMENT OF CIVIL AND MARITIME ENGINEERING

UNIVERSITY COLLEGE, AUSTRALIAN DEFENCE FORCE ACADEMY

UNIVERSITY OF NEW SOUTH WALES

June 1995

STATEMENT

The contents of this thesis are entirely my own work except where otherwise indicated.

ABSTRACT: Mathematical models are a valuable tool for predicting the behavior of aquatic systems. However, many of the parameters required by these models are not known with certainty. Reliability analysis provides a means of including uncertainties in the modelling process. Prediction limits of the model response can be established when the uncertainties involved in the analysis are taken into account. These prediction limits can have a significant influence on the decision making process.

A number of new reliability techniques for estimating the uncertainty of a hydraulic system are demonstrated. These include the point estimate method and an exact random field generator, which is used to produce realizations required in Monte Carlo simulation. Hypothetical examples and a case study are used to assess the performance of these techniques with other well known reliability methods. First-order analysis and the point estimate method were found to be suitable for simple problems. Monte Carlo simulation combined with the embedding circulant matrix approach, for generating spatially correlated random fields, is robust, efficient and provides results that are physically plausible for complicated multi-dimensional problems.

The behavior of the freshwater lens on Bonriki was chosen as the case study. A simple groundwater model was used to model the behavior of the freshwater lens. In the groundwater model, the permeability of the aquifer was considered as a spatially correlated model parameter with uncertainty. Measured data was used to establish the statistical properties of the permeability of the aquifer on Bonriki. The model was used to assess the impact of increasing the rate of freshwater extraction from the lens and reducing the amount of vegetation on Bonriki on the sustainability of the freshwater lens. Various reliability techniques were considered for estimating the prediction limit of the thickness of the freshwater lens for various management strategies. Only Monte Carlo simulation was suitable. The results for the case study show that managers who base their decisions on deterministic model results alone, may compromise the freshwater lens and jeopardize the survival of the inhabitants on the atoll. The stochastic-deterministic modelling approach also suggests that the removal of the vegetation may not provide the additional freshwater yield anticipated. There is a high probability that the freshwater lens could be compromised because of the uncertainty in the model parameters.

Acknowledgements

I wish to acknowledge the assistance of the following people who have been involved in this study.

Dr. K.S. Li who supervised this project for the first six months and Dr. I. Young who assumed responsibility of supervision after Dr. Li's departure overseas. Although the topic of the study is not within Dr. Young's field of expertise, he has provided moral support and advice during the project. I am indebted to Dr. A.T.A Wood from the Centre of Mathematics and its Applications, Australian National University, who late in the project filled the void left by Dr. Li. His knowledge of the generation of random fields and kernel filtering has enabled me to complete this study. I appreciate his patience in demystifying the mathematics of the subject.

All the people involved in the supervision of this project have limited expertise in water resource problems considered in this study. I have assumed the responsibility of providing the appropriate expertise in this area. The supervisors that have been involved in the study have been chosen for their expertise in reliability analysis and probability theory.

I am also grateful to Mr. A.C. Falkland for providing the data for the case study and for his assistance in the interpretation of this data.

I acknowledge the assistance provided by A.C.T. Electricity and Water and the Department of Urban Services, A.C.T. Government for seeing the benefit of and funding the project.

Finally, I appreciate the moral support provided by my wife Alix.

Table of contents

List of symbols

A	cross-sectional area
$\boldsymbol{C}$	circulant matrix
$\boldsymbol{D}$	covariance matrix
E	evaporation and evapotranspiration per unit area
$F_X(x)$	cumulative distribution function of a random variable X
$G(\omega)$	radial spectral distribution function
$G'(\omega)$	radial spectral density function
I	interception
K	permeability
L	length of the computational domain
M	number of lines used in the turning band technique
N'	number of harmonics
O	abstraction rate per unit area
P	precipitation per unit area
Q	outflow
S	storage
S_f	friction slope $S_f = \eta^2 Q\|Q\| W^{4/3}/A^{10/3}$
R	recharge rate per unit area
$\boldsymbol{R}^d$	domain in d-dimensional Eucliden space
T	transmissivity, $T = (1 + \alpha)Kh$
V	separation distance
V_0	correlation distance or scale
W	wetted perimeter
$\boldsymbol{X}$	vector of random variables, $\boldsymbol{X} = (x_1,x_2,\ldots,x_k)$
Y	model response, $Y = f(\boldsymbol{X})$
$\boldsymbol{Z}$	uncorrelated random vector of *iid* $N(0,1)$ variables, $\boldsymbol{Z} = (z_1,z_2,\ldots,z_k)$.
a	constant
b	covariance reduction factor
d	dimension of the problem
$f(\boldsymbol{X})$	model response
$f(\boldsymbol{\mu})$	$f(\mu_1,\mu_2,..,\mu_k)$
$f_j\pm$	$f(\mu_1,..,\mu_{i-1},\mu_i\pm\sigma_i,\mu_{i+1},..,\mu_k)$
f_{ij}^{++}	$f(\mu_1,..,\mu_{i-1},x_i\pm\sigma_i,..,\mu_{j-1},x_j\pm\sigma_j,..,\mu_k)$
g	acceleration due to gravity
h	height of the water table above mean sea level
h_f	height of the freshwater table above mean sea level
h_s	depth of the seawater-freshwater interface below mean sea level
k	number of random variables
m	dimension of a circulant matrix
n	number of observations in a sample
q	flow rate through the elemental volume
t	time
$\mathbf{t}$	vector of co-ordinate directions
w	sampling interval
x_i	random variable
x_i^+	$x_i^+ = \mu_i + \sigma$

x_i^- $x_i^- = \mu_i - \sigma$
x_j distance to node j in the x-direction
x co-ordinate direction
y co-ordinate direction
y_i distance to node i in the y-direction

ΔR change in recharge per unit area of an incremental volume
ΔS change in storage in an incremental volume
ΔV change in volume of the lens
Δx width of an elemental volume in the x-direction or distance between two computational points in the x-direction
Δy width of an elemental volume in the y-direction or distance between two computational points in the y-direction
Δq change in flow rate through the elemental volume
Δs change in soil storage
Δt computational time increment

Λ diagonal matrix of eigenvalues of a circulant matrix $\boldsymbol{C}$
Ω frequency
α Ghyben-Herzberg ratio, $\alpha \simeq 40$
β effective porosity
$\kappa(\mathbf{x})$ kernel function
$\gamma(\mathbf{x})$ covariance function, $\gamma(\mathbf{x}) = \sigma^2\rho(\mathbf{x})$
σ standard deviation
$\rho(\mathbf{x})$ or ρ_{ij} correlation coefficient
μ mean
ς kurtosis
ϑ skewness
ω frequency or wave number
ρ_s seawater density
ρ_f freshwater density
λ_i eigenvalue
$\boldsymbol{\mu}$ vector of mean values, $\boldsymbol{\mu} = (\mu_1,\mu_2,\ldots,\mu_k)$
η Manning's resistance coefficient
ρ $\rho = \sum_i \rho_i$
ρ_i $\rho_i = \sum_j \rho_{ij}$
ρ_{ii} $\rho_{ii} = 1.$

Operators or functions

E[.] expected value
Cos Cosine
Sin Sine
sinh Hyperbolic Sine
tan Tangent
exp exponentiation
ln natural logarithm

$U(a,b)$	uniform distributed in the interval $[a,b]$
$N(\mu,\sigma)$	standard normally distribution with mean, μ and standard deviation, σ

Matrix notation

{ }	vector
[ ]	rectangular matrix

Abbreviations

μS	micro Siemens
iid	independently identically distributed

List of figures

List of tables

Chapter 1.

Introduction

Water resources are threatened by the encroachment and the increasing demand placed on this resource by human beings. For example, an expanding metropolis may encroach flood prone areas thereby increasing the risk of damage and loss of life. Mathematical models can be used to predict the behaviour and consequences of these natural events and to predict the consequences of new or increased demands on water resources. A reasonable compromise between the acceptable risk of failure and utilization of the water resources may be achieved with accurate predictions.

1.1 Modelling techniques in water resources

The tendency in water resources problems has been to use increasingly more complex models based on the presumption that they will provide greater accuracy. The accuracy of the model response is not directly proportional to the model complexity. Model accuracy is also influenced by uncertainties in the modelling process.

Uncertainty in the modelling process may arise from; (*i*) *natural* or *inherent* uncertainty which is due to the random variability of the hydrological processes, (*ii*) the use of a simplified equation to describe a complex physical process which is known as *model* uncertainty and (*iii*) *parameter* uncertainty which is due to parameters in hydraulic and hydrologic models that cannot be quantified exactly.

Uncertainties arising from (*i*) can be included in the model formulation. However, uncertainties arising from (*ii*) and (*iii*) are generally ignored in the modelling process. Decision makers involved with water resources problems are usually provided with a single model response, obtained using a sample set of model parameters. As such, the model response only represents a single sample from a number of possible outcomes. Reliability analysis provides a means of quantifying the range of possible outcomes for the predicted model response by including uncertainties in the modelling process. Prediction limits of the model response can be established if the range of possible outcomes is known.

The credibility of models can be greatly enhanced if the prediction limits of the model response can be quantified. This can be important in; (*i*) model selection, (*ii*) decision-making and (*iii*) the collection of data.

As hydrological models become larger and more complex, the number of parameters increase, as well as the amount of data needed to estimate these parameters. The availability and quantity of suitable data generally decreases with increasing model complexity. Consequently there is greater uncertainty in complex models compared to their simpler counterparts. Therefore, it is necessary to balance model complexity against parameter uncertainty.

The range of model responses which are acceptable for the problem under study can affect the choice of a model. Large model prediction limits may be consistent with parameter uncertainty propagating

through the model. If the influence of these uncertainties on the predicted model response is ignored, a suitable model may be prematurely rejected. Once a model has been chosen, the appropriate data required by the model can be collected.

Prediction limits of the model response can be established when the uncertainties involved in the analysis are taken into account. These prediction limits can be used to quantify the risks associated with various management strategies. Generally, only parameter uncertainty is considered in a problem.

1.1.1 Uncertainty models

Uncertainty in water resources problems has traditionally been analyzed using *single-random-variable* models.

The random variation of the Manning coefficient η in space is represented by a single random variable in the single-random-variable model as illustrated in Figure 1.1 for an open channel flow problem. This approach implies that all realizations of the parameter η are the same everywhere, although the exact magnitude of the realization remains random. If the realizations of η at section 1 is η_1, the values of η at all other sections will also be equal to η_1.

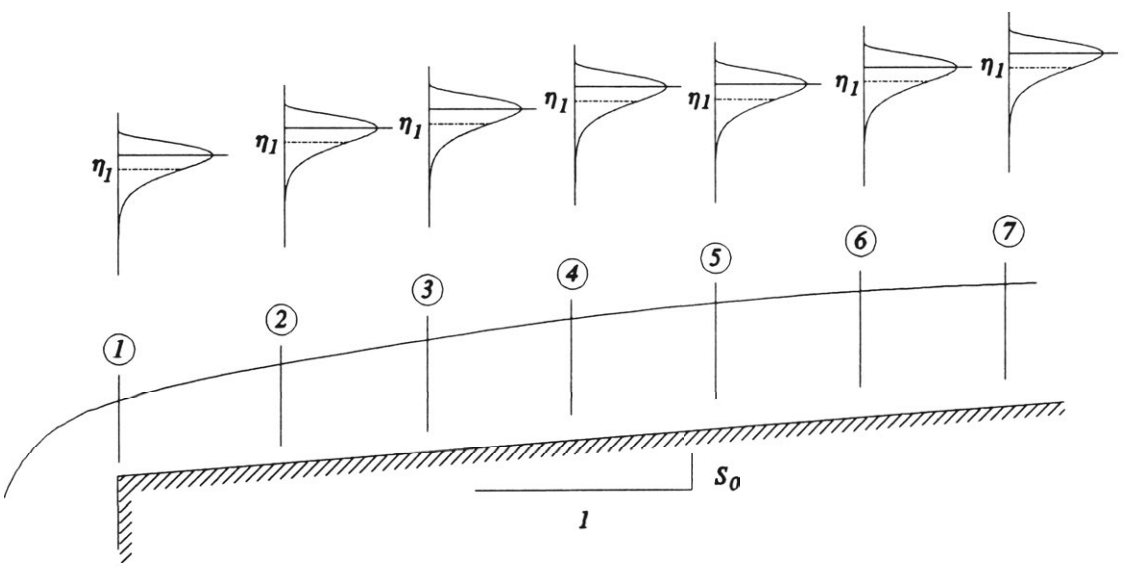

Figure 1.1 Variation of Manning's coefficient in the single-random-variable model

This is erroneous, since if the model is correct, the value of η for the entire channel can be determined with absolute certainty by measuring the value of the parameter η, using a single sample taken anywhere in space. This is contrary to the expectation that η would vary from one location to another.

The use of the single-random-variable model generally results in a gross overestimation of the prediction limit of the model response, since it ignores the variance reduction due to spatial averaging (see, for example Zoppou and Li [1993]).

A more realistic approach is to apply a *random field* model to the problem, as shown in Figure 1.2. In this model, the value of parameter η at different locations is treated as an independent or as a spatially correlated random variable.

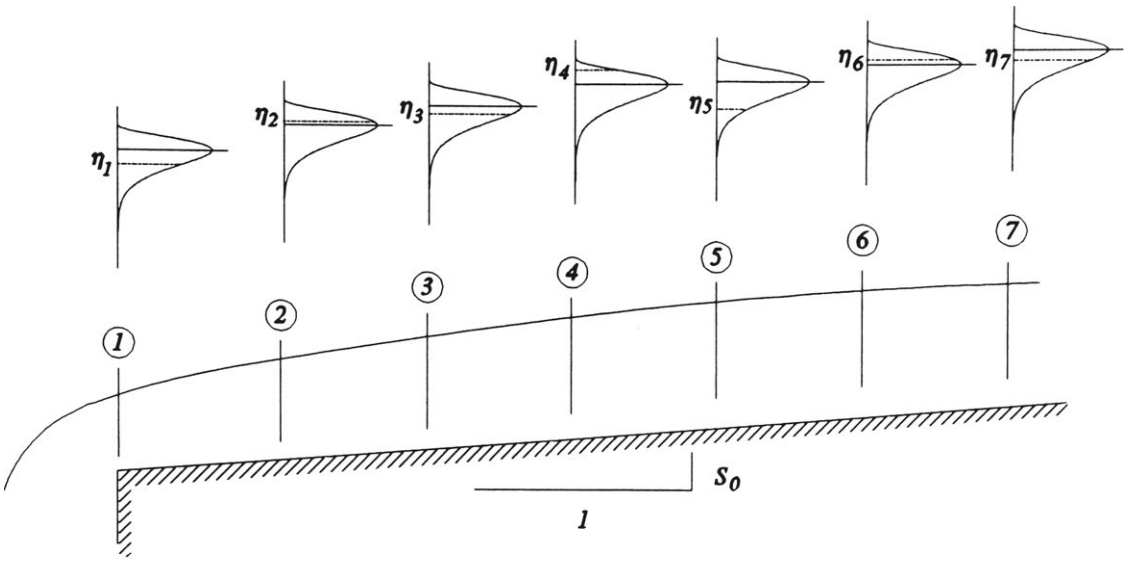

Figure 1.2 Variation of Manning's coefficient in the random field model

1.1.2 Methods of reliability analysis

Techniques for estimating the influence of parameter uncertainty on a model's response include; (*i*) *first-order analysis*, (*ii*) *point estimate method*, (*iii*) *Monte Carlo simulation*, (*iv*) using the *Mellin transform* and (*v*) using *stochastic* equations.

The model input variables are positively correlated in many water resources problems. Zoppou and Li (1993) have shown that ignoring the spatial correlation between the random variables has a significant influence on the predicted model response. Only the first-order analysis and the point estimate method can readily accommodate correlated random variables.

The Mellin transform is only applicable to problems where the random variables are independent. The use of stochastic equations require the use of complicated and numerically intensive techniques for their solution. For these reasons they are considered to have little practical value (Li and McLaughlin [1991]).

The application of Monte Carlo simulation is relatively straightforward if the random variables are independent. Values for the random variables are sampled at random from independent probability distributions. Monte Carlo simulation is not an appropriate method for determining the effect of uncertainties on a model's response unless realizations of correlated random variables can be generated efficiently.

There are a number of algorithms for generating spatially correlated random variables in one-, two- and three-dimensions. A number of these algorithms are described in this thesis and are used to predict the prediction limits of the response of one- and two-dimensional hydraulic models.

The Monte Carlo simulated model response is compared with the predicted model response determined using the first-order analysis and a new point estimate method. Data collected on Bonriki, an island on Tarawa atoll in the Pacific Ocean, was used as the case study for the comparison.

1.2 Bonriki island

Water resources do not exist for many coral atolls found in the Pacific and Indian Oceans. The main source of potable water comes from rainfall collection systems and groundwater. The major advantage of groundwater is the large storage volumes that are achieved in comparison to any manmade reservoir that could be contemplated on many atolls. Therefore, on small islands the groundwater is an important resource.

Groundwater on the islands of an atoll normally occurs in the form of a thin lenticular shaped freshwater body called a *lens* which rests upon saline water beneath the island. The formation which contains groundwater and through which it flows is known as the *aquifer.*

The quality of the freshwater in the aquifer can be impaired either by intrusion of seawater into the aquifer or by the contamination of the lens from sewerage, stormwater runoff, fertilizers, pesticides and industrial effluent. The greatest threats to the freshwater lens on many small islands are over-abstraction of groundwater which can decrease the size of the freshwater lens on heavily populated islands and pollution. The groundwater must be managed effectively to avoid depleting the resource.

Some freshwater lenses have been modelled mathematically in order to effectively manage the groundwater resource. Mathematical modelling of the lens enables the quantitative assessment of the effect of various influences on the freshwater lens. The behaviour of the lens on Bonriki was modelled mathematically using an unsteady groundwater flow model based on the Ghyben-Herzberg relationship. This model was used to estimate the thickness of a freshwater lens on Bonriki.

The parameters in the model are not known with certainty. The prediction limits of the thickness of the freshwater lens was estimated by considering the permeability of the aquifer as a model parameter with uncertainty. Therefore the permeability, which is a measure of the aquifer medium to allow the movement of fluid under a pressure gradient, is treated as a spatially correlated random field. First-order analysis, Monte Carlo simulation and the point estimate method were used to estimate the prediction limits of the thickness of the freshwater lens for various extraction rates and vegetation cover.

The prediction limits of the model response can be used to estimate the sustainable yield of the freshwater lens. The sustainable yield is a subjective quantity and is defined as the rate at which freshwater may be extracted from the lens without compromising its renewability.

1.3 Objectives of the study

The major objective of this study is to demonstrate a number of new reliability techniques for estimating the uncertainty of a hydraulic system. This includes the point estimate method which is used to calculate the statistical moments of the model response and an efficient random field generator which is used to produce correlated realizations required in Monte Carlo simulation. The results of these models are compared to the classical first-order analysis of the model response.

There have been a number of original contributions to the vast knowledge on reliability analysis of water resources problems. These include:

(*i*) The first practical illustration using a case study of an exact method for generating correlated random fields.

(*ii*) Demonstrating the application of the new point estimate method for estimating the moments of the response of a hydraulic and hydrological model.

(*iii*) This study is one of the very few applications of reliability theory for estimating the prediction limits of a freshwater lens on an island in a coral atoll.

These aspects alone are a significant contribution to the advancement of reliability theory in water resources problems.

1.3.1 Outline of the thesis

The sources of uncertainty, their influence on a model's response and their importance in the modelling process are discussed in Chapter 1. The fundamental difference between the single-random-variable and the random field models is also described. Several techniques for quantifying the effect of uncertainties on a model response are briefly described in this chapter. The case study used to demonstrate and compare these techniques is introduced in this chapter.

The data collected on Bonriki is described in Chapter 2. The unsteady groundwater flow model describing the behaviour of the freshwater lens on Bonriki is described in Chapter 3. The sharp interface single aquifer model and the solution method used in the model is described in detail in this chapter. In addition, the data collected on Bonriki which is required by the model and the model calibration results are also described.

The first-order analysis, Monte Carlo simulation and point estimate methods are discussed in Chapter 4. Methods for estimating the covariance structure of the data are also described in this chapter.

Methods for generating spatially correlated random fields, including an exact random field generator is described in Chapter 5. A comparison based on efficiency, ease of use and applicability of the generators is discussed in this chapter. Hypothetical one- and two-dimensional problems have been used to facilitate this comparison. The exact random field generator and the point estimate method are described in detail because they are relatively new techniques with very few applications in water resources. Other techniques are well known and have been used in many water resources problems, therefore these techniques are only briefly described.

The statistical properties, mean, variance and covariance structure of the measured permeability on Bonriki are established in Chapter 6.

Prediction limits of the freshwater lens on Bonriki are estimated in Chapter 7 using the first-order analysis, the point estimate method and Monte Carlo simulation for a number of extraction rates and vegetation cover. The exact random field generator, described in Chapter 5 is used to produce realizations of the permeability of the aquifer used in Monte Carlo simulation. The efficiency, accuracy and applicability of the reliability techniques is also discussed in this chapter.

The performance of the reliability techniques in the one-dimensional problem and in the case study is discussed in Chapter 8. The practical aspects of applying the three reliability analysis techniques is also reviewed using the case study. The usefulness of reliability analysis as a management tool is also discussed. Further research directions are also recommended.

Chapter 2.

The freshwater lens on Bonriki

There are four main groups of islands forming the Republic of Kiribati in the Pacific Ocean, see Figure 2.1. The total land area is only 710 square kilometres while the islands cover over 5 million square kilometres. In 1980 there were 58,000 inhabitants in the Republic.

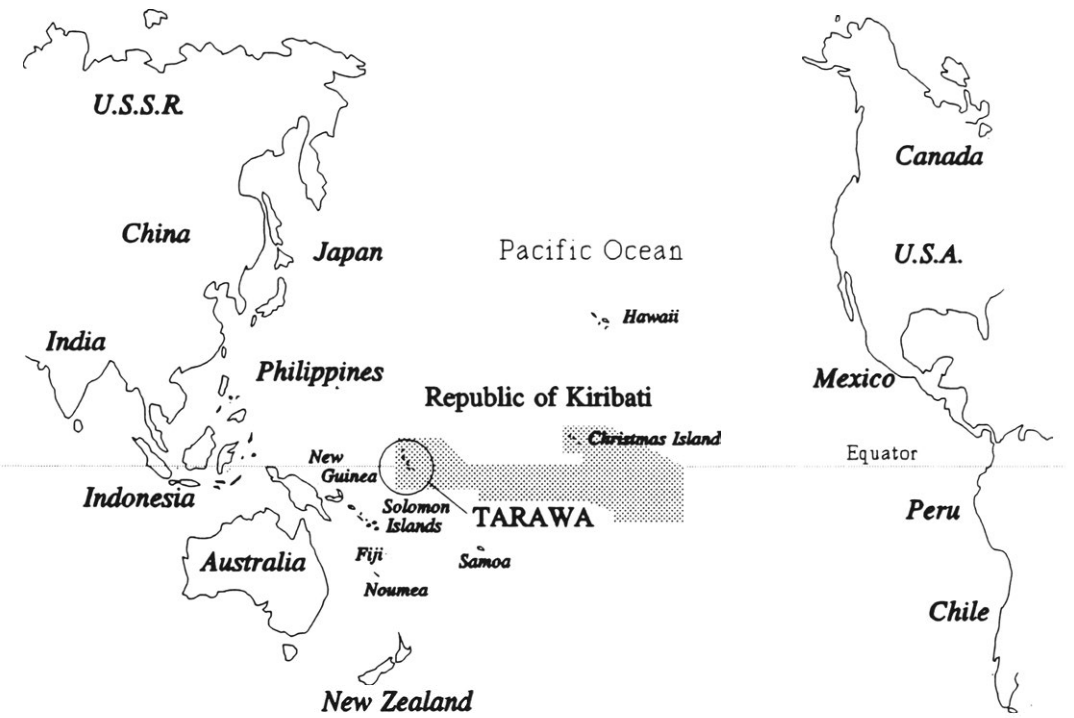

Figure 2.1 Location of the Republic of Kiribati

Tarawa atoll located at 1°30'N, 173°00'E is one of 33 island groups within the Republic of Kiribati. It has the largest population of any of the island groups with a population of 20,150. Tarawa is a typical atoll comprised of a ring of islands and fringing reefs enclosing a central seawater lagoon, see Figure 2.2. The atoll consists of over 24 islands with a total surface area of 30.6 square kilometres.

The series of islands have formed on top of a rim of an old volcano which rises 4,000 metres from the ocean floor, although on the western side they are entirely submerged. The lagoon coincides with the original crater and is rarely more than 20 metres deep. The land areas are flat and low-lying, with a maximum height above mean sea level of approximately 4 metres.

The majority of inhabitants reside on the islands on the southern rim, known as South Tarawa. The islands on the eastern rim, North Tarawa are uninhabited.

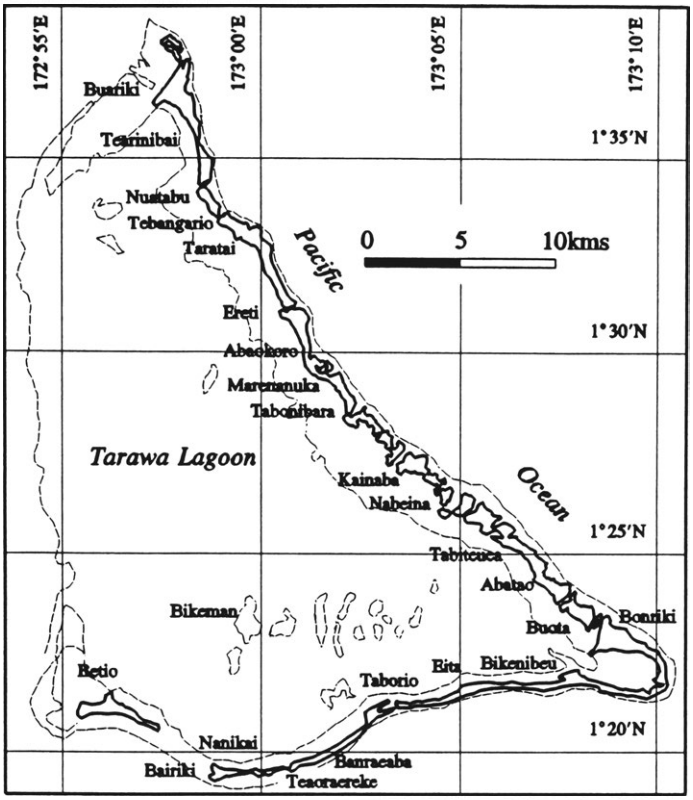

Figure 2.2 Location of Bonriki island on Tarawa atoll

The soil on these islands is very porous, consisting mainly of coral and sand. Only babai (taro), coconuts and pandanus are the major crops because the layer of soil is thin.

The average daily minimum temperature is 25°*C*. Temperatures below 23°*C* are rare. Maximum temperatures are high, averaging between 31 to 33°*C*, but seldom rise above 34°*C*. Irregularities in the temperature on atolls are small because the sea temperature is almost constant throughout the year.

Relative humidity is high, ranging from 70-80% throughout the year. The lowest humidity, which is seldom below 55%, occurs during September to November. The highest humidity occurs between December and May.

No tropical cyclones have occurred in Kiribati due to the close proximity of Kiribati to the equator. Winds seldom exceed gale force. When seas are rough, large waves do not reach the land because the islands are protected by their surrounding coral reefs. Wind directions are often variable during the wetter part of the year (December to May), however, winds between north and east are the most frequent. South-easterlies are more frequent during the drier part of the year (June to November) (Burgess [1987]).

Approximately 60-65% of the annual rainfall occurs between December and May and 35-40% occurs between June to November (Burgess [1987]). January is normally the wettest month and October is the driest month. The average annual rainfall on Tarawa is approximately 2000 millimetres which is typical of many of the atolls in Kiribati.

2.1 Aquifers on atoll islands

The main source of potable water for many coral atolls comes from groundwater in the aquifer system below the surface of the island. A basic conceptual model of the aquifer system of an atoll island is shown in Figure 2.3.

Aquifers on atoll islands vary substantially in their composition and also in their hydraulic properties such as permeability and porosity.

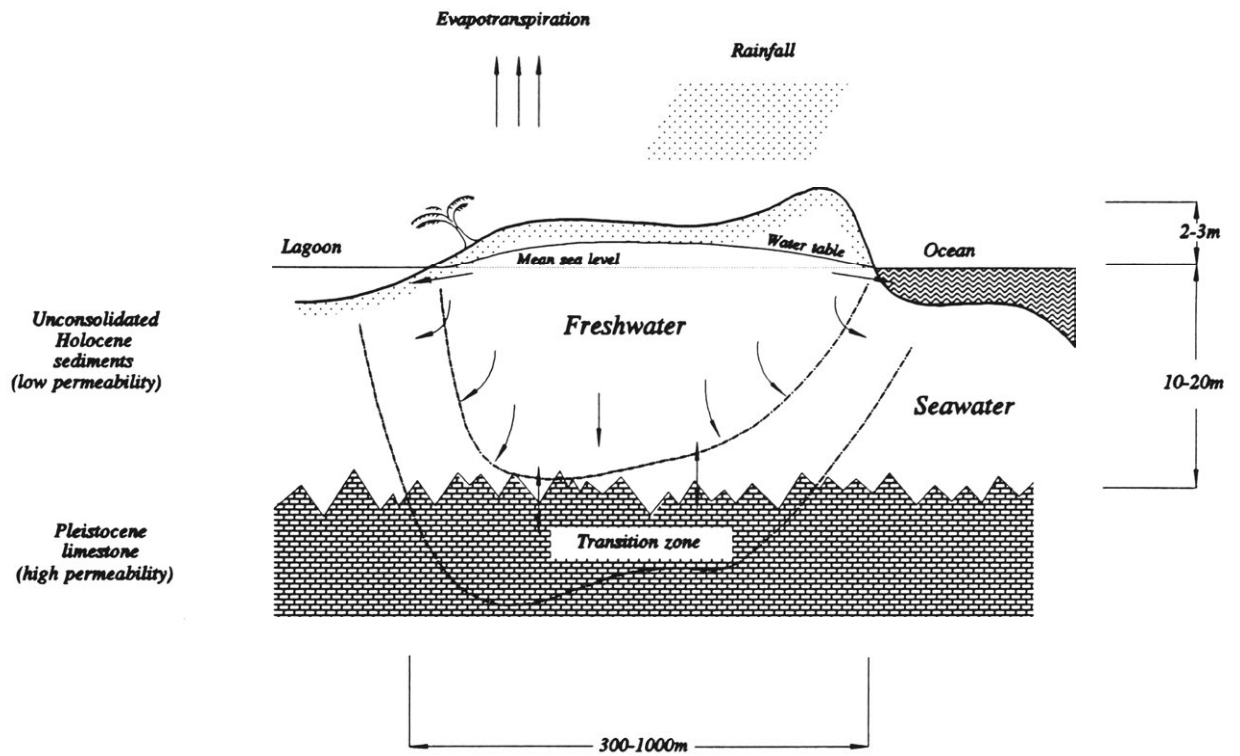

Figure 2.3 Form of the freshwater lens beneath atoll islands

The upper aquifer which usually consists of Holocene-age unconsolidated sand, gravel and silt has moderate permeability. The lower aquifer is comprised of Pleistocene-age sediments that have undergone diagenetic change during numerous episodes of eustatic sea level changes. These limestones form a more permeable aquifer than the overlying Holocene sediments.

2.2 Freshwater lens on atoll islands

Groundwater on an atoll island normally occurs in the form of a thin lenticular shaped freshwater body called the lens, see Figure 2.3. The freshwater lens on an island floats on seawater due to the differences in density between sea and fresh water. The upper surface of a freshwater lens is the water table and the lower surface is a boundary between the freshwater and seawater. The lower boundary is not sharp but is a transition zone of brackish water.

Within the island, the upper surface of the unconfined freshwater lens is domed, being higher in the center of the island than at the margins. This gives the lens a head which is the reason why water flows horizontally from the island's interior to its periphery.

The lens cross-section is often asymmetric with the deepest part skewed towards either the ocean or lagoon depending on the relative permeability of the sediments.

The central depression in the island plays an important role in the water balance of the island. Water tends to concentrate in the depression and recharges the lens during wetter periods of the year. During the dry season water is lost more rapidly from this area by evaportranspiration because the water table is closer to the surface. The groundwater is more accessible to plant roots if there is a depression in the island. Direct evaporation of the water surface is also greater if there is a pool in the depression.

Tidal range can be important because it influences the thickness of the transition zone. Semidiurnal tidal and recharge fluctuations have the effect of inducing mixing. The piezometric surface of the freshwater lens fluctuates up and down with the tides. A consequence of this is that the interface is not a sharp discontinuity. Instead there is a brackish transition zone. The width of the transition zone can be as thick, if not thicker, than the thickness of the freshwater above it. The transition zone between freshwater and seawater is narrow on Tarawa, where there is a relatively high recharge compared to other atolls (Daniell [1983]).

2.3 Ghyben-Herzberg ratio

The earliest work on the dynamics of coastal aquifers was done by Ghyben (1888) and Herzberg (1901). They established a steady-state relationship between the shape of the freshwater-seawater interface and its position based on the density difference between these waters.

By assuming static conditions at the sharp seawater-freshwater interface, hydrostatic equilibrium gives

$$\rho_s g h_s = \rho_f g h_f + \rho_f (h_s + h_f)$$

where h_s is the depth of the seawater-freshwater interface below mean sea level, g is the acceleration due to gravity, h_f is the height of the water table above sea level, ρ_s is the seawater density and ρ_f is the freshwater density.

Re-arranging

$$h_s = h_f \left[\frac{\rho_f}{\rho_s - \rho_f} \right].$$

The density of seawater is usually 1.025, therefore $h_s = 40 h_f$. This is known as the Ghyben-Herzberg ratio. To illustrate the significance of the Ghyben-Herzberg ratio, consider a cone of depression formed about a pumping well in fresh water. An inverted cone of seawater will rise into the freshwater. The seawater rise of approximately 40 times the freshwater drawdown may occur. This can significantly affect the quality of the freshwater in the vicinity of the pumping well. The construction of horizontal galleries for extracting the groundwater are commonly used to avoid this problem.

2.4 The size of a freshwater lens

The size of the freshwater lens on atoll islands depends on; (*i*) recharge, (*ii*) width of the island, (*iii*) permeability, (*iv*) porosity, (*v*) evapotranspiration and (*vi*) abstractions.

The size and shape of the freshwater lens is essentially a balance between what comes in and what is lost from the lens. This can be expressed mathematically as

$$R = P - I - E - \Delta s \tag{2.1}$$

where R is the recharge, P is the precipitation, I is the interception, E is the evaporation and evapotranspiration and Δs is the change in soil storage.

Rainfall is the sole source of recharge to the lens. The amount and type of vegetation on an island, as well as man-made modifications to the surface of the island, influence the proportion of rainfall reaching the lens as recharge. A small proportion of the rainfall reaching the ground is also held above the water table in the capillary zone.

Interception, which includes all retention of water by vegetation before it gets to the ground, can be as much as 15% on islands and is particularly high where there are coconuts. Evaporation and evapotranspiration also depend on vegetation. Coconuts have high transpiration rates with estimates suggesting 70-130 litres per tree per day. This compares with human consumption of water ranging between 20-350 litres per person per day on similar islands to 1000 litres per day in some tourist resorts (Falkland [1991]).

The long-term recharge to the freshwater lenses on Tarawa from rainfall is estimated to be about 35% of the rainfall in areas with good vegetation cover. This can increase to 50% of the rainfall in cleared areas (Falkland [1992]). As a general rule, recharge is generally less than 50% of rainfall.

Using the conservation of mass, the simple water balance can be established for the lens given by

$$R = O + Q + \Delta V \tag{2.2}$$

where O is the abstraction rate, Q is the outflow at the lens circumference and ΔV is the change in the volume of the lens.

The effect of abstractions on the volume of the lens can be estimated if the outflow is known using equation (2.2) and equation (2.1) to estimate the recharge. The Ghyben-Herzberg ratio can be used to estimate the position of the freshwater-seawater interface if the surface area of the lens is known.

The solution of equations (2.1) and (2.2) is relatively straight forward for steady state conditions. However, under transient conditions it is more convenient to develop and solve a numerical model describing the behavior of the lens. The numerical model can be used to estimate the sustainable yield from a freshwater lens for various management strategies.

2.5 Sustainable yield of a lens

Sustainable yield is the volume of water which can be safely abstracted from the lens without deleteriously affecting the long term viability of the aquifer. Mink (1976) defines the sustainable yield as the volume rate of water that can be withdrawn from an aquifer continuously without affecting the quality of the water being withdrawn.

The sustainable yield can be approximately equal to the average annual recharge for inland aquifers. However, in coastal and small island groundwater bodies this is not true, since part of the recharge is required to maintain the freshwater lens. If all the recharge was withdrawn, there would be no freshwater to flow through the lens to prevent the intrusion of sea or brackish water from below. Mink (1976) suggests that it is common in thin lens situations to extract only 25% of the recharge. Hunt and Peterson (1980) used this criterion as a means of estimating the sustainable yield of the freshwater lens on Kwajalein atoll in the Marshall Islands. They also considered local destruction of the freshwater lens that can be caused by inappropriate pumping methods resulting in upconing of the underlying transition zone. Chidley and Lloyd (1979) indicated that a value of 25 to 30% of the recharge was an appropriate extraction rate for the lens on Grand Cayman Island in the Caribbean Sea.

Griggs and Peterson (1989) modelled the freshwater lens on Laura, an island on the Majuro atoll, Marshall Islands, Pacific Ocean. They showed that extracting an equivalent of 20% of the mean annual recharge had a minor influence on the long term sustainability of the freshwater lens. Extracting 40% of the mean annual recharge caused major upconing of the lens, whilst an extraction rate of 60% of the mean annual recharge resulted in the destruction of the lens.

Falkland (1994) defines sustainable yield as 17-20% of the mean annual recharge for freshwater lenses on small coral islands, such as those found on South Keeling atoll in the Cocos (Keeling) Islands, Indian Ocean. Sustainable yield varies from island to island but is probably 20-30% of recharge, which is approximately 6-12% of the rainfall.

There are numerous factors which influence what yield is sustainable. It is as much a social problem as a hydrologic one (Wentworth [1951]). Sustainable yield is a subjective quantity. Establishing the sustainable yield of the freshwater lens on Bonriki will not be attempted in this study. Instead, the probability density function of the lens thickness will be estimated for different pumping rates and vegetation cover using an unsteady flow model based on the Ghyben-Herzberg ratio. This information can be used to estimate the probability of the lens thickness not meeting certain management constraints.

2.6 Bonriki island

Bonriki is a small island of 154 hectares, located on the south western corner of the Tarawa atoll, see Figure 2.2. The major features on Bonriki are the airfield, see Figure 2.4 and naturally growing coconut trees which cover 80% of the island's surface. Coconuts are the major crop for the residents of Tarawa.

Figure 2.4 Geographical map of South Tarawa

The climate of Tarawa, particularly the rainfall pattern, is affected by the El Niño Southern Oscillation phenomenon. Burgess (1987) illustrated the correlation between the annual rainfall at Tarawa (Betio) and the Southern Oscillation Index, which is an indicator of the severity of the El Niño Southern Oscillation activity. It was found that the annual rainfall on Tarawa is usually above normal when the Southern Oscillation Index is negative and below normal when the Southern Oscillation Index is positive.

The mean annual rainfall at Tarawa, recorded at Betio meteorological station for the period 1947-1980, was 1976 millimetres, which is similar to the amount of rainfall observed on many Pacific atolls.

The freshwater lenses on Biota and Bonriki are used to provide a significant proportion of the potable water for South Tarawa. The freshwater lens on Bonriki contributes approximately 70%, Buota 20% and the remaining freshwater is from lenses from other islands and roof catchments. The government declared a large portion of the lands owned by the Bonriki people as a water reserve because the groundwater on Bonriki is an important resource for Tarawa (van Trease [1993]), thereby restricting development and population on the island. The population on Bonriki was only 848 in 1985 with the majority of the residents of Bonriki located in a single village in the south-eastern corner of the island.

Groundwater is extracted from 17 infiltration galleries on Bonriki. Pumps attached to each gallery have a nominal pumping rate of 55 cubic metres per day. The effect of intensive pumping of fresh water from the lens has had a detrimental effect on vegetation on the island with the production of coconuts decreasing dramatically (van Trease [1993]). It is thought that this decline has resulted from an increase in salinity of the groundwater due to seawater intrusion.

There has been extensive monitoring of water levels and salinity in the aquifer on Bonriki due to the importance of the freshwater lens on Bonriki to the residents on Tarawa. A total of sixteen bores over the period 1980-1993 have been used for this purpose. The monitoring program showed that the freshwater lens on Bonriki can be as deep as 29 metres. In addition, the thickness of the Holocene limestone is uniform with a thickness varying between 15 and 22 metres. DHC (1982) concluded by using some of this data, that in the long term, the extraction of freshwater from the lens on Bonriki should not be greater than 30% of the recharge.

Chapter 3.

Modelling the thickness of the freshwater lens on Bonriki

The behavior of freshwater lenses beneath small islands is usually modelled using either the dual aquifer model or the traditional sharp interface single aquifer based on the Ghyben-Herzberg relationship. Important differences between the various models that have been used are given by Underwood *et al.* (1992).

3.1 Lens models

Models based on the Ghyben-Herzberg relationship depend upon the long-term balance between recharge and outflow of freshwater from around the perimeter of the lens. The primary mechanism for loss of freshwater in the dual aquifer model is degradation by downward mixing into the transition zone. Models based on the Ghyben-Herzberg relationship are two-dimensional in plan. The dual aquifer models, such as SULTRA (Saturated Unsaturated TRAnsport) (Voss [1984]), are two-dimensional in the vertical plane. Three-dimensional models are available, for example HST 3D (Kipp [1987]) and the quasi-three-dimensional model SHARP (Essaid [1990]). Recent application of the HST 3D model to the aquifer system on the Pacific island of Nauru by Ghassemi *et al.* (1990) failed to produce physically meaningful results. Difficulties were also encountered in implementing the model as a two-dimensional cross-sectional model.

Since this study is interested in the long term behaviour of a lens, an unsteady single aquifer model based on the traditional Ghyben-Herzberg relationship is used. The computational effort required for multiple simulations necessary for this study, prohibits the use of more sophisticated dual aquifer models. For example, Ghassemi *et al.* (1990) found that the SULTRA model with 127 $\times$ 33 nodes to discretize the Nauru island aquifer system, required 10 hours, 145 minutes and 18 minutes of execution time on a VAX 11/785, VAX 8700 and FACOM VP-100 (Fujitsu) supercomputer systems respectively. Approximately 1000 time steps of 15 days each were used to simulate a 41 year period. This is the time required for the simulation of a single realization. In a Monte Carlo simulation for example, 100's of simulations are required. The computational time required to perform the simulation required for the reliability analysis considered in this thesis would be prohibitive.

Vacher (1988) suggests that the Ghyben-Herzberg relationship is valid for small islands with very permeable and highly recharged aquifers. Chapman (1985) argues that the Ghyben-Herzberg relationship is appropriate for modelling the behaviour of a shallow freshwater lens. Therefore, the simpler less computationally intensive sharp interface single aquifer model, based on the Ghyben-Herzberg relationship has been adopted in this study.

3.1.1 Theory of the sharp interface single aquifer models

The following assumptions are made in the single aquifer sharp interface model: (*i*) A sharp interface occurs between the freshwater and seawater boundary at the base of the lens. (*ii*) The freshwater lens is unaffected significantly by the ebb and flood of the tide. This implies that the sea is tideless and not affected by barometric variations. (*iii*) The aquifer is isotropic but nonhomogeneous. (*iv*) The pressure distribution in the lens is hydrostatic. This is equivalent to assuming that the groundwater velocity is horizontal. (*v*) All natural flow from the freshwater lens to the surrounding seawater occurs at the perimeter of the lens. (*vi*) A Ghyben-Herzberg type of relationship holds. The depth below a datum of the interface between saltwater and freshwater is some fixed ratio, α times the height of the water table above sea level, even in the dynamic situation. (*vii*) Flow is laminar and Darcy's Law applies. (*viii*) The groundwater system is treated as a single layer aquifer system.

It is possible to derive a simple unsteady flow model describing the behaviour of a freshwater lens based on the Ghyben-Herzberg relationship with these assumptions.

Consider the element of dimensions Δx by Δy shown in Figure 3.1, where Δt is the time interval, x and y are distance dimensions, q is the flow rate through the elemental volume, t the time, R is the recharge rate per unit area, α is the Ghyben-Herzberg ratio and h is the height of the water table above sea level.

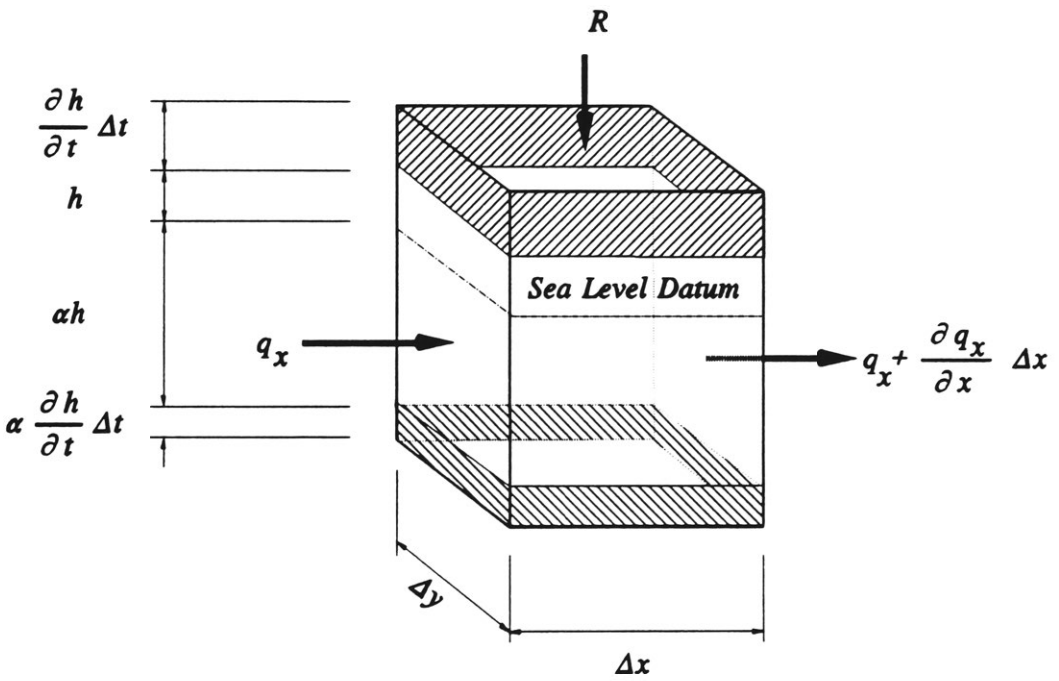

Figure 3.1 Advection and turbulent diffusion in a fluid element

To derive the equation governing the flow through an aquifer, consider the mass balance of freshwater flowing through an element of the aquifer during the time increment Δt. During Δt the continuity equation for the element is

$$\Delta S = \Delta t(\Delta q + \Delta R)$$

which simply states that over a time increment Δt the change in lens storage ΔS is equal to the inflow

minus the outflow from the element.

The net inflow into the element during Δt is

$$\Delta q = -\frac{\partial q_x}{\partial x}\Delta x - \frac{\partial q_y}{\partial y}\Delta y.$$

The net outflow due to recharge during Δt is

$$\Delta R = R\Delta x\Delta y.$$

The change in storage of freshwater during Δt is

$$\Delta S = \beta(1 + \alpha)\frac{\partial h}{\partial t}\Delta x\Delta y\Delta t$$

where β is the effective porosity or storage coefficient.

From the equation of continuity

$$\beta(1 + \alpha)\frac{\partial h}{\partial t}\Delta x\Delta y = -\frac{\partial q_x}{\partial x}\Delta x - \frac{\partial q_y}{\partial y}\Delta y + R\Delta x\Delta y. \tag{3.1}$$

If it is assumed that Darcy's Law applies to the flow, it follows that for flow in the x-direction

$$q_x = -(1 + \alpha)Kh\frac{\partial h}{\partial x}\Delta y$$

where K is the permeability or the hydraulic conductivity. The quantity $T = (1 + \alpha)Kh$ is known as the transmissivity. Substituting Darcy's equation into equation (3.1) yields the following equation of motion for the system under the assumptions given above.

$$\frac{\partial}{\partial x}\left[Kh\frac{\partial h}{\partial x}\right] + \frac{\partial}{\partial y}\left[Kh\frac{\partial h}{\partial y}\right] - \frac{\beta\partial h}{\partial t} + \frac{R}{(1+\alpha)} = 0. \tag{3.2}$$

3.1.2 Solution of the equation of motion

The numerical solution of equation (3.2) generally involves replacing the partial derivative in this equation by finite differences. The first two terms in equation (3.2) represent the net inflow into a node. For node i these terms can be approximated by

$$\sum_{j=1}^{k} C_{ij}(h_j - h_i)/\Delta x/\Delta y$$

where k is the number of nodes adjacent to node i and $C_{ij} = (1 + \alpha)(K_i + K_j)(h_i + h_j)/4$. Therefore equation (3.2) can be approximated by

$$\sum_{j=1}^{k} C_{ij}(h_j - h_i) + R_i\Delta x\Delta y - \beta_i(1 + \alpha)\Delta x\Delta y\frac{\partial h_i}{\partial t} = 0. \tag{3.3}$$

Equation (3.3) is written for each node in the computational domain. Using matrix notation, the system of equations can be written as

$$[M]\{H\} = [B]\left\{\frac{\partial H}{\partial t}\right\} - \{R\}$$

or

$$\left\{\frac{\partial H}{\partial t}\right\} = [B]^{-1}[M]\{H\} + [B]^{-1}\{R\}$$

in which $[M]$ is a $p \times p$ matrix, the coefficients of which are the coefficients C_{ij} or their sum on the diagonal, $[B]$ is a diagonal $p \times p$ matrix, with $\beta_i(1 + \alpha)\Delta x\Delta y$ as the coefficients, $\{R\}$ is a column vector with coefficients $R_i\Delta x\Delta y$, $\{H\}$ is the vector of known height of the water table above sea level, $\{\partial H/\partial t\}$ is the unknown derivatives and p is the number of computational nodes. The inverse of the diagonal matrix $[B]$ is simply a diagonal matrix with $1/(\beta_i(1 + \alpha)\Delta x\Delta y)$ as the coefficients.

A suitable approximation is required for the temporal derivative. A forward difference scheme will produce an explicit finite difference scheme which is relatively simple to solve. Adopting a backward finite difference scheme will produce an implicit finite difference scheme. Implicit schemes have some desirable properties such as they are unconditionally stable and theoretically there is no restriction on the time step that can be employed. However they are more difficult to solve, generally requiring an iterative procedure for their solution (see, for example Prickett and Lonnquist [1971]). An explicit scheme is used in this study to approximate the temporal derivative. Therefore

$$\{H\}^{t+\Delta t} = \{H\}^t + \Delta t([B]^{-1}[M]\{H\}^t + [B]^{-1}\{R\}^t)$$

where the superscript $t + \Delta t$ refers to the unknown values on the current time level and t to the known values on the previous time level. The unknowns $\{H\}^{t+\Delta t}$ can be solved directly, however there is a limitation on the size of the time step Δt that can be used. de Marsily (1986) showed that the restriction on the time step is given by

$$\Delta t \leq \min_{i=1}^{p} \frac{\beta_i(1 + \alpha)\Delta x\Delta y}{\sum_{j=1}^{k} C_{ij}}. \tag{3.4}$$

The time step depends on the grid size and the properties of the lens.

3.2 Bonriki lens

The single lens model described above requires as input the; (*i*) lens geometry, (*ii*) Ghyben-Herzberg ratio and at each node the (*iii*) permeability, (*iv*) porosity, (*v*) extraction and (*vi*) recharge.

A number of these parameters have been determined from measurements at a set of boreholes drilled on Bonriki. Initially two boreholes were drilled on Bonriki (BH1 and BH2) in September to November 1980. These boreholes were subsequently renamed BN3 and BN18 respectively. This was followed by nine new boreholes drilled in November and December 1980, (BN1 to BN9). The location of these boreholes are shown in Figure 3.2. The co-ordinates of the boreholes on Bonriki are given in Table 3.1.

Only six of these boreholes were drilled through the freshwater zone and into the transition zone (BN1, BN2, BN4, BN5, BN7 and BN9). All but BN4 were cased with slotted PVC (plastic) pipe. No permanent casing was installed in borehole BN4. The remaining boreholes (BN3, BN6 and BN8) were drilled to about 70% of the depth of the freshwater zone. Between March and June 1985 seven new boreholes were drilled on Bonriki (BN11 to BN17). All sixteen boreholes have been used to monitor the salinity of the water in the lens. In the period July to August 1983 remedial works consisted of

removing the existing monitoring system and the PVC casing, redrilling of boreholes and reinstallation the monitoring system. A new borehole BN10, was drilled near BN1 and fitted with a monitoring system. The original shallow boreholes BN3, BN6 and BN8 were backfilled with sand and abandoned.

Table 3.1 Co-ordinates of the boreholes on Bonriki

Borehole Number	Tarawa Grid Easting	Tarawa Grid Northing
BN1	53067	32290
BN2	52979	32140
BN3	52933	32035
BN4	52782	31947
BN5	52614	31698
BN7	52667	32754
BN9	52519	32505
BN10	53049	32323
BN11	53189	31547
BN12	52958	31740
BN13	52610	32646
BN14	52509	32849
BN15	52818	32375
BN16	52695	32270
BN17	52600	31860
BN18	52670	32400

A cross-section of the island through boreholes BN1, BN2, BN3, BN4 and BN5 is shown in Figure 3.3 and 3.4. Selected salinity profiles (2500, 1000 and 25000 μS per centimetre) of the water in the lens recorded on the 12/03/1985 and 26/02/1989 in these boreholes are also plotted in Figures 3.3 and 3.4 respectively. These limits coincide with the freshwater limit, 2500 μS per centimetre, the mid-point of the transition zone, 25000 μS per centimetre, which is based on the assumed value of 50000 μS per centimetre for seawater. Standardized potable water has been defined as water up to an electrical conductivity of 2500 μS per centimetre. This is based on the WHO (1971) standard and is equivalent to 600 milligrams per litre of chloride ion concentration.

The results in these figures reveal that the freshwater lens varies in both space and time. This observation was confirmed by Falkland (1992) using a more comprehensive data set. The water table is about 1.5 to 2.5 metres below the ground surface.

The lens is asymmetric, with the deepest part of the lens located towards the lagoon. This could be attributed to any of the following: (*i*) Higher permeability on the ocean side due to the fractured limestone sequences being closer to the surface. This allows the lens to drain more rapidly to the sea. (*ii*) Increased recharge in this area due to the clearing of coconut trees near the runway. (*iii*) The majority of the extraction from the lens occurs on the ocean side.

In 1989 the measured thickness of the freshwater lens was greater than that recorded in 1985. The thickness of the freshwater lens in 1985 corresponds to a period of below average annual rainfall on Bonriki. Prior to 1989 above average rainfall occurred on Bonriki.

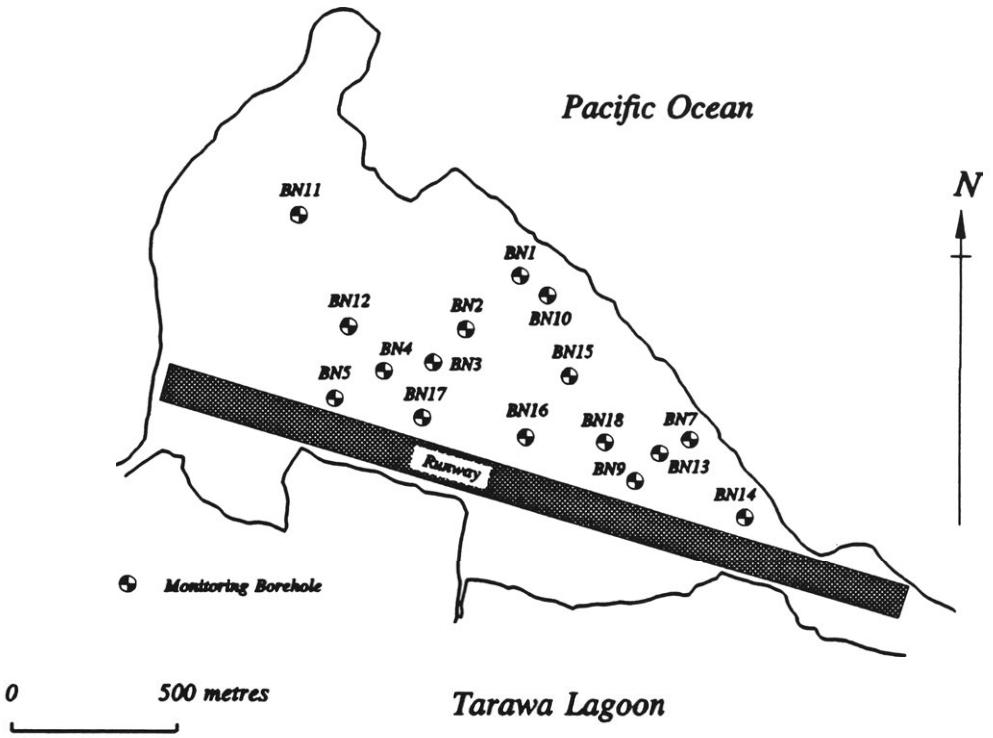

Figure 3.2 Location of the monitoring boreholes on Bonriki

The nonconformity between the less permeable Holocene and more permeable Pleistocene limestone is also shown in these figures at selected boreholes. The thickness of the Holocene limestone seems to be uniform with a thickness varying between 15 and 22 metres.

Vacher (1988) suggests that to correctly model islands with transition zones which occupy a large fraction of the thickness of a freshwater lens, it is necessary to use a variable density advective-dispersion model. These models include seawater flux into the transition zone. From Figures 3.3 and 3.4 the transition zone does not occupy a large portion of the lens thickness in comparison to other atolls (see also Daniell [1983]). Therefore, models based on the simpler Ghyben-Herzberg ratio are appropriate in this case.

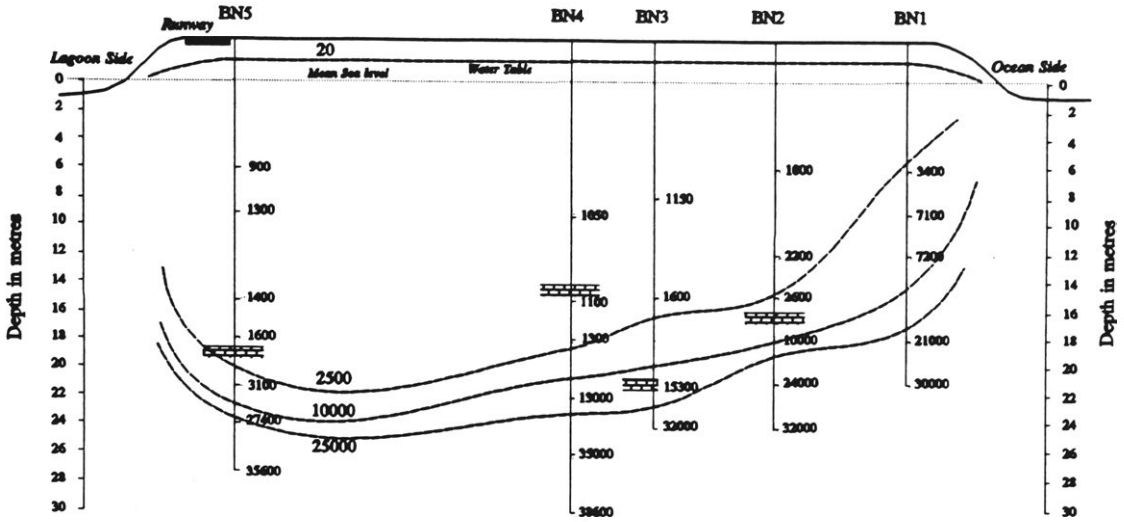

Figure 3.3 Cross-section through bores BN1 to BN5, Bonriki, showing electrical conductivity contours in μS per centimetre of the freshwater lens recorded on the 12/05/1985

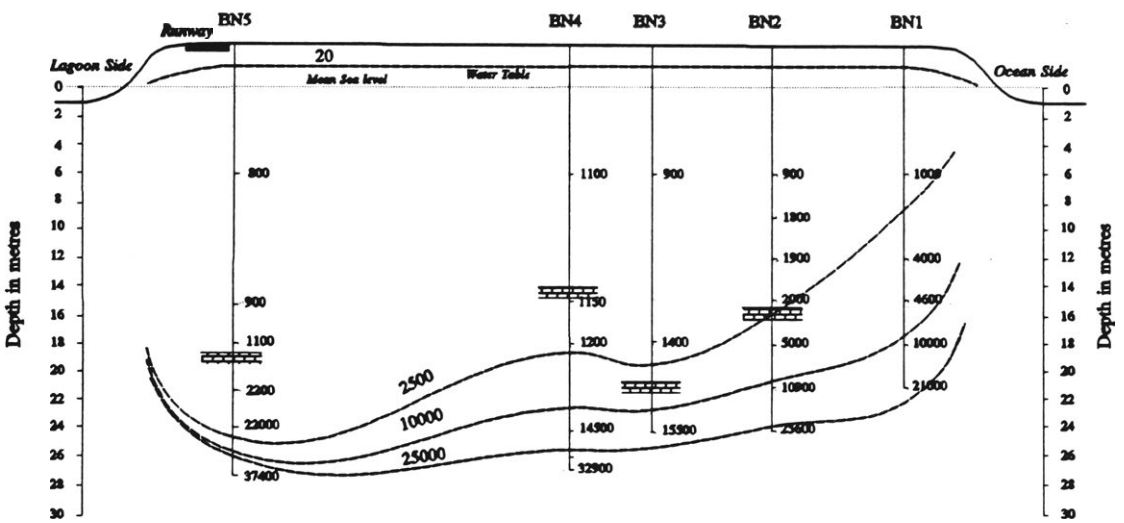

Figure 3.4 Cross-section through bores BN1 to BN5, Bonriki, showing electrical conductivity contours in μS per centimetre of the freshwater lens recorded on the 26/02/1989

3.2.1 Lens geometry

The boreholes on Bonriki were used to determine the hydraulic properties of the aquifer, to monitor the salinity in the water in the lens and to establish the lens thickness and its shape.

The boundaries of the freshwater lens were established by comparing the surface resistivity with the conductivity readings in the boreholes. Contours of the lens thickness, defined by the conductivity reading of 2500 μS per centimetre, are shown in Figure 3.5.

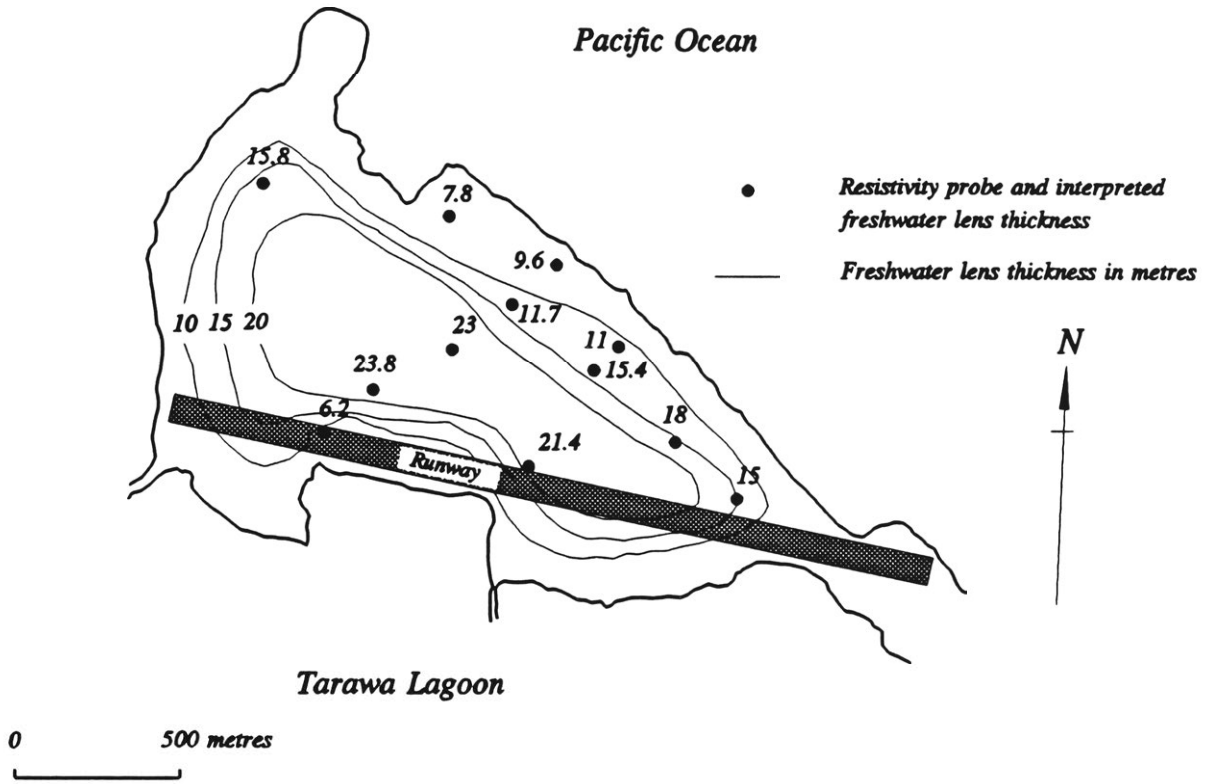

Figure 3.5 Contours of the thickness of the freshwater lens estimated from resistivity probe measurements

The stored volume of potable water is large in comparison to the surface area of the island, which is 154 hectares. Assuming that 30% of the total volume of the lens is extractable freshwater, there is approximately 6×10^6 cubic metres of potable water on Bonriki. In practice however, this volume of freshwater is not available, as it would significantly deplete the freshwater lens and may adversely affect the quality of the remaining freshwater.

The area enclosed by the 10 metre contour of the lens thickness is considered as the extraction area of the lens. The approximate surface area of the lens is 76 hectares (Volker *et al.* [1985]). It is within this area that freshwater may be safely extracted and is of potable quality.

The location of the boundary nodes and the extraction points used in the model are illustrated in Figure 3.6. A total of 22 × 15 nodes were used in the model to define the freshwater lens and

boundary nodes on Bonriki. The distance between each node is 100 metres in both principle directions.

The freshwater-seawater interface is generally taken to be the mid-point of the transition zone for the application of models based on the Ghyben-Herzberg relationship. The initial thickness of the freshwater lens is taken as the depth to the mid-point of the transition zone for this study. This corresponds to 25000 μS per centimetre in the transition zone. The influence of the initial lens thickness on the final model results is negligible for this study .

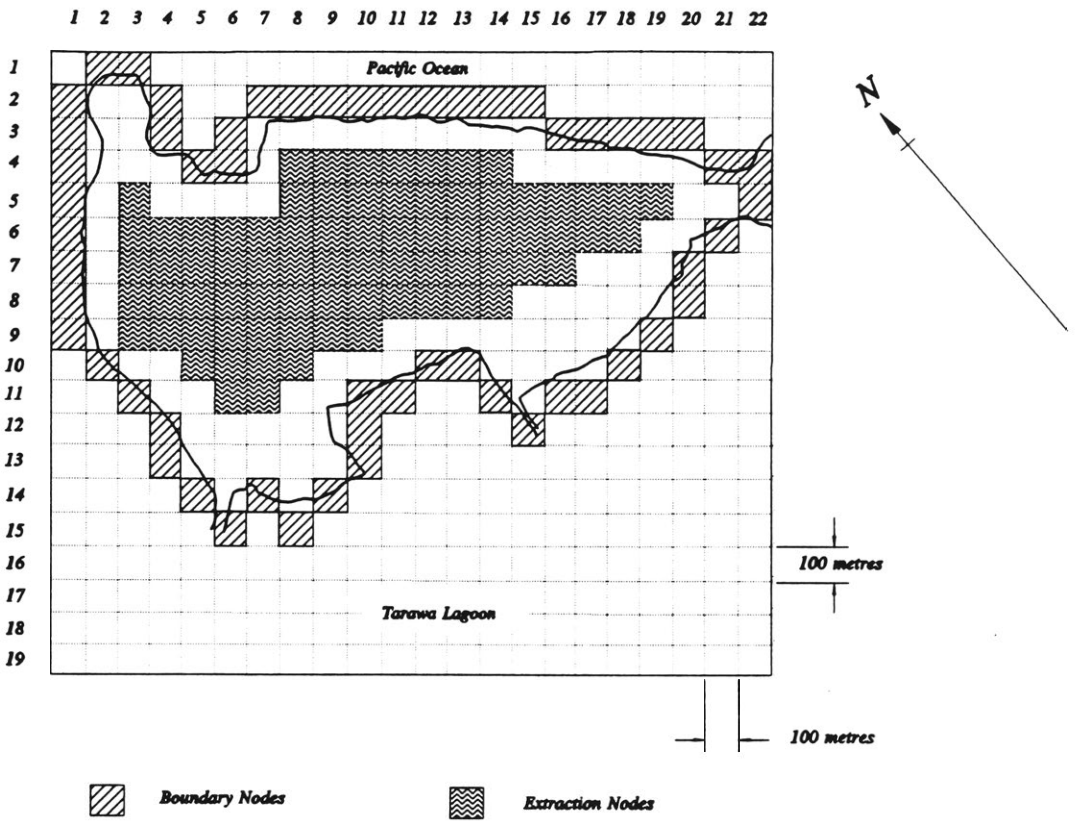

Figure 3.6 Bonriki island boundary and extraction nodal layout

3.2.2 Ghyben-Herzberg ratio

The Ghyben-Herzberg constant α should only depend on the relative density of freshwater and seawater. Although it may also depend on temperature, it should be in the range 36 to 40. However, values of the Ghyben-Herzberg constant that have been used in various studies, vary between 20 to 40. Lloyd *et al.* (1980) and Falkland (1983) have used a value as low as 20 for α. They argue that this delimits the lower limit of the freshwater.

The appropriate demarcation between freshwater and seawater in the single aquifer sharp interface model is the mid-point of the transition zone (Chapman [1985]). This is also consistent with the assumptions made in deriving the equations governing the behaviour of the single aquifer sharp interface model, equation (3.2). Therefore, a constant value of 40 was used for the Ghyben-Herzberg constant, α in the analysis, as representative of the ratio of the height of the water table above mean sea level to the depth below mean sea level to the mid-point of the transition zone.

3.2.3 Porosity

Porosity is the ratio of voids to the total volume of a sediment. Effective porosity, or *specific yield* is that proportion of the voids through which flow actually occurs. It is generally 10-30% and is always less than the total porosity, which is characteristically 40-60% (Woodroffe [1989]).

No insitu tests for the determination of porosity of the aquifer on Bonriki exists, however laboratory analysis showed a typical value would be 40% (Daniell [1983]).

3.2.4 Permeability

Permeability is a measure of the ability of the aquifer medium to allow the movement of fluid under a pressure gradient with appreciable velocity. It depends on the stratification, consolidation, arrangements of grains, size distribution and porosity of the aquifer medium. Unconsolidated Holocene sediments tend to show permeabilities of 1 to 10 metres per day (Lloyd *et al.* [1980]), whereas the permeability of the underlying Pliesocene limestones is likely to be around 1000 metres per day (Hunt [1979]). Coral-rich Holocene sediments often have intermediate permeabilities of approximately 200 metres per day (Lloyd *et al.* [1980]). Permeability cannot be effectively estimated from core samples. It can however be measured from test wells using pumping experiments.

Little information is known about the variation of permeability with depth and lateral extent on Bonriki. Insitu falling head and constant head tests were performed at selected boreholes on Bonriki to estimate the permeability of the aquifer. These tests were performed in the deepest boreholes on Bonriki, (BN1, BN2, BN4, BN5, BN7 and BN9 shown in Figure 3.2). Permeability tests of the aquifer were obtained at approximately 3 metre depth intervals. The results of these tests can be found in Murphy (1981).

The permeabilities obtained for the constant head (pump out) tests were higher than for the falling head tests. Falkland (1983) considered the falling head test results more reliable than the constant head results. The constant head tests require water to be pumped out, which can dislodge particles of loose material in the borehole, thus increasing the size of the voids in the aquifer and yielding higher permeability values. This form of testing may also cause upconing of the transition zone and seawater in the vicinity of the pump. Therefore, large scale pump tests are not considered appropriate on atolls.

Falling head tests involve pumping water into the borehole at very low rates. The rate of pumping is not considered to be sufficient to disturb the aquifer medium during the test. The rate at which water drops in the borehole is used to calculate the permeability of the aquifer.

Several tests were performed for a number of depths below the ground surface at many of the boreholes. The fall in water level over a time interval was used to estimate the permeability for a particular depth. This may have been performed for a number of time intervals. There are 178 measurements of permeability from 6 boreholes. These have been summarized in Table 3.2. A, B and C denote different pump tests performed at the indicated depth. The numbers in the square brackets are the permeabilities estimated over a number of time intervals for each pump test. These results will be used to estimate the mean, variance and correlation structure of the permeability of the aquifer.

Table 3.2 Measured permeabilities in various bores on Bonriki

Bore Hole Number	Depth in metres	Permeability in metres per day
BN1	5.2 to 6.0	A[9.1,8.4,3.2,13.9,6.6,10.2,9.3]:B[4.3,12.0,7.2,9.8,8.0,8.9]
	8.2 to 9.0	A[12.1,4.1,16.2,9.4,11.6,14.0]:B[9.0,16.1,10.5,13.1,11.9,11.8]
	14.2 to 15.0	A[7.0,14.7,12.3,7.6]
BN2	5.9 to 6.4	A[2.0,1.2,2.3,0.0]:B[1.9,2.0,2.0,2.8,1.3]:C[2.7,2.8,2.8,2.9,2.9]
	8.9 to 9.4	A[5.8,2.1,1.5]:B[8.0,3.8,2.2]
	14.75 to 15.55	A[9.7,7.0]:B[20.4,9.0,9.5,7.9,10.8,7.2,9.0,6.2]
	20.25 to 21.05	A[11.3,17.8,17.1,16.4,16.9,22.1,26.5]:B[14.7,12.1,12.9,16.4,16.7,18.1,25.8,26.2]
	23.25 to 24.05	A[9.4,6.7,10.0,3.6,6.6,4.1,2.9]:B[8.6,11.7,7.8,6.9,4.1,2.1]
BN4	2.7 to 3.55	A[3.5]:B[3.9]
	5.8 to 6.3	A[3.5]:B[4.1]
	10.05 to 10.55	A[4.7,4.6,4.2]:B[5.3,1.3,5.6,5.9]
	14.85 to 15.35	A[12.1]:B[15.2]
	23.25 to 24.05	A[17.5,15.8,16.9,5.6]:B[10.2,14.0,13.8,20.8]:C[8.7,11.4,13.4]
BN5	9.15 to 9.65	A[6.9,18.9]:B[7.2,7.4]
	11.25 to 12.05	A[18.5]:B[18.5]:C[16.4]
	14.25 to 15.05	A[18.5,12.2]:B[14.8,12.7]:C[14.8,13.1]
	17.25 to 18.05	A[9.9,10.0]:B[13.0,9.7]:C[10.7,8.9]
	20.25 to 21.05	A[13.6,11.7]:B[12.3,11.7]:C[11.3,11.7]
	23.25 to 24.05	A[24.5,20.2]:B[24.5,20.2]:C[24.5,18.2]
BN7	8.10 to 8.9	A[19.9,29.3]:B[19.9,29.3]:C[26.5,25.1]
BN9	5.2 to 6.0	A[12.2,9.6]:B[15.2,11.1]:C[12.2,9.6]
	8.2 to 9.0	A[10.2,7.2]:B[10.2,6.9]:C[8.7,7.2]
	11.2 to 12.0	A[7.6,7.9]:B[7.6,8.3]:C[8.6,8.3]
	20.2 to 21.0	A[33.1,22.8]:B[26.5,26.6]:C[22.1,20.0]
	23.2 to 24.0	A[26.7,40.2]:B[44.4,40.2]:C[44.4,35.7]

The results from the falling head pump tests indicate that the permeability of the Holocene sediments vary between 0 to 20 metres per day, while much greater values, in excess of 44 metres per day, were found in the Pleistocene limestones. These values were confirmed by laboratory analysis of collected samples (DHC [1982]).

Permeability tends to increase with depth, however there is significant variation in permeabilities with location, depth and for multiple tests at a particular depth.

3.2.5 Extraction rate

Groundwater is extracted from 17 infiltration galleries located between 1.0 and 2.0 metres below the ground surface on Bonriki. The location of these galleries are shown in Figure 3.7.

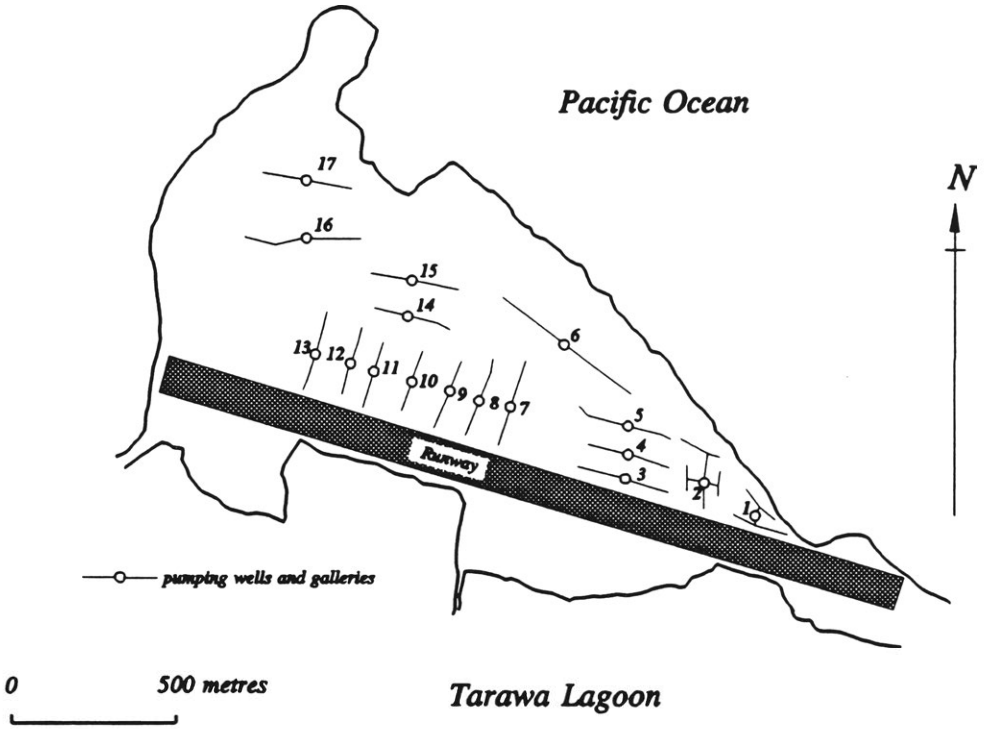

Figure 3.7 Location of the pumping wells and galleries on Bonriki

Pumps attached to each gallery have a nominal pumping rate of 55 cubic metres per day. The construction of horizontal galleries for extracting the groundwater are commonly used to avoid upconing of seawater into the freshwater lens.

The predicted demand from the lenses on South Tarawa is approximately 750 cubic metres per day (Volker *et al.* [1985]). It is possible to satisfy this requirement from the freshwater lens on Bonriki. If this volume of freshwater is withdrawn uniformly from the lens area it would be equivalent to a net withdrawal rate of approximately 360 millimetres per year. This represents 18% of the annual rainfall on Bonriki, see Figure 3.8.

The galleries are distributed over the whole island. Therefore, constant extraction of the freshwater is assumed to occur uniformly over the entire area of the lens. A constant pumping rate is assumed for several important reasons: (*i*) It is undesirable to vary the pumping rate because it can have a detrimental effect on the performance of the aquifer. A variable pumping rate may increase the likelihood of dislodging particles in the aquifer. (*ii*) Water restrictions are imposed on many islands. All the water that is extracted is generally utilized and the volume required necessitates pumping continuously. (*iii*) A variable pumping rate may promote mixing between freshwater and seawater

thereby increasing the mixing zone and reducing the available potable water.

3.2.6 Recharge

Recharge is a major factor influencing the sustainability of the freshwater lens. It can be estimated using a number of techniques. A water balance was used by Falkland (1992) to determine the recharge on Bonriki during the period 1954 to 1991. The water balance is simply the net input to the lens from rainfall, major sources of evaporation and storage in the soil. Sources of evaporation include; (*i*) plants, (*ii*) roots, (*iii*) the soil capillary zone and (*iv*) roots which transpire water directly from the freshwater lens. The recharge on Bonriki was estimated by assuming 80% tree cover, which is the existing vegetation condition on Bonriki. The recharge to the freshwater lens on Bonriki was calculated by considering all these sources. The recharge and corresponding annual rainfall during the period 1954 to 1991 is depicted in Figure 3.8.

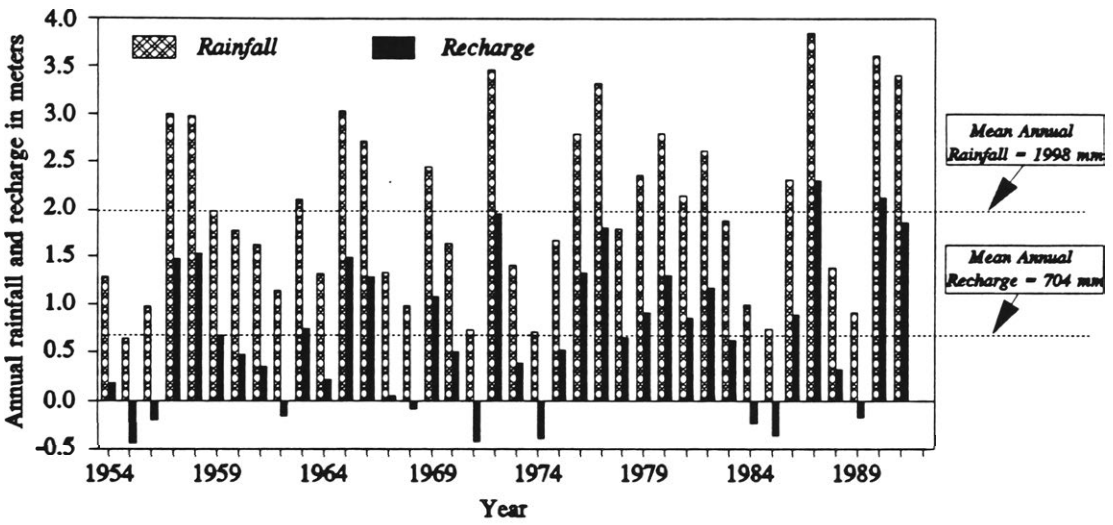

Figure 3.8 Annual recharge and rainfall on Bonriki during 1954 to 1991, for 80% vegetation cover (after Falkland [1992])

The rainfall record was obtained from the meteorological station on Betio. Whilst the average annual rainfall is of the order of 2,000 millimetres, there is considerable variation from year to year. The highest recorded annual rainfall recorded during this period is 3843 millimetres and the lowest is 647 millimetres.

There is considerable variability in the recharge rate. Falkland (1992) found that as expected, there was a strong correlation between rainfall and recharge. The peak recharge rates coincide with periods of above average rainfall. Negative recharge coincides with periods where the evaporation from the sources described above exceeds the precipitation, resulting in a depletion of the water from the lens. When dry years follow wet years where the water table is high, there is a net loss of water from the lens by deep-rooted vegetation and evaporation.

The estimated recharge during the period 1954 to 1991 for 40% and 20% of the vegetation cover is shown in Figures 3.9 and 3.10 respectively. It is obvious from these figures that the recharge increases with

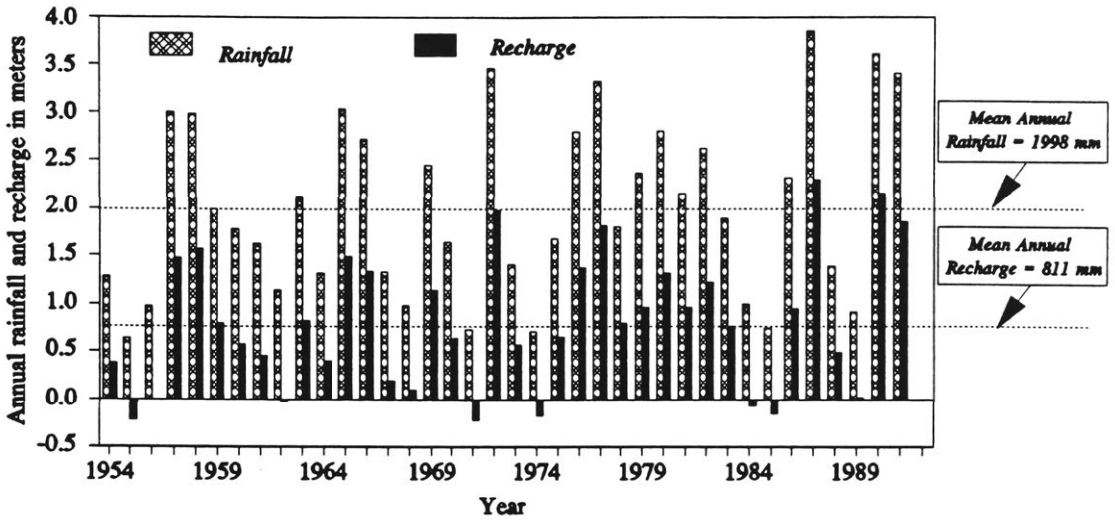

Figure 3.9 Annual recharge and rainfall on Bonriki during 1954 to 1991, for 40% vegetation cover (after Falkland [1992])

decreasing vegetation cover. A management strategy for increasing the sustainability of the freshwater lens is to reduce the amount of vegetation on Bonriki.

3.3 Calibration of the model

Despite the amount of data collected on Bonriki, Falkland (1992) found it necessary to calibrate the sharp interface single aquifer model. The single aquifer sharp interface model was calibrated by assuming that the recharge, shown in Figure 3.8, occurred uniformly over the entire area of the lens with no extraction due to pumping occurring. A computational time step, Δt = 30 days, which satisfies the stability criterion given by equation (3.4) and a value of 40 was used for the Ghyben-Herzberg ratio, α. The model parameters mean effective porosity and mean permeability were adjusted until there was a reasonable agreement between the simulated and observed lens thickness at borehole BN4.

No pumping was assumed because actual pumping from the freshwater lens on Bonriki commenced in 1987. The effect of pumping on the lens thickness is observed to occur several years after pumping commences. The duration of pumping was not considered sufficient on Bonriki to influence the thickness of the lens.

Borehole BN4 was chosen because the best data sets were available for this borehole. The data included the depth to the mid-point of the transition zone over the period from 1981 to 1990

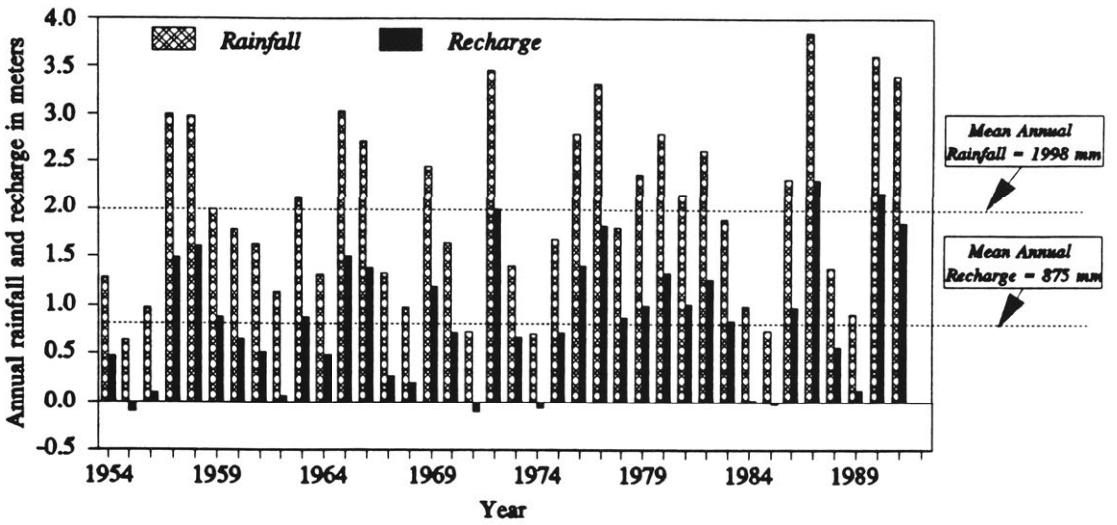

Figure 3.10 Annual recharge and rainfall on Bonriki during 1954 to 1991, for 20% vegetation cover (after Falkland [1992])

(beginning of 1981, 1985, 1986, 1988, 1989 and 1990) as shown in Figure 3.11.

The results from the calibrated model for the period 1954-1992 and the recorded lens thickness at borehole BN4 are also shown in Figure 3.11. There is close agreement between the modelled 'no pumping' curve with the recorded lens thickness.

The calibration parameters were the mean effective porosity $\beta = 0.4$ and the permeability $K = 14$ metres per day. Falkland (1992) also verified the calibrated values of specific yield and permeability with measurements of salinity at a number of other boreholes on Bonriki.

There is an apparent contradiction with the use of the Ghyben-Herzberg relationship which is a steady relationship in an unsteady flow model. The Ghyben-Herzberg relationship has been used in unsteady flow models by Chidley and Lloyd (1977), Anderson (1976), Hunt (1979), Llody *et al.* (1980), Ayres and Vacher (1983) and Vacher (1988). However, Herman *et al.* (1986) suggests that it may not be appropriate to base models of atoll islands on the Ghyben-Herzberg relationship because the horizontal flow assumption may be violated by tidal influences. It is acknowledged that models based on the Ghyben-Herzberg relationship are not appropriate if the short term behaviour of the lens is of interest because the Ghyben-Herzberg model depends on the long term balance between recharge and outflow of freshwater from the extraction and circumference of the island (Woodroffe [1989]). Ghassemi (1994) suggests that for the large time step used, the model results may be considered as steady over the interval Δt. The calibration results shown in Figure 3.11 suggest that the use of the Ghyben-Herzberg relationship in an unsteady flow model is valid for the time scale considered in this study.

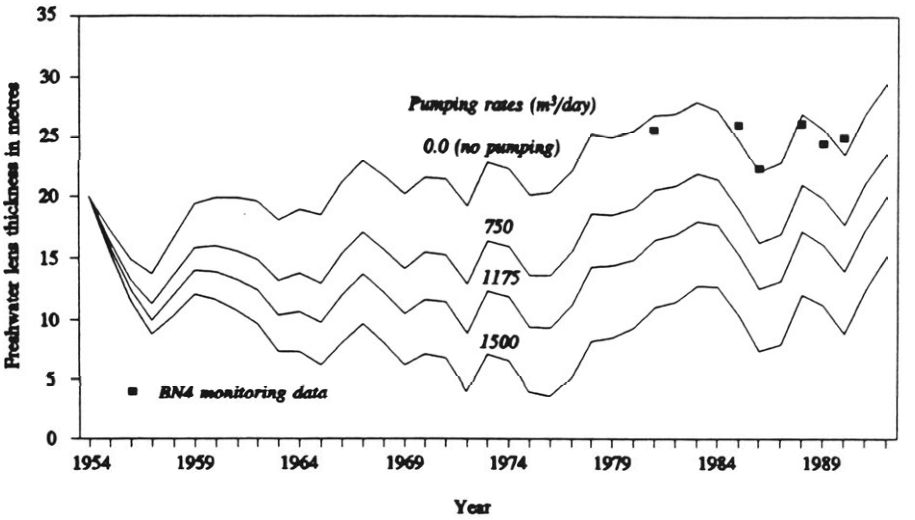

Figure 3.11 Observed and simulated lens thickness at borehole BN4 on Bonriki, for various pumping rates and 80% vegetation cover, during the period 1954-1992

Values of the aquifer properties permeability and porosity and the estimated recharge for Bonriki are consistent with those used for other atoll islands. Values for these parameters for other atoll islands can be found in Table 3.3.

Table 3.3 Atoll island aquifer characteristics from the Holocene (adapted from Underwood *et al.* [1992])

Atoll Island	Source	Permeability (m/d)	Measurement Type	Effective Porosity	Lens Thickness (m)	Maximum Thickness of the Lens (m)	Estimated Recharge Rate (m/yr)
South Keeling	*Falkland* (1994)	5-50			3-10	15	0.85
Tonga Tongatapu	*Hunt* (1979)	1296	field pump test			20	0.43
Nauru	*Ghassemi et al.* (1990)	900		0.3		4.7 (average) (potable) up to 7.0	0.54
Enewetak Enjebi	*Herman et al.* (1986)	60 (Holocene) 6000 (Pleistocene)		0.3	15 (Holocene) 200 (Pleistocene)		
Enewetak Enjebi	*Wheatcraft and Buddemeier* (1981)	54 30-75 60	field pump tests lab-permeameter	0.2	12-15	16-22	0.50
Tarawa Buota	*Lloyd et al.* (1980)	4.5 (average) 2.9-7.3	pumping test	0.1-0.15	5-10	15-23	1.30
Pingelap Deke	*Ayers and Vacher* (1986)	0.01-0.44 (0.11 average) 1.0-10.0	in situ permeameter reef-plate cores Holocene cores	0.15 (reef) 0.25 (Holocene)	15-25 17-24	14-22 (potable)	1.78
Majuro Laura	*Anthony* (1987)	(3.4 average) 60 (upper sediment) 60-600 (lower sediment)	grain-size analysis grain-size analysis				
Christmas Banana Village	*Falkland* (1983)	5.5 2-39	in situ permeameter	0.4		6-12 (potable)	0.12
Tarawa Bonriki	*Falkland* (1992)	14	in situ permeameter	0.4	10-24	29	0.7
Kwajalein Kwajalein	*Hunt and Peterson* (1980)	56-223 60-175	pump tests lab-permeameter		6-12	14-18 (potable)	1.17
Cocos Home Island	*Jacobson* (1976)					15 (potable)	0.50
Grand Cayman Island	*Chidley and Lloyd* (1977)	27.4 (average)				10-15	0.28
Bikini Eneu	*Underwood* (personal data)	35-70	lab-permeameter			8 (potable)	

Chapter 4.

Reliability analysis

There are a number of techniques for estimating uncertainties in a model response. These include the use of; (*i*) the *Mellin transform* (Epstein [1948], Park [1987] and Tung [1990]), (*ii*) *stochastic equations* (Unny [1984], Zielinski [1988], Tumeo and Orlob [1989] and Leduc *et al.* [1986, 1988]), (*iii*) *first-order analysis* (Sagar [1978], Dettinger and Wilson [1981], Scavia *et al.* [1981], Malone *et al.* [1983], Ang and Tang [1984], Townley and Wilson [1985] and Ünlü [1994]), (*iv*) the *point estimate method* (Evans [1967,1972], Rosenblueth [1975], Li and Lumb [1985], Harr [1989], Yen and Guymon [1990] and Zoppou and Li [1993]) and (*v*) *Monte Carlo simulation* (Freeze [1975], Smith and Freeze [1979a,b], Malone *et al.* [1983], Jones [1990] and Ünlü [1994]).

First-order methods were first used for water resources problems by Tang and Yen (1972). Subsequently they have been applied to the design of; (*i*) sewers by Tang *et al.* (1975) and by Yen and Tang (1976), (*ii*) culverts by Yen *et al.* (1980) and by Tung and Mays (1980) and (*iii*) levees by Tung and Mays (1981), Tung (1988) and Cesare (1991). It has been used; (*i*) in flood warning predictions by Yen and Tang (1977) and by Melching *et al.* (1991), (*ii*) for selecting rainfall-runoff models and (*iii*) by Melching and Yen (1986) to establish the influence of sewer slope on the capacity of a sewer. First-order analysis was used by; (*i*) Tung (1987) to establish the uncertainty of the United States National Weather Service rainfall frequency atlas, (*ii*) Chadderton *et al.* (1982) to provide a measure of uncertainty in a dissolved oxygen deficit model and (*iii*) Jaffe and Parker (1984) for the analysis of uncertainty in a simple first-order decay water quality model.

There are many examples of the use of Monte Carlo simulation in water resources problems. These include: (*i*) Burges and Lettenmier (1975) who analyzed the accuracy of a simplified Streeter-Phelps equation for dissolved oxygen and biochemical demand using both the Monte Carlo simulation and first-order second moment analysis. (*ii*) Scavia *et al.* (1981) who estimated the variance of a non-linear lake eutrophication model using Monte Carlo simulation and first-order second moment analysis. (*iii*) Garen and Burges (1981) who used both Monte Carlo simulation and first-order second moment analysis to determine the uncertainty in the results obtained from the Stanford Watershed model due to model input uncertainty. (*iv*) Huang (1986) who established the reliability of a trapezoidal open channel design to convey discharge controlled by sluice gates using both Monte Carlo simulation and first-order second-moment analysis. (*v*) Jones (1990) who used Monte Carlo simulation to estimate the statistical moments of the head in a confined groundwater flow in an aquifer subject to different pumping rates. (*vi*) Malone *et al.* (1983) who used Monte Carlo simulation, first-order analysis and the stochastic equation approach to analyze the effect of uncertainty of the phosphorous loading term on the long term phosphorous levels in Lake Washington.

There are few examples of the application of the point estimate method to water resources problems. These include: (*i*) Yen and Guymon (1990) who developed a probabilistic model of the water table elevations in an aquifer. (*ii*) Ünlü (1994) who used the point estimate method to establish the exceedence probability of contaminants in soil and groundwater downstream from a waste pit. (*iii*) Zoppou and Li (1993) who used the point estimate method to estimate the confidence limits of the

predicted water level in a backwater model.

Although the Mellin transform is well known, there are very few applications of the Mellin transform to water resources problems. Recently these have included; (*i*) Tung (1989) for estimating the uncertainty of travel time in open channel routing which was estimated using kinematic wave theory and (*ii*) Tung (1990) for the analysis of uncertainty of flood travel time and stormwater drain design (see also Zoppou and Li [1992]).

4.1 The Mellin transform

The mean, variance and higher statistical moments of the model response can be obtained using the Mellin transform. The technique has a number of limitations: (*i*) The model response must be an explicit function of the random variables, which is not always possible. (*ii*) The Mellin transform may not exist or is readily available for some functions (Park [1987]). (*iii*) The random variables are independent. (*iv*) The model response $Y = f(X)$ must have the multiplicative form

$$Y = f(X) = a_0 \prod_{i=1}^{k} x_i^{a_i}$$

in which $X = (x_1, x_2, \ldots, x_k)$ is a vector of random variables and $a_0, a_1, \ldots, a_k$ are constants. Clearly the problems considered in this thesis do not satisfy these conditions. Hydraulic and hydrologic problems that do satisfy these conditions can be found in Zoppou and Li (1992).

In practice, random variables encountered in hydraulics and hydrological problems are not independent. Random variables closer to each other tend to have similar properties rather than if they were farther apart. This is true for many spatial random variables encountered in water resources modelling. Therefore, only those techniques which are capable of handling correlated random variables will be considered. With the exception of the Mellin transform, all the above techniques are applicable to problems with correlated random variables.

4.2 Stochastic equations

Stochastic differential equations can be obtained by adding white Gaussian processes to each of the random variables in the deterministic equations used in the model. The use of Gaussian white noise to describe the uncertainty in the random variables facilitates the solution of the resulting equations. The equations can be transformed into a system of Itô differential equations (see, for example Zwillinger [1989]). The solution of the Itô differential equation is a Markov process and the joint probability density function of the random variables can be found using the Fokker-Plank equation (see, for example Zwillinger [1989]).

Alternatively, the mean and variance of the model response can be estimated from the Itô *lemma* in stochastic calculus. This is commonly referred to as the *moment equation* approach. The moment equation approach is not practical for large problems (Li and McLaughlin [1991]).

The perturbation method is another approach for deriving stochastic equations in which each random variable in the governing equations is expanded into a deterministic component and a fluctuating component. The deterministic component may be considered as the central tendency or the mean and the fluctuation, the variance or variation about the mean. This perturbation expansion of the governing

equations results in a system of stochastic equations. The stochastic equations are solved providing estimates of the mean and variance of the model response. These two moments do not entirely describe the distribution of the model response, except in the case of two parameter distributions such as the normal distribution.

Tumeo and Orlob (1989) employed the perturbation technique to estimate the first two moments of a biochemical oxygen demand and oxygen deficit model of the Sacramento River. Satish and Zhu (1994) described a stochastic analysis of a two-dimensional steady state ground-water flow model of a leaky aquifer using the perturbation based boundary element method. Zielinski (1988) developed a stochastic river water quality model based on the Streeter-Phelps model. The model was used to predict the dissolved oxygen in the Thames River, Ontario. The stochastic differential equations were derived using the moment equation approach. Leduc *et al.* (1986) used the Fokker-Plank equation to estimate the probability density function of a biochemical oxygen demand model and the moment equation approach to estimate the mean and variance of the model response. A stochastic biochemical oxygen demand model was developed by Leduc *et al.* (1988) for the Waterloo Pollution Control Plant. Leduc *et al.* (1988) used the moment equation approach to develop stochastic equations for this problem.

The basic assumption in the perturbation analysis is that the important information about the random variables of interest can be provided by the mean and variance. Therefore, in many stochastic equation methods, Gaussian distributions are assumed for the random variables (Tumeo and Orlob [1989]). The use of stochastic differential equations only provide estimates of the first two moments of the model response in many applications. This severely restricts the description of the model response to two parameter distributions. There is generally no closed form solution to stochastic differential equations. Complicated and numerically intensive algorithms are usually required (see, for example Satish and Zhu [1994]). The stochastic equation approach is an approximate technique. Alternative reliability techniques are capable of providing comparable results at a fraction of the computational effort. For example, Zoppou and Li (1994) used the point estimate method and produced results comparable to the analytical solution at a fraction of the computational effort required by the boundary integral stochastic model formulation of Satish and Zhu (1994).

The perturbation method and Monte Carlo simulation will generally not give the same results. The differences would be small only if the variability of the random variables is small (Li and McLaughlin [1991]). The Monte Carlo simulation is not limited by the small perturbation assumption or the assumption of Gaussian white noise description for the uncertainty in random variables.

Li and McLaughlin (1991) emphasize the fact that numerical limitations have greatly restricted the application of stochastic methods to real-world problems. Numerical methods for solving stochastic groundwater problems need to be made much more efficient if they are to have any practical value (Li and McLaughlin [1991]). Other approaches used in reliability analysis are currently preferred.

4.3 First-order analysis

First-order analysis is useful in obtaining approximations of the mean and variance of the model response. The basis of the first-order analysis is a truncated Taylor series expansion of the function $Y = f(x_1,x_2,\ldots,x_k)$ such that $E[f(X)] \simeq f(\mu_1,\mu_2,\ldots,\mu_k)$ (Hahn and Shapiro [1967], Garen and Burges [1981] and Yen *et al.* [1986]) and

$$\sigma^2[Y] \simeq \sum_{i=1}^{k}\sum_{j=1}^{k} \left.\frac{\partial f}{\partial x_i}\right|_{\mu_{x_1},\mu_{x_2},\ldots,\mu_{x_k}} \left.\frac{\partial f}{\partial x_j}\right|_{\mu_{x_1},\mu_{x_2},\ldots,\mu_{x_k}} \times \rho_{ij}\sigma_{x_i}\sigma_{x_j}. \tag{4.1}$$

in which μ_i is the mean value of parameter x_i, σ_{x_i} is the standard deviation of the parameter x_i, k is the number of random variables and ρ_{ij} is the correlation coefficient between x_i and x_j.

If the random variables x_i are uncorrelated, then

$$\sigma^2[Y] \simeq \sum_{i=1}^{k} \left[\left.\frac{\partial f}{\partial x_i}\right|_{\mu_{x_1},\mu_{x_2},\ldots,\mu_{x_k}} \right]^2 \times \sigma_{x_i}^2. \tag{4.2}$$

These relationships are exact if the function $f(X)$ is linear. Wood (1976) pointed out that in a nonlinear system, as watershed models generally are, first-order analysis may give incorrect values for the mean model response because $f(E[x]) \neq E[f(x)]$. The left side of the inequality represents the standard modelling procedure, whereas the right hand side represents the desired result. These two values can be significantly different in situations where the model response is highly nonlinear. If the model response is not linear then the variance of the random variables must be small to obtain reasonably accurate results from first-order analysis (Yen and Guymon [1990]).

The approximation of the mean model response in first-order analysis involves running a model with the mean values of the parameters, whereas the variance of the model response requires the evaluation of the derivatives in equations (4.1) or (4.2).

Analytical expressions for the derivatives of complex models are usually impossible to derive. The derivatives can however be approximated conveniently using finite differences. The standard finite difference approach involves incrementing each parameter of the model one at a time by some small amount Δx_i, and observing the change in the model response ΔY. The partial derivative of the model response with respect to the model parameter is approximated by $\Delta Y/\Delta x_i$.

Garen and Burges (1981) used a centered scheme involving the average of two perturbations $x_i + \Delta x_i$ and $x_i - \Delta x_i$, of each parameter to obtain a better estimate of the partial derivatives.

For a bivariate function $f(x,y)$, where $k = 2$, the $2k + 1$ model evaluations $f(\mu_x,\mu_y)$, $f(\mu_x + \Delta x,\mu_y)$, $f(\mu_x - \Delta x,\mu_y)$, $f(\mu_x,\mu_y + \Delta y)$ and $f(\mu_x,\mu_y - \Delta y)$ required by first-order analysis could be reduced to $k + 1$, $f(\mu_x,\mu_y)$, $f(\mu_x + \Delta x,\mu_y)$ and $f(\mu_x,\mu_y + \Delta y)$. However, there is some loss of accuracy if the partial derivatives for each parameter are approximated by the less accurate forward differences (see, for example Yen *et al.* [1986]).

Equations (4.1) or (4.2) can be used to estimate the model response variance once the partial derivatives for all parameters have been estimated. Approximate prediction limits of the model response can be estimated by assuming that the model response is described by a two parameter probability distribution.

First-order analysis is generally the simplest and involves significantly less computational effort than other reliability techniques involving correlated random variables.

There is another approach used by water resources managers for establishing the sensitivity of a model response to variations in the model parameters. This is commonly referred to as *sensitivity analysis*. This usually involves perturbing each model parameter independently and observing the response of the model response to the perturbation.

The first-order analysis can be considered intuitively to be a weighted sensitivity analysis with the sensitivity coefficient $\Delta f(x_i)/\Delta x_i$ weighted by the variance of x_i. This weighting coefficient is important in reliability analysis. Although the process may be insensitive to a perturbed parameter, the sensitivity coefficient multiplied by its variability, measured by $\sigma_{x_i}^2$, may have a significant influence on the outcome of the process. Although this is similar to first-order analysis, it treats each parameter independently and it fails to account for the correlation between the parameter values (Townley and Wilson [1985]). In addition, it ignores the effect of the variability of the model parameter on the model response. Therefore, simple sensitivity analysis is an inadequate technique for estimating the effect of uncertainty in the model parameters on the model response.

4.4 Point estimate method

Point estimate methods refer to those methods which enable the statistical moments of a random function $Y = f(\boldsymbol{X})$ to be calculated using the values of $Y = f(\boldsymbol{X})$ at a specified set of values of $\boldsymbol{X}$. Point estimate methods may be more convenient than other reliability techniques, as neither the calculation of derivatives nor the explicit formulation of the function $Y = f(\boldsymbol{X})$ is required (Li and Lumb [1985]). The latter is very difficult to attempt for complex models that are used in hydrology and hydraulics.

The point estimate method developed by Evans (1967,1972) is of limited use because it assumes that the random variables are independent. Rosenblueth (1975,1981) developed a two-point estimate method for correlated random variables. The joint probability density of $\boldsymbol{X}$ in this method is assumed to be concentrated at points in the 2^k hyperquadrants of the space defined by $\boldsymbol{X}$. The expected value of $Y = f(\boldsymbol{X})$ is obtained by summing the product of $f(\boldsymbol{X})$ and the probability content of $\boldsymbol{X}$ for all $\boldsymbol{X}$ in the 2^k hyperquadrants. Rosenblueth's method involves 2^k evaluations of $f(\boldsymbol{X})$. As the number of evaluations increases exponentially with k, the method becomes computationally prohibitive when k is large.

The exact expected value can only be obtained in Rosenblueth's point estimate method if the first- and second-order statistical moments of the random variables are known and $Y = f(\boldsymbol{X})$ is a quadratic polynomial expressed in the general form (Li [1991])

$$Y = f(\boldsymbol{X}) = f(\boldsymbol{\mu}) + \sum_i a_i(x_i - \mu_i) + \sum_i b_i(x_i - \mu_i)^2 + \sum_{ij} c_{ij}(x_i - \mu_i)(x_j - \mu_j) \qquad (4.3)$$

where μ_i is the mean value of x_i, $\boldsymbol{\mu} = (\mu_1,\mu_2,\ldots,\mu_k)$ for a function of k variables and a_i,b_i and c_{ij} are coefficients.

Taking expectation on both sides of equation (4.3), then

$$E[f(\boldsymbol{X})] = f(\boldsymbol{\mu}) + \sum_i b_i\sigma_i^2 + \sum_{ij} c_{ij}\sigma_i\sigma_j\rho_{ij} \tag{4.4}$$

where σ_i is the standard deviation of x_i and ρ_{ij} is the correlation coefficient between x_i and x_j.

If $f(..,\pm,...,\pm,...) = f(..,\mu_i\pm\sigma_i,...,\mu_j\pm\sigma_j,...)$, it can be shown that

$$f(\boldsymbol{\mu}) + \sum_i b_i\sigma_i^2 = \frac{1}{2^k}\sum_{p=0}^{1}\sum_{q=0}^{1}..\sum_{s=0}^{1} f((-1)^p,..,(-1)^q,....,(-1)^s) \tag{4.5}$$

$$c_{ij}\sigma_i\sigma_j = \frac{1}{2^k}\sum_{p=0}^{1}\sum_{q=0}^{1}..\sum_{s=0}^{1} \eta f(-1)^p,..,(-1)^q,..,(-1)^s) \tag{4.6}$$

where $\eta = 1$ if $q + r$ is even and $\eta = -1$ if $q + r$ is odd.

Substituting equations (4.5) and (4.6) into equation (4.4) yields the two-point estimate method developed by Rosenblueth (1975) for multivariate functions. The procedure described by equations (4.5) and (4.6) is not an efficient way for obtaining the different terms in equation (4.4) as it requires a total of 2^k evaluations of $f(\boldsymbol{X})$.

The modified point estimate method by Harr (1989) is an extension of Rosenblueth's 2-point estimate method. Although more efficient than Rosenblueth's method, it only provides estimates of the expected value and standard deviation and is only applicable to independent random variables.

A relatively new point estimate method was developed by Li (1992) which has the same order of accuracy as Rosenblueth's two-point estimate method for multivariate functions, but it is more efficient because it requires fewer evaluations of $f(\boldsymbol{X})$.

The more efficient new point estimate method can be obtained using the following procedure.

Define $f_i(x_i) = f(\mu_1,..,\mu_{i-1},x_i,\mu_{i+1},..,\mu_k)$. According to equation (4.3), $f_i(x_i)$ can be expressed as

$$f_i(x_i) = f(\boldsymbol{\mu}) + a_i(x_i - \mu_i) + b_i(x_i - \mu_i)^2. \tag{4.7}$$

Since $f_i(x_i)$ is a quadratic function in x_i, application of the two-point estimate method developed by Rosenblueth (1975) for a univariate function to equation (4.7) will yield the exact expectation of $f_i(x_i)$.

Therefore,

$$E[f_i(x_i)] = \frac{1}{2}[f_i(x_i^-) + f_i(x_i^+)] = f(\boldsymbol{\mu}) + b_i\sigma_i^2 \tag{4.8}$$

where $x_i^+ = \mu_i + \sigma_i$, $x_i^- = \mu_i - \sigma_i$. Summing equation (4.8) for all i, then

$$f(\boldsymbol{\mu}) + \sum_i b_i\sigma_i^2 = (1 - k)f(\boldsymbol{\mu}) + \frac{1}{2}\sum_i [f_i(x_i^+) + f_i(x_i^-)]. \tag{4.9}$$

Equation (4.9) gives the first two terms on the right hand side of equation (4.4). To obtain the last term in equation (4.4), it is necessary to calculate the coefficient c_{ij}. It can be shown that $c_{ij} = \partial^2 f(\boldsymbol{X})/\partial x_i\partial x_j$ for a quadratic function. This derivative can be approximated by the following finite difference formula

$$c_{ij} = \frac{f_{ij}(x_i^+, x_j^+) - f_i(x_i^+) - f_j(x_j^+) + f(\mu)}{\sigma_i \sigma_j} \tag{4.10}$$

where $f_{ij}(x_i^+, x_j^+) = f(\mu_1, .., \mu_{i-1}, x_i^+, .., \mu_{j-1}, x_j^+, .., \mu_n)$. Substituting the results of equations (4.9) and (4.10) into equation (4.4), the following formula is obtained.

$$E[f(X)] = (1 - \frac{3k}{2} + \frac{\rho}{2}) f(\mu) + \frac{1}{2}\sum_i [(3 - 2\rho_i) f_i(x_i^+) + f_i(x_i^-)] + \sum_{i<j} f_{ij}(x_i^+, x_j^+)\rho_{ij} \tag{4.11}$$

where

$$\rho_i = \sum_j \rho_{ij}, \quad \rho = \sum_i \rho_i \quad \text{and} \quad \rho_{ii} = 1 \quad \text{by definition.}$$

Higher-order statistical moment of $f(X)$ can be computed using

$$\begin{aligned} E[(f(X) - \mu)^2] &= E[f(X)^2] - E[f(X)]^2 \\ E[(f(X) - \mu)^3] &= E[f(X)^3] - 3E[f(X)]E[f(X)^2] + 2E[f(X)^3] \\ E[(f(X) - \mu)^4] &= E[f(X)^4] - 4E[f(X)]E[f(X)^3] + 6E[f(X)^2]E[f(X)^2] - 3E[f(X)]^4 \end{aligned} \tag{4.12}$$

with $E[f(X)^r]$ obtained from equation (4.11) and where $\sigma = (E[x - \mu)^2])^{1/2}$, $\vartheta = E[(x - \mu)^3]/\sigma^3$ and $\varsigma = E[(x - \mu)^4]/\sigma^4$.

If the random variables are independent, equation (4.11) can be simplified to the following point estimate method which only requires $2k + 1$ evaluations of $f(X)$.

$$E[f(X)] = (1 - k) f(\mu) + \frac{1}{2}\sum_i [f_i(x_i^+) + f_i(x_i^-)]. \tag{4.13}$$

Equation (4.11) requires $(k^2 + 3k + 2)/2$ evaluations of $Y = f(X)$ as compared to 2^k evaluations for Rosenblueth's two-point estimate method. The proposed second-order point estimate method is more efficient than Rosenblueth's method for $k > 3$, but not as efficient as the first-order analysis. It is as accurate as Rosenblueth's two-point point estimate method. With a moderate number of variables it is potentially more efficient than Monte Carlo simulation in many practical problems. It provides an exact expected value for a quadratic polynomial and an exact variance for a linear polynomial.

Equation (4.11) assumes that only the mean and variance of x_i are known. If higher statistical moments are known for x_i, then the following fourth-order accurate expression is more accurate than equation (4.11).

$$\begin{aligned} E[f(X)] &= (1 - \frac{3k}{2} + \frac{\rho}{2} + \sum_i \omega_i^0) f(\mu) \\ &+ \sum_i [(\omega_i^+ - \rho_i + 1) f_i(x_i^+) + \sum_{i<j} f_{ij}(x_i^+, x_j^+)\rho_{ij} \end{aligned} \tag{4.14}$$

in which

$$x_i^+ = \mu_i + \alpha_i^+ \sigma_i, \qquad x_i^- = \mu_i + \alpha_i^+ \sigma_i,$$

$$\omega^+ = \frac{1}{\alpha^+(\alpha^+ - \alpha^-)}, \qquad \omega^- = \frac{1}{\alpha^-(\alpha^- - \alpha^+)} \tag{4.15}$$

and $\omega^0 = 1 - \omega^+ - \omega^-$.

The coefficients $\alpha^\pm$ are estimated using

$$\alpha^+ = \frac{\upsilon + \sqrt{4\zeta - 3\upsilon^2}}{2} \quad \text{and} \quad \alpha^- = \frac{\upsilon - \sqrt{4\zeta - 3\upsilon^2}}{2}. \tag{4.16}$$

In equation (4.11) $\alpha^+ = \alpha^- = 1$.

Equation (4.15) is more accurate than Rosenblueth's method because the former gives an exact expected value of a fourth-order multivariate polynomial, while the latter can only give an exact answer for a multivariate quadratic polynomial. It will provide exact variance for a second-order polynomial and exact skewness and kurtosis for a linear function.

There is no need to generate realizations for the random variables in the point estimate method. The correlation structure of the process is considered explicitly in equation (4.11). No assumption has been made about the distributions of the random variables in deriving equation (4.11). It is applicable to both Gaussian and non-Gaussian random variables.

The point estimate method is very efficient for a moderate number of random variables. For problems with a large number of random variables and for higher-dimensional problems, the number of function evaluations may be prohibitive. In addition, the point estimate method may not provide accurate estimates of the statistical moments if the model response is highly nonlinear (Yen and Guymon [1990]). Estimates of the expected value and standard deviation of the model response may not be sufficient to characterize it for highly nonlinear problems.

The point estimate method only provides approximations of the moments of the model response. It is necessary to assume or fit a suitable distribution to these moments if the prediction limits are required.

4.5 Curve fitting

The exact probability density of the model response is difficult to determine. However, if the moments of the model response are available, it is possible to fit a distribution to these moments and the prediction limits of the model response can be inferred from the fitted distribution. This procedure is known as *curve fitting*, see Figure 4.1.

Only the statistical moments of the model response are estimated in the first-order analysis, the point estimate method, the method of moments, perturbation and the Mellin transform (for independent random variables). The first-order analysis only provides estimates of the mean and variance of the model response. Therefore, only two parameter distributions can be fitted. Generally the normal distribution is chosen. For many hydraulic and hydrologic models these two moments may not be adequate to describe the model response. This is particularly true if the model response is nonlinear, which may result in a skewed distribution for the model response. Higher-order moments are required in this case. It is possible to estimate these moments using the point estimate method and the Mellin transform. These moments can be used to fit more general distributions which include the normal distribution to the model response.

moments using the point estimate method and the Mellin transform. These moments can be used to fit more general distributions which include the normal distribution to the model response.

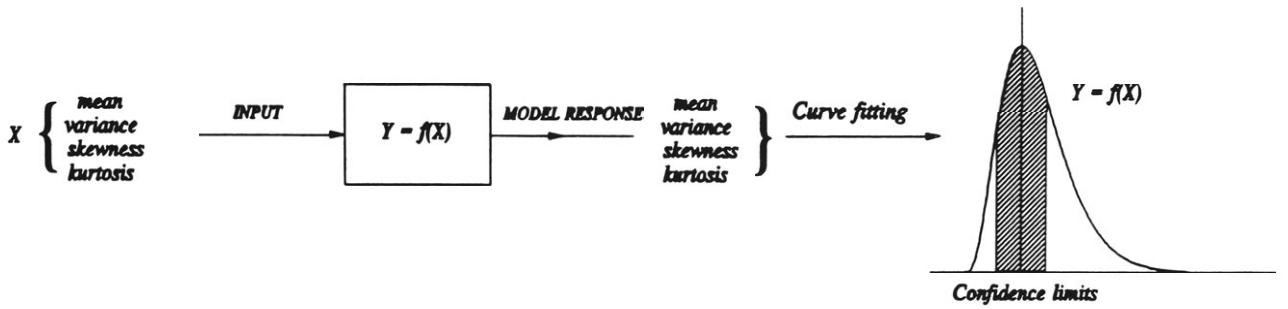

Figure 4.1 Estimating the probability density function for the model response, $Y = f(X)$, using higher-order moments

The probability density functions of many continuous probability distributions can be described as solutions of the differential equation (Kendall *et al.* [1987])

$$\frac{df(x)}{dx} = \frac{(x - b_0)f(x)}{b_1 + b_2x + b_3x^2}. \tag{4.17}$$

Solving this equation will produce the probability density function $f(x)$ for the random variable x. The parameters b_i ($i = 0, 1, 2, 3$) are functions of the first four statistical moments of the distribution.

The distributions defined by equation (4.17) can be classified according to the nature of the roots of its denominator.

The Pearson family of frequency curves, which is defined uniquely by the first four statistical moments, are derived from this differential equation. Twelve types of distributions can be described by Pearson distributions, for example, the Pearson Type III distribution is equivalent to the Gamma distribution. The Pearson Type I, II and VI distributions are forms of the Beta distribution and the normal distribution is a member of the Pearson family. Solomon and Stephens (1978) showed that the Pearson distribution gives an excellent approximation to the long tail of a distribution when the first four moments are known exactly.

The relationship between the numerous distributions within the Pearson family can be established given the skewness and kurtosis (see, for example Li and Lumb [1985]).

Another family of curves attempts to transform one distribution to a more convenient distribution. Johnson curves attempt to transform the distribution to normality. There are three types of Johnson curves (Johnson [1949]);

(*i*) S_L (the lognormal system), where the standardized normal variable is given by

$$z = \zeta + \delta \ln\left[\frac{x - \xi}{\lambda}\right] \quad \text{for} \quad \xi < x,$$

(*ii*) S_U (unbounded system), where the standardized normal variable is defined by

$$z = \zeta + \delta \sinh^{-1}\left[\frac{x - \xi}{\lambda}\right] \quad \text{and}$$

(*iii*) S_B (bounded system), where the standardized normal variable is expressed as

$$z = \zeta + \delta \ln\left[\frac{x - \xi}{\xi + \lambda - x}\right] \quad \text{for} \quad \xi < x < \xi + \lambda.$$

The parameters ζ, ξ, δ, and λ are chosen so that z is approximately normal.

The most appropriate transformation depends on the skewness and kurtosis (see, for example Kendall *et al.* [1987]). Hill *et al.* (1976) developed an algorithm for fitting Johnson curves given the first four statistical moments of a probability density function.

4.6 Monte Carlo simulation

Monte Carlo simulation involves executing the hydraulic or hydrological model repeatedly, with each run containing a new set of randomly sampled parameters. The results from a large number of runs are combined to provide an approximation of the probability distribution of the model response, which may provide some insight into the model's behaviour.

Once the distribution of each independent variable is established in the Monte Carlo simulation, a pseudo-random number is generated for each dependant variable and a sample value for the model response $Y = f(X)$ is determined.

Suppose that m samples are simulated, then using the *law of large numbers*, the probability distribution for $Y = f(X)$ can be estimated and the probability that the model response is less than some limit Z is given by

$$p_f = Pr(Y = f(X) \leq Z) = \lim_{m \to \infty} \frac{k}{m}$$

where k is the number of trials in which $Y = f(X) \leq Z$. p_f is commonly known as the *probability of failure* of the hydraulic system.

Establishing the number of samples required to define a density function of the model response in Monte Carlo simulation is very difficult and considered an art by Burges and Lettenmaier (1975). Very large samples are required in some problems. This increases with increasing variance and skewness of the distribution. Scavia *et al.* (1981) used 1,000 samples in their Monte Carlo simulation of a lake eutrophication model which contained seven parameters. Huang (1986) used 2,000 samples in the Monte Carlo simulation of flow in a trapezoidal channel controlled by sluice gates. There were eleven independent variables in their study. Wallis *et al.* (1974) found that for skewness coefficients greater than five, 100,000 samples were inadequate to describe the tails of the distribution beyond the 99.9% probability level. Monte Carlo simulation can be computationally expensive when the probability of failure of the hydraulic system is small (Yen *et al.* [1986]). Burges and Lettenmaier

The sample size is problem dependent. An adequate sample size can be established by estimating the probability density function of the model response for a number of sample sizes and by selecting a sample size which produces very little improvement in the estimated probability density function. However, this may not ensure that an optimum sample size has been selected. Robinson and Maul (1991) observed a false plateau in the estimated risk associated with the geological disposal of radioactive wastes using Monte Carlo simulation and various sample sizes. They were able to obtain an analytical solution for this problem using the Laplace transform. Without the analytical solution, the sample size in the region of the false plateau may have been interpreted as the converged result. The sample size was increased by at least an order of magnitude in order to produce an acceptable estimate of the true risk associated with the disposal of the radioactive waste. Unfortunately an exact solution to a problem is seldom available. Therefore, it may be necessary to use an independent reliability method to verify the parameters and the results used in another.

All the methods described in this chapter may yield similar estimates of average values of the model response, however variance estimates can be quite different. Scavia *et al.* (1981) point out that the first-order analysis estimates the variability about a single sample from the population, while Monte Carlo simulation estimates the variance of the population, or the expected variability in the system. They further suggest that Monte Carlo simulation represents the *truth* and can be used to check the accuracy of other reliability techniques. Another major advantage is that unlike other reliability techniques, knowledge of the form of the probability density function for the model response, $Y = f(X)$ is not required.

Monte Carlo simulation is a powerful technique and intuitively appealing (see, for example Schweppe [1973]). Fewer assumptions are made in Monte Carlo simulation in comparison to other reliability methods. It is a very flexible method that can be applied to solve a wide variety of problems.

A deficiency of the Monte Carlo method is that the probability density function of the independent variables must be known or assumed. This may not be possible if there is insufficient data to establish these distributions. However, this problem also arises in other methods.

The model input parameters are usually positively correlated in many water resources problems. Zoppou and Li (1993) have shown that ignoring spatial correlation between the random variables has a significant influence on the predicted model response. Standard Monte Carlo simulation techniques are not capable of incorporating correlations between the random variables because they rely on random sampling from independent probability distributions. Unless realizations of correlated spatially random variables can be generated, Monte Carlo simulation cannot be used to determine the effect of uncertainties on a model's response. The next chapter has been devoted to the generation of spatially correlated random fields.

Chapter 5.

Generation of spatial random fields

Consider a spatially variable quantity x, which is a function of spatial co-ordinate $\mathbf{t}$, where $\mathbf{t}$ is the one- two- or three-dimensional location vector. The function $x(\mathbf{t})$ is not known everywhere, but is generally estimated from available data. However, the data is one sample from an infinite collection of possible data sets. The ensemble of these infinite data sets or functions defines a *spatial stochastic process*.

Instead of specifying all possible functions $x(\mathbf{t})$, it is more convenient to define the ensemble by statistical moments. It is possible to reconstruct the spatial function $x(\mathbf{t})$ with these statistical moments. *Random field generators* provide a means of using the statistical information of a spatial stochastic process to generate the spatial function $x(\mathbf{t})$. The grid of generated spatially random values is known as a *random field* and the individual values are known as *realizations*. A random field generator can produce a large number of unique random fields, each having equal likelihood of occurrence, which can be used in Monte Carlo simulation.

Aquifer properties are usually described on a rectilinear grid in space in many groundwater models. In practice however, aquifer characteristics are usually measured over a limited region on a nonuniform grid. A major advantage of random field generators is that they provide a means of using statistical information gathered for a random variable at a few sites to generate values for that spatially random variable on a uniform grid.

Current approaches to generating random fields usually involve the generation of a Gaussian random field. To fully define a Gaussian random field only the mean at each point and the covariance function at each pair of points is required. Assuming a Gaussian process considerably simplifies the stochastic problem (Hasofer [1993]).

5.1 Second-order stationary process

The first two statistical moments of a Gaussian random field are defined as the *mean* (first moment) which gives the expected value at any point $\mathbf{t}$

$$E[x(\mathbf{t})] = \overline{x(\mathbf{t})}$$

and the *covariance* function (second moment) between the values $x(\mathbf{t}_1)$ and $x(\mathbf{t}_2)$, located at $\mathbf{t}_1$ and $\mathbf{t}_2$ respectively, is given by

$$\gamma(\mathbf{t}_1,\mathbf{t}_2) = E[(x(\mathbf{t}_1) - \overline{x(\mathbf{t}_1)})(x(\mathbf{t}_2) - \overline{x(\mathbf{t}_2)})].$$

The covariance represents the degree of linear association of the random variable at two different locations $\mathbf{t}_1$ and $\mathbf{t}_2$.

When $t_1 = t_2$ then

$$\gamma(t_1,t_2) = \sigma^2(t)$$

which is the variance. The relationship

$$\rho(t_1,t_2) = \frac{\gamma(t_1,t_2)}{\sigma(t_1)\sigma(t_2)}$$

is the *correlation coefficient* between $x(t_1)$ and $x(t_2)$.

The term correlation function is often used synonymously with covariance function, however they are different. Covariance is an established statistical term and correlation is a normalized quantity within the range $-1 \leq \rho(t_1,t_2) \leq 1$.

These moments are not known in practice and must be deduced from the data or from previous experience. *Stationarity* and *isotropy* are simplifications which assist in estimating statistical moments from the measured data.

Stationarity assumes that the mean and variance are constant and the correlation between any two observations $x(t_1)$ and $x(t_2)$ depends only on their relative location in space, $t_1 - t_2$. This can be expressed mathematically as

$$E[x(t)] = \mu \quad \text{and} \quad E[(x(t_1) - \mu)(x(t_2) - \mu)] = \gamma(t_1,t_2).$$

Isotropy assumes that the covariance function depends only on the separation distance and not on the direction of the separation vector. Therefore,

$$E[(x(t_1) - \mu)(x(t_2) - \mu)] = \gamma(|t_1 - t_2|)$$

in which $|t_1 - t_2|$ is the separation distance. If these conditions are satisfied then the stochastic process is called a *second-order stationary process*.

5.2 Covariance functions

The covariance function should decrease to zero for large separation distances because spatial random variables in water resources problems tend to have similar properties if they are closer together than farther apart.

Several covariance functions have been used in water resources modelling (see, for example Bras and Rodríguez-Iturbe [1976a,b]). They include the following one-dimensional covariance functions;

(i) Exponential function

$$\gamma(V) = \sigma^2 \exp\left[\frac{-|V|}{V_0}\right]$$

(ii) Quadratic exponential or Gaussian function

$$\gamma(V) = \sigma^2 \exp\left[\frac{-V^2}{V_0^2}\right]$$

(*iii*) *Whittle or Bessel function*

$$\gamma(V) = \sigma^2 \frac{V}{V_0} K_1 \left[\frac{V}{V_0} \right]$$

(*iv*) *Power model*

$$\gamma(V) = \begin{cases} \sigma^2 \left[1 - \frac{|V|}{V_0} \right]^{\alpha} & \text{for } 0 \leq V \leq V_0 \\ 0 & V > V_0 \end{cases}$$

(*v*) *Spherical model*

$$\gamma(V) = \begin{cases} \sigma^2 \left[1 - \frac{3}{2}\frac{V}{V_0} + \frac{1}{2}\frac{V^3}{V_0^3} \right] & \text{for } 0 \leq V \leq V_0 \\ 0 & V > V_0 \end{cases}$$

(*vi*) *Hole-effect model*

$$\gamma(V) = \sigma^2 \left[1 - \frac{V}{V_0} \right] exp \left[-\frac{V}{V_0} \right]$$

where, $\alpha > 0$ is an arbitrary constant, V is the separation distance $|\mathbf{t}_i - \mathbf{t}_j|$ between the random variables in the random field, $V_0 > 0$ is the *correlation distance* also known as the *integral scale*, K_1 is a first-order modified Bessel function of the second kind and σ is the standard deviation.

A plot of the above covariance functions can be found in Figure 5.1. These curves were produced using $V_0 = 1.0$, $\alpha = 1.0$, $0 \leq V \leq 100$ and $\sigma = 1$. Other examples of covariance functions can be found in Vanmarcke and Grigoriu (1983).

The correlation distance reflects how the relationship between values of the random variable depends on distance. A large value of V_0 implies that the random variable is correlated over a large spatial extent. The random variables become perfectly correlated $\rho_{ij} = 1$, as $V_0 \rightarrow \infty$ and the random field model degenerates into the single-random-variable approach.

The most commonly used covariance function used in water resources problems is the exponential function. This is not because data in water resources problems have been found to exhibit exponential covariance properties. Instead it is chosen because it is a simple covariance function to evaluate. Bras and Rodríguez-Iturbe (1976a,b) recommend the use of the Bessel type or the single exponential type covariance function and caution the use of the quadratic exponential covariance function.

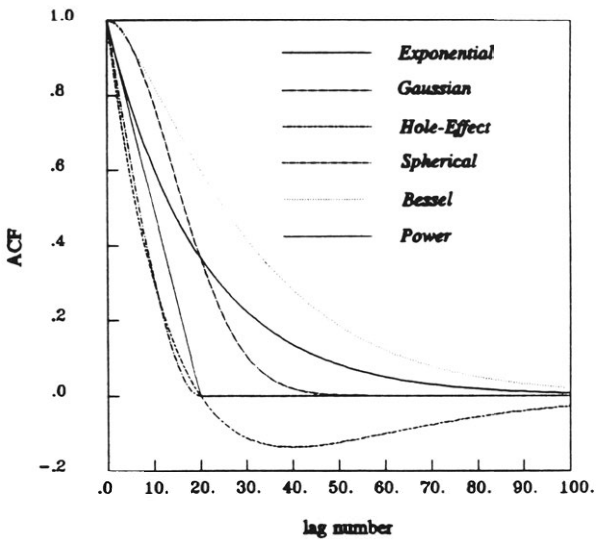

Figure 5.1 Well known correlation functions used in hydrology

5.3 Generation of Gaussian realizations

The problem is how to generate realizations with a given probability distribution and covariance structure efficiently. There are a number of techniques suitable for generating the realization of a homogenous stationary Gaussian scaler random process, which attempt to preserve the covariance structure. These include; (*i*) *matrix decomposition*, (*ii*) *spectral*, (*iii*) the *nearest neighborhood approach*, (*iv*) *turning bands* and (*v*) the *circulant embedding approach.*

5.3.1 Matrix decomposition

A k-dimensional multivariate normal distribution, with mean $\mu = (\mu_1,\mu_2,\ldots,\mu_k)^T$ and covariance matrix $\boldsymbol{D}$, has the joint density function given by Larson (1973) as

$$f(\boldsymbol{X}) = \frac{|\boldsymbol{D}|^{-1/2}}{(2\pi)^{k/2}} exp\left[\frac{[-(\boldsymbol{X} - \mu)^T\boldsymbol{D}^{-1}(\boldsymbol{X} - \mu)]}{2}\right]$$

where $\boldsymbol{X} = (x_1,x_2,\ldots,x_k)^T$ are the random variables, $|\boldsymbol{D}|$ is the determinant of $\boldsymbol{D}$, k is the number of realizations required and the superscript T denotes transpose.

Since the covariance matrix is symmetric and positive-definite, it can be written as $\boldsymbol{D} = \boldsymbol{B}\boldsymbol{B}^T$, where, $\boldsymbol{B}$ is a $k \times k$ lower tridiagonal matrix. If $\boldsymbol{Z}^T = (z_1,z_2,\ldots,z_k)$ are *iid* $N(0,1)$ distributed variables, then $\boldsymbol{X}$ can be represented as (Fishman [1978])

$$\boldsymbol{X} = \boldsymbol{B}\cdot\boldsymbol{Z} + \mu. \tag{5.1}$$

The decomposition of $\boldsymbol{D}$ can be performed by standard techniques such as the *bordering technique* (George and Liu [1981]), which is also known as Cholesky decomposition. After $\boldsymbol{B}$ is computed, then from equation (5.1)

$$x_i = \mu_i + \sum_{j=1}^{i} B_{ij} z_j \quad \text{for } i = 1,\ldots,k.$$

No approximations have been assumed in generating realizations of x_i. Matrix decomposition via Cholesky factorization is exact and does not require stationarity. It is only necessary are evaluate the covariance $\boldsymbol{D}$ and it is applicable to problems of any dimension. The only restriction are computational resources. The number of floating point operations required by this method for one-dimensional problems are $O(k^3)$ and the storage requirement is $O(k^2)$. The prohibitively large storage requirements of matrix methods for moderate values of k prevent their generalized use. This is particularly valid for two- and three-dimensional problems. For example, the current best algorithms for triangularization of a correlation matrix (see for example Dietrich [1993]) required to generate a random field on a two-dimensional rectangular grid $p \times q$, require at least $O(p^3q^2)$ floating point operations. Even with a modest grid size the computational resources are very demanding. For this reason multi-dimensional simulations are usually generated by alternative methods.

Matrix decomposition has been used recently by Touran and Wiser (1992) to estimate the total cost variance of a construction project. It has also been used in a Monte Carlo simulation model of one-dimensional groundwater flow in a nonuniform homogeneous media by Freeze (1975). The three parameters; (*i*) hydraulic conductivity, (*ii*) porosity and (*iii*) compressibility were considered as correlated and normally distributed, however they were not spatially correlated.

5.3.2 Spectral method

A stationary process can also be described by its mean, variance and *spectral density function*. The normalized spectral density function is the Fourier transform of the correlation function, which is mathematically equivalent (see for example Box and Jenkins [1976] and Chatfield [1989]). Therefore, the spectral representation of a homogeneous and isotropic random field provides a means of generating sample functions of that field when its' spectral density function is known.

The one-dimensional random field can be generated using the classical spectral method described by Rice (1954) and improved by Shinozuka and Jan (1972). Other methods have been proposed by Shinozuka (1971) and Mejía and Rodríguez-Iturbe (1974).

Mejía and Rodríguez-Iturbe (1974) derived the following equation for the generation of a spatial random process using spectral theory

$$x(\mathbf{t}) = \left[\frac{2}{N'}\right]^{1/2} \sum_{m=1}^{N'} Cos[\omega_m(\mathbf{t}^T \cdot y_m) + \phi_m] \tag{5.2}$$

in which $\mathbf{t}$ represents a vector of co-ordinates $(\mathbf{t}_1,\mathbf{t}_2,\ldots,\mathbf{t}_d)$ in $\mathbb{R}^d$, y_m is an d-dimensional random variable $(y_{m1},y_{m2},\ldots,y_{md})$ uniformly distributed on a unit surface in d-dimensional space $\mathbb{R}^d$, ω_i is a random variable whose distribution is the *radial spectral distribution function*, $G(\omega)$ corresponds to the isotropic correlation function of $x(\mathbf{t})$, ϕ_m is a uniformly distributed random angle between 0 and 2π, $(\mathbf{t}^T \cdot y_m)$ denotes the vector inner product and N' is the finite number of harmonics.

Mejía and Rodríguez-Iturbe (1974) have shown that the above process is homogeneous and isotropic as $N' \to \infty$. It is also a Gaussian process with zero mean, unit variance and as $N' \to \infty$ it has a correlation function with radial spectral distribution corresponding to $G(w)$.

A general family of isotropic random process is characterized by the correlation function (Mejía and Rodríguez-Iturbe [1974]).

$$\rho(t) = 2\left[\frac{|t|}{2V_0}\right]^{s-d/2} K_{s-d/2}\left[\frac{|t|}{V_0}\right]\left[\Gamma\left[s - \frac{d}{2}\right]\right]^{-1} \tag{5.3}$$

in which K is the modified Bessel function of the second kind, d is the dimension of the process, s is the degrees of freedom, V_0 is the correlation distance and $|t| = (t_1^2 + t_2^2 + \ldots + t_d^2)^{1/2}$.

The spectral density of equation (5.3) is given by

$$f(\omega) = a\left(1 + \omega^2 V_0^2\right)^{-s}$$

where a is a constant and ω is some point on $\mathbf{R}^d$.

The radial density function is related to the spectral density by (Mejía and Rodrígueze-Iturbe [1974] and Bras and Rodrígueze-Iturbe [1985])

$$G'(\omega) = \frac{f(\omega)2\pi^{d/2}\omega^{d-1}}{\Gamma(d/2)}$$

therefore

$$G'(\omega) = a\frac{\omega^{d-1}}{\left[1 + (\omega^2 V_0^2)\right]^s}.$$

When $s = (d+1)/2$ then $\rho(V) = exp(-|V|/V_0)$, which is the classical exponential decaying correlation function. It can be used in one- two- or three-dimensions. For a process varying over an area $d = 2$, then

$$G'(\omega) = \frac{\omega V_0^2}{\left[1 + (\omega^2 V_0^2)\right]^{3/2}} \quad \text{for } 0 \leq \omega \leq \infty$$

and

$$G(\omega) = 1 - \frac{1}{\left[1 + (\omega^2 V_0^2)\right]^{1/2}} \quad \text{for } 0 \leq \omega \leq \infty.$$

For $d = 1$, the radial density function for a one-dimensional or line process is given by

$$G'(\omega) = \frac{1}{1 + (\omega^2 V_0^2)} \quad \text{for } 0 \leq \omega \leq \infty.$$

which is the derivative of the radial spectral distribution function

$$G(\omega) = \frac{Tan^{-1}(\omega V_0)}{V_0} \quad \text{for } 0 \leq \omega \leq \infty.$$

A major advantage of the correspondence between the radial spectral distribution and a given correlation function is that it allows sampling the random variable ω by the inverse method. Generating uniformly distributed values between 0 and 1 and their substitution for $G(\omega)$ results in a series of ω values belonging to the population defined by the radial spectral density and distribution function.

A set of commonly used isotropic correlation functions are; (*i*) single exponential, (*ii*) quadratic

exponential and (*iii*) Bessel form. The corresponding radial spectral density functions and distributions for these and other correlation functions are given by Mejía and Rodríguez-Iturbe (1974) and Mantoglou and Wilson (1982).

For a two-dimensional space, $d = 2$, y_m is equally distributed on the unit circle, therefore

$$y_i = (Cos\,\theta_m,\ Sin\,\theta_m)$$

where θ_m is uniformly distributed between 0 and 2π.

Equation (5.2) becomes

$$x_{ij} = x(x_1,x_2) = \left[\frac{2}{N'}\right]^{1/2} \sum_{m=1}^{N'} Cos[\omega_m(x_1 Sin\theta_m + x_2 Cos\theta_m) + \phi_m] \tag{5.4}$$

where θ_m and ϕ_m are chosen from a uniform distribution over the range 0 to 2π so that θ_m and ϕ_m are $U(0,2\pi)$ distributed. The random variable ω_m must be sampled from the radial spectral distribution function corresponding to a selected spatial correlation function $\rho(x_1,x_2)$.

The random variable ω_m is given by

$$\omega_m = \frac{1}{V_0}\left\{\left[\frac{1}{1 - G(\omega_m)}\right]^2 - 1\right\}^{1/2} \tag{5.5}$$

for a two-dimensional process and

$$\omega_m = \frac{Tan(G(\omega_m)V_0)}{V_0}$$

for a line process.

Generated values of $x(t_1,t_2)$ through equation (5.4) are samples of a stationary and isotropic two-dimensional process in the variables t_1 and t_2. The spatial correlation of the generated values approach equation (5.3) as the number of harmonics goes to infinity. Bras and Rodríguez-Iturbe (1976a) suggest that the influence of N' is not crucial provided it is larger than 50.

The generation of a two-dimensional random field is a seven-step process;

(*i*) choose $N' \geq 50$,

(*ii*) generate N' values of G from $U(0,1)$,

(*iii*) calculate N' values of ω_m from equation (5.5),

(*iv*) generate N' values of θ_m from $U(0,2\pi)$,

(*v*) generate N' values of ϕ_m from $U(0,2\pi)$,

(*vi*) calculate the realizations x_{ij} from equation (5.4), and

(*vii*) repeat steps (*vi*) to (*vii*) for $i = 1,2,\ldots,I$; $j = 1,2,\ldots,J$.

It is possible to generate a random process using these simple steps in the R^2 space defined by $t_1 = y$ and $t_2 = x$. For a one-dimensional process, $y_i = 1$ and $J = 0$.

A more detailed development and explanation of the generation algorithm can be found in Bras and Rodríguez-Iturbe (1985).

It is reported by Mantoglou and Wilson (1982) that in terms of accuracy and cost Shinozuka and Jan's method is superior to the methods described by Shinozuka (1971) and Mejía and Rodríguez-Iturbe (1974).

Shinozuka and Jan (1972) propose the following equation

$$x(t) = \sqrt{2} \sum_{m=1}^{N'} H(\omega_m) Cos[\omega_m' \cdot y_m + \phi_m] \tag{5.6}$$

in which the *Cosine* amplitudes $H(\omega_m) = (f(\omega_k)\Delta\omega)^{1/2}$ are derived from the correlation function $f(\Delta k)$.

In the above equation ϕ_k are independently random angles uniformly distributed between 0 and 2π, $\omega_k = (k - 1/2)\Delta\omega$ and $\omega_k' = \omega_k + \delta\omega$ for $k = 1,\ldots, N'$ and N' is the number of harmonics chosen. The discretization frequency $\Delta\omega = \Omega/N'$ and Ω is the maximum frequency at which the spectrum is truncated. The frequency $\delta\omega$ is a small random frequency added in order to avoid periodicity and is uniformly distributed between $-\Delta\omega'/2$ and $\Delta\omega'/2$, where $\Delta\omega'$ is a small frequency such that $\Delta\omega' \ll \Delta\omega$. Shinozuka and Jan (1972) obtained reasonably accurate results with $\Delta\omega' = \Delta\omega/20$ and $N' = 50$ when simulating a line process.

Both the correlation and spectral density functions of the simulated process converge as $(1/N')^2$ to the true correlation function and the target spectral density function respectively. The improvement in convergence from $(1/N')^{1/2}$ for (5.2) to $(1/N')^2$ for (5.6) results in a significant reduction in computer resources.

A major advantage of the spectral methods is that they are not restricted to evenly spaced observations and they can be extended to multi-dimensional applications. However, spectral methods are approximate and are only asymptotically exact. The use of the spectral method requires careful analysis and fine tuning of parameters if spurious features in the resulting realizations are to be avoided, as was shown in a recent study by Black and Freyberg (1990). Furthermore, the method requires explicit knowledge of the spectral density function of the covariance function.

5.3.3 Nearest neighborhood approach

This approach is fully described by Whittle (1954) and Bartlett (1975). The domain is discretized into rectangles. A simple linear equation is used to express the dependence of the realization in a rectangle with realizations in surrounding rectangles. The correlation between adjacent rectangles is imposed by a moving average or an autoregressive model.

The first-order nearest-neighbor autoregressive relation in two-dimensions can be written as (Smith and Freeze [1979b])

$$x_{ij} = \alpha_x(x_{i-1j} + x_{i+1j}) + \alpha_y(x_{ij-1} + x_{ij+1}) + z_{ij} \tag{5.7}$$

in which x_{ij} is the generated realization for the rectangle located at ij, z_{ij} is an *iid* $N(0,1)$ distributed variable, α_y is an autoregressive parameter expressing the degree of spatial dependence of x_{ij} on its

two neighboring values $x_{i\,j-1}$ and $x_{i\,j+1}$ in the y direction ($|\alpha_y| < 1$) and α_x is the degree of spatial dependence of x_{ij} on its two neighboring values in the x direction, $x_{i-1\,j}$ and $x_{i+1\,j}$ ($|\alpha_x| < 1$), see Figure 5.2.

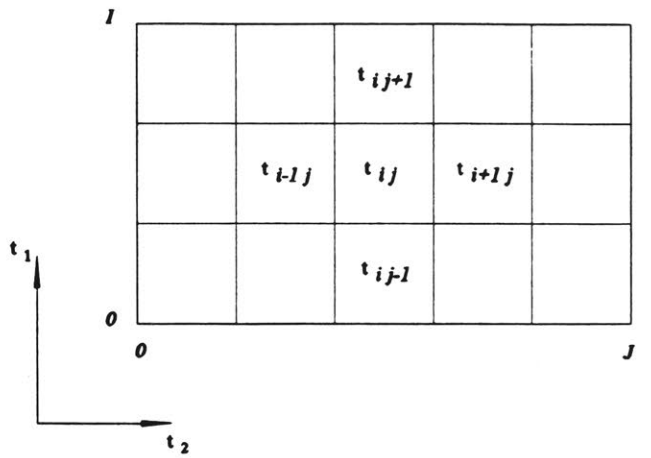

Figure 5.2 Schematic illustration of the nearest neighbor grid, first-order model (after Smith and Freeze [1979b])

A single value x_{ij} applies everywhere within the rectangle $i\Delta x \times j\Delta y$ and equation (5.7) is assumed to be valid for the entire field for a statistically homogeneous process.

The stochastic process model for the entire set of p blocks (I rows and J columns) can be written as a system of p linear equations

$$\boldsymbol{X} = \boldsymbol{W}\boldsymbol{X} + \boldsymbol{Z} \tag{5.8}$$

where the matrix $\boldsymbol{W}$ is a spatial lag operator of scaled weights w_{kl}. These scaled weights are defined by

$$w_{kl} = w_{kl}^{*}/r$$

where $k = 1,2,\ldots,p$; $l = 1,2,\ldots,p$; $k \neq l$, with $w_{kl}^{*} = \alpha_y$ if rectangles k and l are contiguous in the y direction, $w_{kl}^{*} = \alpha_x$ if rectangles k and l are contiguous in the x direction, $w_{kl}^{*} = 0$ otherwise and r is the total number of contiguous rectangles surrounding rectangle k. The scaling r is required to preserve statistical homogeneity in the generated sequence. The matrix $\boldsymbol{W}$ defines the relationship between the rectangles.

Solving for vector $\boldsymbol{X}$, equation (5.8) yields

$$\boldsymbol{X} = (\boldsymbol{I} - \boldsymbol{W})^{-1}\boldsymbol{Z} \tag{5.9}$$

in which $\boldsymbol{I}$ is an identity matrix.

For a p rectangular system, a $p \times p$ banded matrix $\boldsymbol{I} - \boldsymbol{W}$ must be inverted once during the simulation and the storage proportional to p is required.

Tompson *et al.* (1989) and Bellin *et al.* (1992) suggest that the nearest neighbor method may not produce a stationary process and it is difficult or impossible to specify a desired covariance structure

a priori. The reason for this is that there is no explicit use of an correlation structure in the derivation of equation (5.9). King and Smith (1988) show that a stationary random field is only generated using the nearest neighbor method when $\alpha < 1/2$ in the one-dimensional case and for $\alpha < 1/4$ in the two-dimensional case. Although it is possible to preserve the covariance structure in the principal directions of the grid, there is some doubt that it will be preserved on the diagonal.

The nearest neighborhood approach has been applied to groundwater flow and transport problems by Smith and Freeze (1979a,b) and Smith and Schwartz (1981).

5.3.4 Turning bands

An alternative approach for the synthesis of multi-dimensional processes is the turning bands method developed by Matheron (1973).

Instead of simulating the two- or three-dimensional field directly, several line processes are generated each using a one-dimensional covariance function that corresponds to the desired two- or three-dimensional field covariance function. A weighted sum of the corresponding values of the line processes is assigned to each point in the random field.

Let A represent the two-dimensional field where generated realizations with a given covariance structure is required at discrete points, see Figure 5.3

The steps are as follows;

(*i*) choose an arbitrary origin 0 in the two-dimensional computational domain $\mathbb{R}^2$,

(*ii*) generate lines such that the corresponding direction vectors $\mathbf{u}$ are uniformly distributed on the unit circle,

(*iii*) the angle θ_i formed between a line i and a fixed χ axis is uniformly distributed between 0 and 2π,

(*iv*) along each line i, generate a second-order stationary line process having zero mean and covariance function $\gamma_1(\zeta)$, where ζ is the coordinate on line i,

(*v*) onto line i, orthogonally project those points of the field where the realizations are required. Assign to these points the corresponding value of the one-dimensional process. For example, in Figure 5.3, if N is a point of the region with the location vector $\mathbf{t}_N$, then the assigned value from line i will be $z_i(\zeta_{Ni})$, where $\zeta_{Ni} = \mathbf{t}_N \cdot \mathbf{u}_i$ is the projection of the vector $\mathbf{t}_N$ onto line i, $\mathbf{u}_i$ the unit vector in line i and $\mathbf{t}_N \cdot \mathbf{u}_i$ represents the inner product of the vectors $\mathbf{t}_N$ and $\mathbf{u}_i$,

(*vi*) synthesize M independent line processes using $\gamma_1(\zeta)$ as the covariance function so that at every point N of the region there are M assigned values $z_i(\zeta_{Ni}) = z_i(\mathbf{t}_N \cdot \mathbf{u}_i)$, where $i = 1, \ldots, M$, and

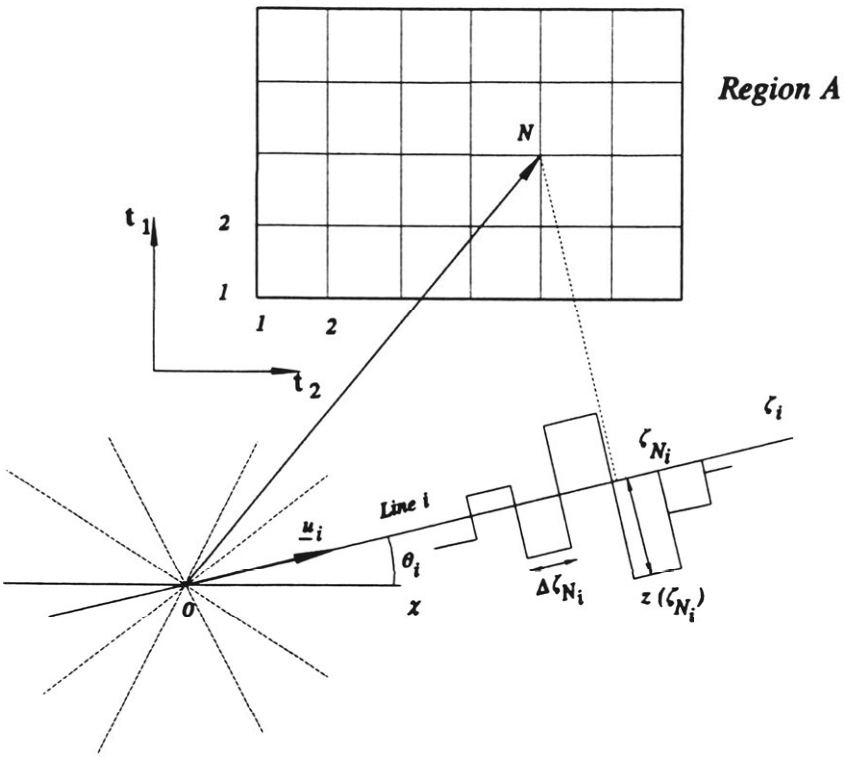

Figure 5.3 Schematic representation of a random field and turning bands lines, i (after Mantoglou and Wilson [1982])

(*vii*) finally, assign to the point N the value given by

$$x(t_N) = t_{ij} = \frac{1}{\sqrt{M}} \sum_{i=1}^{M} z_i(t_N \cdot u_i)$$

as the realizations of the two-dimensional random field.

Either the fast Fourier transform (FFT) technique (Brooker [1985], Miller and Borgman [1985]) or the traditional spectral method (Shinozuka and Jan [1972], Mantoglou and Wilson [1982]) can be used to generate the line process. Mantoglou and Wilson (1982) adopted the approach of Shinozuka and Jan (1972) to generate the line processes. Tompson *et al.* (1989) used the fast Fourier transform. Bellin *et al.* (1992) used both.

Equation (5.6) can be used to generate the line process. However, a relationship is required between the spectral density function of the line process and the radial spectral density function of the two-dimensional process.

Mantoglou and Wilson (1982) proved that the spectral density function of the line process along the turning bands line is given by one-half the radial spectral density function of the two-dimensional process multiplied by the variance. Therefore, $f(w) = \sigma^2 G'(w)/2$, which can be used to derive the

spectral density function of the line process for various two-dimensional covariance or correlation functions, given the radial spectral density function $G'(w)$.

The simulated covariance approaches the theoretical covariance as M increases (Brooker [1985]). Mantoglou and Wilson (1982) found that $M = 16$ provides a very accurate approximation of the process and that $M = 4$ - 16 is sufficient for almost all applications in two-dimensions. Tompson *et al.* (1989) suggest that at least 100 or more randomly orientated lines are required to alleviate the distortion effect associated with the appearance of line-like patterns in the simulated three-dimensional random fields. For a rectangular grid with spacing Δx, Δy the origin of the turning bands line is chosen so that $\Delta\zeta < min(\Delta x,\Delta y)$ (Mantoglou and Wilson [1982]). Evenly spaced lines are preferred in practice because of their rapid convergence. The direction of the M lines therefore, are simply a rotation of $2\pi/M$ radians from the previous line process with the angle of the first line, $\theta_1 = 0$.

Mantoglou and Wilson (1982) found that for $\Omega = 40/V_0$ and $N' = 100$, both the variance and correlation were preserved at large distances relative to the correlation length or integration scale when equation (5.6) was used to generate a two-dimensional random field.

Mantoglou and Wilson (1982) claim that turning bands is much more efficient than matrix decomposition or the nearest neighborhood approach. The costs are those of generating line simulations and appropriately projecting the resulting one-dimensional simulations onto the sampling grid. If M lines are used with each containing n intervals, the total cost will be $O(pql) + Mc(n)$, where $c(n)$ is the cost of generating a single line realization. Compared to the exact matrix factorization method, the spectral and turning band methods have much more modest computational requirements.

The turning bands method for simulating isotropic Gaussian processes is approximate because it depends on the application of the central limit theorem. That is, the correlation structure of the ensemble of realizations approach the required structure only if enough lines are generated. It can only be applied to processes with stationary and radially symmetric correlation functions.

Turning bands has been used extensively in groundwater flow and transport problems in a porous medium. Rubin *et al.* (1992) used this method to produce two-dimensional realizations of the permeability of an aquifer. Delhomme (1979) used the method of turning bands to generate two-dimensional realizations of transmissivity for an aquifer. Bellin *et al.* (1992) used turning bands to generate transmissivity in a two-dimensional solute transport in porous medium. Ababou (1991) used turning bands to generate conductivity values in a three-dimensional groundwater flow model.

5.3.5 Circulant embedding approach

The theoretical basis of a random field generator based on the properties of the circulant matrix will be described in detail for the simulation of a one-dimensional stationary Gaussian process on a fine rectangular grid in $[0,1]^d \subset \mathbb{R}^d$, where $d = 1$ for one-dimension.

(*a*) ONE-DIMENSIONAL Realizations

Consider a stationary Gaussian process $\boldsymbol{X} = (x_1,x_2,\ldots,x_k)$ with zero mean and symmetric covariance function $\gamma(x) = \sigma^2\rho(x)$. Stationarity and equally spaced sampling ensures that the covariance matrix $\boldsymbol{D}$ has the following Toeplitz form

$$\boldsymbol{D} = \begin{bmatrix} r_0 & r_1 & r_2 & r_3 & r_4 \\ r_1 & r_0 & r_1 & r_2 & r_3 \\ r_2 & r_1 & r_0 & r_1 & r_2 \\ r_3 & r_2 & r_1 & r_0 & r_1 \\ r_4 & r_3 & r_2 & r_1 & r_0 \end{bmatrix}$$

where $r_i = \gamma(\Delta x^i)$, $k = 5$, Δx is the grid spacing and the diagonal elements have common elements.

If a symmetric matrix $\boldsymbol{B}$ could be found such that

$$\boldsymbol{D} = \boldsymbol{B}^T\boldsymbol{B} = \boldsymbol{B}^2$$

then by multiplying $\boldsymbol{B}$ by an uncorrelated random vector $\boldsymbol{Z}$ of independent identically distributed (*iid*) variables which are $N(0,1)$ distributed, $\boldsymbol{X} = \boldsymbol{BZ}$ would be distributed as $N(0,\boldsymbol{D})$ because

$$E[\boldsymbol{X}] = E[\boldsymbol{BZ}] = \boldsymbol{B}E[\boldsymbol{Z}] = 0 \tag{5.10}$$

and

$$E[\boldsymbol{XX}^T] = E[\boldsymbol{BZZ}^T\boldsymbol{B}^T] = \boldsymbol{B}E[\boldsymbol{ZZ}^T]\boldsymbol{B}^T = \boldsymbol{BIB}^T = \boldsymbol{BB}^T = \boldsymbol{B}^2 = \boldsymbol{D}. \tag{5.11}$$

The existence of $\boldsymbol{B}$ must be established.

For a symmetric positive-definite matrix $\boldsymbol{A}$, an orthogonal matrix $\boldsymbol{Q}$ and a diagonal matrix $\boldsymbol{\Lambda}$ exists such that

$$\boldsymbol{A} = \boldsymbol{Q\Lambda Q}^T$$

where columns of $\boldsymbol{Q}$ are eigenvectors of $\boldsymbol{A}$ and $\boldsymbol{\Lambda} = \text{diag}(\lambda_0,\lambda_1,\ldots,\lambda_{k-1})$, where λ_i is the eigenvalue associated with the eigenvectors. Because $\boldsymbol{A}$ is positive definite, all λ_is are positive and

$$\boldsymbol{\Lambda}^{1/2} = \text{diag}(\lambda_0^{1/2},\lambda_1^{1/2},\ldots,\lambda_{k-1}^{1/2}).$$

Matrix $\boldsymbol{B}$ may now be defined as

$$\boldsymbol{B} = \boldsymbol{Q\Lambda}^{1/2}\boldsymbol{Q}^T$$

because

$$\boldsymbol{B}^2 = \boldsymbol{Q\Lambda}^{1/2}\boldsymbol{Q}^T\boldsymbol{Q\Lambda}^{1/2}\boldsymbol{Q}^T = \boldsymbol{Q\Lambda}^{1/2}\boldsymbol{I\Lambda}^{1/2}\boldsymbol{Q}^T = \boldsymbol{Q\Lambda Q}^T = \boldsymbol{A}.$$

So if $\boldsymbol{A}$ is symmetric and positive-definite $\boldsymbol{B}$ exists.

The computational effort required for the calculation of the complete set of eigenvalues and eigenvectors of a large matrix is greater than that required for the decomposition of the covariance matrix in the matrix decomposition method. Fortunately there are more computationally efficient methods of calculating the matrix $\boldsymbol{B}$, which is the square root of the covariance function $\boldsymbol{D}$.

Davis (1987) uses a polynomial of degree 8 to approximate the function $\boldsymbol{D}^{1/2}$, where

$$\boldsymbol{D}^{1/2} = \sum_{i=0}^{8} b_i \boldsymbol{D}^i \quad \text{on} \quad [0,\lambda_u]$$

where, $b_i = (a_i/\lambda_u^i)$, $a_1 = 0.07961$, $a_2 = 3.504$, $a_2 = -16.32$, $a_3 = 63.22$, $a_4 = -156.5$, $a_5 = 240.6$, $a_6 = -220.$, $a_7 = 112.5$, $a_8 = -24.002$ and λ_u is an upper bound for the largest eigenvalue of $\boldsymbol{D}$.

This is not an exact procedure and it requires storing the matrix $\boldsymbol{D}^{1/2}$. Therefore, this approach is computionally expensive for a large number of points.

An alternative technique, called the *circulant embedding approach* has been recently developed by Wood and Chan (1994) utilizing the fast Fourier transform which is exact, very efficiency and avoids storing large matrices. In their approach, the Toeplitz covariance matrix $\boldsymbol{D}$ can be embedded into a $m \times m$ matrix $\boldsymbol{C}$, where $m = 2^g$ for some integer g, and $m \geq 2k$, so that the first $k \times k$ elements in $\boldsymbol{C}$ given here by

$$\boldsymbol{C} = \begin{bmatrix} r_0 & r_1 & r_2 & r_3 & r_4 & r_5 & r_4 & r_3 & r_2 & r_1 \\ r_1 & r_0 & r_1 & r_2 & r_3 & r_4 & r_5 & r_4 & r_3 & r_2 \\ r_2 & r_1 & r_0 & r_1 & r_2 & r_3 & r_4 & r_5 & r_4 & r_3 \\ r_3 & r_2 & r_1 & r_0 & r_1 & r_2 & r_3 & r_4 & r_5 & r_4 \\ r_4 & r_3 & r_2 & r_1 & r_0 & r_1 & r_2 & r_3 & r_4 & r_5 \\ r_5 & r_4 & r_3 & r_2 & r_1 & r_0 & r_1 & r_2 & r_3 & r_4 \\ r_4 & r_5 & r_4 & r_3 & r_2 & r_1 & r_0 & r_1 & r_2 & r_3 \\ r_3 & r_4 & r_5 & r_4 & r_3 & r_2 & r_1 & r_0 & r_1 & r_2 \\ r_2 & r_3 & r_4 & r_5 & r_4 & r_3 & r_2 & r_1 & r_0 & r_1 \\ r_1 & r_2 & r_3 & r_4 & r_5 & r_4 & r_3 & r_2 & r_1 & r_0 \end{bmatrix}$$

is equal to $\boldsymbol{D}$ and the matrix $\boldsymbol{C}$ is called a *circulant* matrix.

As stated by Brockwell and Davis (1991), a real symmetric circulant matrix may be decomposed so that

$$\boldsymbol{C} = \boldsymbol{Q}\Lambda\boldsymbol{Q}^*$$

where $\Lambda = \text{diag}\{\lambda_0,\lambda_1,\ldots,\lambda_{m-1}\}$ is the diagonal matrix of eigenvalues of $\boldsymbol{C}$, $\boldsymbol{Q} = \{q_{jk}\}$ is a complex matrix with elements

$$q_{jk} = \frac{1}{\sqrt{m}} exp\left[\frac{-2\pi ijk}{m}\right] \qquad j,k = 0,1,\ldots,m-1 \tag{5.12}$$

where $i^2 = -1$ and $\boldsymbol{Q}^*$ is the conjugate transpose of $\boldsymbol{Q}$. If $\lambda_j \geq 0$ for $0 \leq j \leq m-1$, then from Proposition 2.1 of Wood and Chan (1994) $\boldsymbol{C}^{1/2} = \boldsymbol{Q}\Lambda^{1/2}\boldsymbol{Q}^*$ is also real and symmetric, where $\Lambda^{1/2} = \text{diag}\{\lambda_0^{1/2},\lambda_1^{1/2},\ldots,\lambda_{m-1}^{1/2}\}$ and $\boldsymbol{C}^{1/2}$ are symmetric, non-definite square roots of Λ and $\boldsymbol{C}$ respectively.

If a vector $\boldsymbol{Z}$ of *iid* variables with $N(0,1)$ distribution can be generated, then from (5.10) and (5.11)

$$\boldsymbol{X} = \boldsymbol{C}^{1/2}\boldsymbol{Z} = \boldsymbol{Q}\Lambda^{1/2}\boldsymbol{Q}^*\boldsymbol{Z} \tag{5.13}$$

is distributed as $N(0,\boldsymbol{C})$.

The problems are how to evaluate the matrices in (5.13) efficiently and avoid storing large matrices for moderate values of m. This is achieved using the efficient fast Fourier transform.

The discrete Fourier transform of the sequence $\boldsymbol{a}$ of complex numbers $a_0,a_1,\ldots,a_{m-1}$ is given by

$$d_a(k) = \sum_{j=0}^{m-1} a_j exp\left[\frac{-2\pi ijk}{m}\right] \qquad k = 0,1,\ldots,m-1.$$

If the dimension of the circulant matrix is highly composite, that is m is of the form 2^g, for integer values of g, the fast Fourier transform can be evaluated very efficiently.

Using Proposition 4.5.1 of Brockwell and Davis (1991) the eigenvalues of $\boldsymbol{C}$, $\lambda_j = d_c(j)$, $j = 0,1,\ldots,m-1$, where the c-sequence is the first row in $\boldsymbol{C}$, can be evaluated efficiently using the fast Fourier transform. Therefore, there is no restriction in this method on the covariance function and only the first row of $\boldsymbol{C}$ needs to be stored.

To generate the complex normal vector $\boldsymbol{Q}^*\boldsymbol{Z}$, *iid* random variables R_0, R_1, W_{jn}, $j = 1,2$, $n = 1,2,\ldots,m/2-1$ which are $N(0,1)$ distributed are required. Set $S_0 = R_0$, $T_0 = 0$, $S_{m/2} = R_1$, $T_{m/2} = 0$ and $S_n = S_{m-n} = 2^{-1/2}W_{1n}$, $T_n = -T_{m-n} = 2^{-1/2}W_{2n}$ for $1 \le n \le m/2-1$. Using the orthogonal properties of the relevant trigonometric functions and Proposition 2.3 (Wood and Chan [1994]), it is possible to establish that $\boldsymbol{Q}^*\boldsymbol{Z} = \boldsymbol{S} + i\boldsymbol{T}$ in distribution, where $\boldsymbol{S} = (S_0,S_1,\ldots,S_{m-1})^T$, $\boldsymbol{T} = (T_0,T_1,\ldots,T_{m-1})^T$ and the superscript T denotes transpose. Therefore, $\boldsymbol{Q}\boldsymbol{\Lambda}^{1/2}\boldsymbol{Q}^*\boldsymbol{Z}$ is equal in distribution to $m^{1/2}\boldsymbol{Q}\boldsymbol{a}$, where $\boldsymbol{a} = (a_0,a_1,\ldots,a_{m-1})^T$ and $a_j = \lambda_j^{1/2}(S_j + iT_j)/m^{1/2}$ for $j = 0,1,\ldots,m-1$. Finally, from (5.12) pre-multiplying the vector $\boldsymbol{a}$ by the matrix $m^{1/2}\boldsymbol{Q}$ is equivalent to calculating the discrete Fourier transform $d_a(n)$ of the sequence $\boldsymbol{a}$. From the transformed m-vector which has a $N(0,\boldsymbol{C})$ distribution, extract a subvector of length n, which will have $N(0,\boldsymbol{D})$ distribution.

The steps can be summarized as follows;

(*i*) apply the fast Fourier transform to the c-sequence to obtain λ_j,

(*ii*) generate S_j and T_j,

(*iii*) calculate a_j, and

(*iv*) apply the fast Fourier transform to the a-sequence.

The required realizations $Y(\boldsymbol{X}) = (d_a(0),d_a(1),\ldots,d_a(k-1))^T$ will have $N(0,\boldsymbol{D})$ distribution.

The only conditions required for this approach to be valid are; (*i*) the mesh of the sampling grid has equal spacing, (*ii*) the random field is stationary, and (*iii*) the embedding matrix $\boldsymbol{C}$ is non-negative definite.

The approach fails if $\boldsymbol{C}$ is not non-negative definite. If the covariance function has bounded support, then C will be non-negative definite and the method can always be implemented. Covariance functions with the property $\gamma(V) = 0$ when $V \ge V_0$ are said to have bounded support on $[0,V_0]$. The power, hole-effect and spherical covariance functions are examples of bounded supported covariance functions. These covariance functions will always produce non-negative embeddings. Dietrich and Newsam (1993) found that the exponential decay and the hole effect covariance functions also produce non-negative embeddings. They showed that the required embedding is always non-negative definite

whenever the sampling grid covers the correlation length scale. This is not true for the Gaussian covariance function. The Gaussian and Whittle covariance functions have infinite support.

More generally, non-negativeness of $\boldsymbol{C}$ can often be achieved by making m sufficiently large (see Proposition 2.2 of Wood and Chan [1994]). Otherwise the method can be modified to produce an approximate stationary Gaussian field (Wood and Chan [1994]). However, to achieve full efficiency of the fast Fourier transform, m should be of the form 2^s.

If simulations are required over a grid that is regular but has an irregular boundary, it is always possible to embed the irregular shaped grid in a larger finely spaced rectangular grid and apply the circulant embedding approach on a larger finely spaced grid.

The circulant embedding approach was first described by Davies and Harte (1987) for the one-dimensional case and later, extended independently by Dietrich and Newsam (1993) and Wood and Chan (1993) for multi-dimensions. As far as the author can establish, this technique has never been implemented in water resources problems, with the exception of Zoppou *et al.* (1994). Algorithms for generating both one- and two-dimensional stationary Gaussian random fields using the above method can be found in Chan and Wood (1994).

(*b*) MULTI-DIMENSIONAL REALIZATIONS

The derivation can be generalized for any dimension d where for $d = 1$, the resulting covariance matrix is Toeplitz. For two-dimensions, $d = 2$ and $\boldsymbol{D}$ is block Toeplitz. For higher dimensions, $d \geq 3$, then $\boldsymbol{D}$ is nested block Toeplitz. The embedding matrix $\boldsymbol{C}$ has a corresponding block circulant structure.

The number of floating point operations required for the method is essentially the cost of the fast Fourier transform of the covariance function values on the extended sampling grid followed by one further fast Fourier transform of an appropriately weighted random vector. This represents an overall operational count of $O(m \log_2(m))$ floating point operations per realization for d-dimensional simulation with $O(m)$ storage, where m is the dimension of the embedding matrix. The computational requirements of the approach are comparable to those of the spectral method using the fast Fourier transform.

Unlike turning bands or the spectral method, this approach yields realizations whose ensemble displays exactly the desired field correlation structure, provided that the embedding matrix is non-negative. The fast Fourier transform is used for computational efficiency. There is no restriction on the covariance function and the technique can cope with $k \geq 50{,}000$ grid points in many cases, even on a relatively modest computer.

5.4 Generation of one-dimensional realizations

A hypothetical one-dimensional study is used to illustrate the use of a number of the above schemes for the generation of a one-dimensional random field. The one-dimensional example consists of a simple backwater analysis in an open channel. The prediction limits of the simulated water surface profile are obtained using the Monte Carlo simulation with; (*i*) the matrix decomposition method, (*ii*) the spectral method and (*iii*) the circulant embedding approach to generate the spatial random field. The prediction limits for the model response obtained using Monte Carlo simulation with these random

field generation techniques were compared with the prediction limits obtained by the point estimate method and first-order analysis for both accuracy and computer resources.

The following elliptic equation is solved in the backwater model

$$\frac{dh}{dx} + \frac{1}{Ag}\frac{d(Q^2/A)}{dx} = S_0 - S_f \tag{5.14}$$

in which A is the cross-sectional area, Q is the discharge, S_0 is the channel bed slope, S_f the friction slope and h is the water depth in the channel. The friction slope is defined by the empirical Manning equation given by

$$S_f = \eta^2 \frac{Q|Q|W^{4/3}}{A^{10/3}}$$

where W is the wetted perimeter and η is the Manning resistance coefficient.

The backwater equation is nonlinear and requires an iterative procedure for its solution. Details of the iterative scheme that was used can be found in Henderson (1966, p. 143).

The water level $h(\eta)$ at fixed distances along the channel, can be treated as a function of the Manning resistance coefficient $\eta(\mathbf{x})$. For simplicity, all other parameters are assumed deterministic. In this problem, the model response $Y = f(\eta)$, represents the backwater profile obtained by solving equation (5.14).

The random variation of η, at different locations, x, was described by a random field model. The exponential correlation function defined by

$$\rho(V) = exp\left[\frac{-2|V|}{V_0}\right] \tag{5.15}$$

is used for the correlation function of the Manning resistance coefficient, where V is the separation distance between the two sections and the integration scale V_0 has been arbitrarily set to 30.5 metres.

The backwater profile in a trapezoidal channel described in Henderson (1966, p. 126) is considered. The channel has a base width of 6.1 metres and side slopes 1.5H:1V, is laid on a slope of 0.001 and carries a discharge of 28.32 cumecs. The channel terminates in a free overfall and therefore critical flow occurs at this point. The critical depth y_c, is equal to 1.17 metres. The channel is divided into 63 segments, each being 7.62 metres in length Δx.

A value of the random variable η is given at each cross-section. Therefore, there is a total of $k = 64$ random variables. The Manning resistance coefficients have a mean value of 0.025 and a coefficient of variation $\sigma_\eta/\mu_\eta = 15\%$ and is considered to be normally distributed.

A modest 2145 function evaluations $Y = f(\eta)$, are required for the point estimate method, compared to 1000 used in the Monte Carlo simulation and only 129 function evaluations for first-order analysis. In the spectral method, given by equation (5.2) $N' = 100$ and the dimension of the circulant matrix, $m \geq 2k = 2^8 = 256$ was used in the circulant embedding approach. These values were chosen to ensure that the circulant matrix was highly composite and non-negative definite.

For illustrative purposes, the 95% prediction limit for the model response shown in Figures 5.4 for

first-order analysis and the point estimate method was obtained by assuming that $Y = f(\eta)$ is normally distributed. The 95% prediction limits for Monte Carlo simulation, also shown in Figure 5.4 were obtained from the 1000 model simulations. There is very little difference for practical purposes between the model response simulated using all the above methods.

First-order analysis proved to be an accurate and efficient method for estimating the mean and variance of the model response. This is despite the fact that the backwater model is nonlinear. The first-order analysis has produced results that are comparable to all the other methods. Therefore, it is not unreasonable to assume that for this simple problem the model response is linear. The first-order analysis produced the largest model variances. It may not have produced accurate results with larger values for the coefficient of variation of the Manning resistance coefficient. As pointed out by Yen and Guymon (1990), first-order analysis is only accurate for linear problems where the coefficient of variation of the random variables is small.

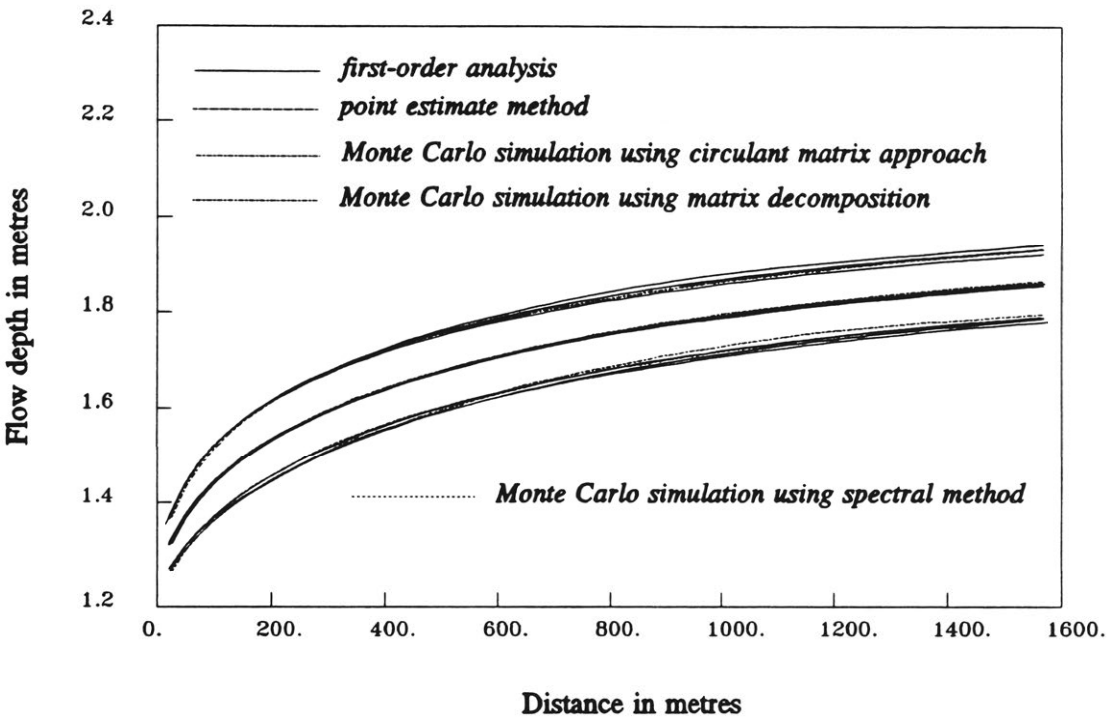

Figure 5.4 Mean and 95% prediction limits of the backwater model response using several reliability techniques

The difference in the variance of the model response predicted by the first-order, point estimate method and Monte Carlo simulation is relatively insignificant compared to the variance reduction due to adopting a random field model.

Using the first-order analysis and assuming a traditional single-random-variable approach produced the mean and 95% prediction limits shown in Figure 5.5 for the backwater model. Also shown in this figure is the predicted model response assuming a random field model. Similar results were obtained using other reliability techniques.

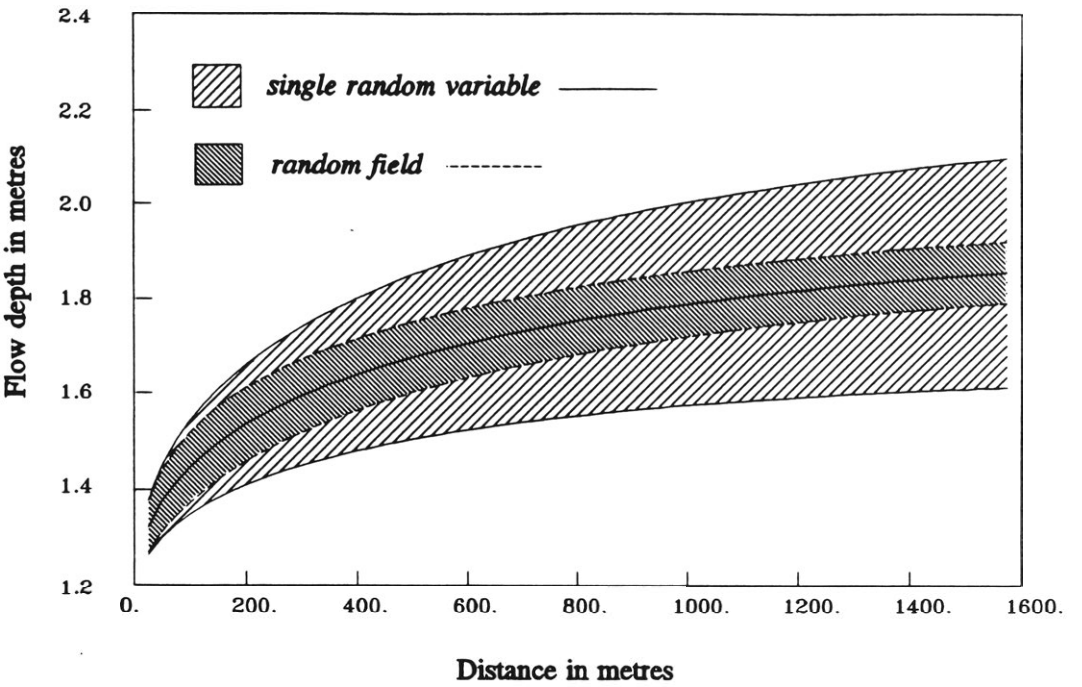

Figure 5.5 Mean and 95% prediction limits of the backwater model response using single-random-variable and random field models in first-order analysis

The random field model produces significantly smaller variance estimates in comparison to the traditional single-random-variable approach. This illustrates the importance of selecting an appropriate model for establishing the influence of spatially random variables on the response of a model.

The large variance in the model response reflects the effect of assuming that the value of a random variable can be determined with absolute certainty by a single sample. In nature large values are usually accompanied by low values. The result is that these extreme values are averaged or smoothed in space. The single-random variable model is not a realistic representation of the spatial averaging observed in nature, whereas the random field model is a more realistic description of the natural process. Therefore, the use of the random field model results in realistic confidence limits of the model's response when compared to the single-random-variable model.

To check that the methods used to generate the random fields have produced realizations that have the desired correlation structure, the correlation coefficient was estimated using

$$\rho(n) = \frac{\frac{1}{k-n-1}\sum_{i=1}^{k-n}(\eta_i - \bar{\eta})(\eta_{i+n} - \bar{\eta})}{\sigma_\eta^2} \tag{5.16}$$

where n is the lag and k is the number of observations.

The correlation function estimated using (5.16), with the realizations generated by the spectral method, matrix decomposition and circulant embedding approach, have been plotted against the exact

where n is the lag and k is the number of observations.

The correlation function estimated using (5.16), with the realizations generated by the spectral method, matrix decomposition and circulant embedding approach, have been plotted against the exact correlation coefficient, given by equation (5.15) in Figure 5.6. The values for the estimated correlation function are the average values obtained using 1000 realizations of the one-dimensional field. Although there seems to be a significant difference between the estimated and exact correlation coefficient, this is attributed to the fact that only when $L/\Delta x \to \infty$ and the number of realizations approaches ∞ will the estimated correlation function approach $\rho(V)$. Therefore, all the methods for producing spatial random fields have produced realizations that preserve the desired correlation structure.

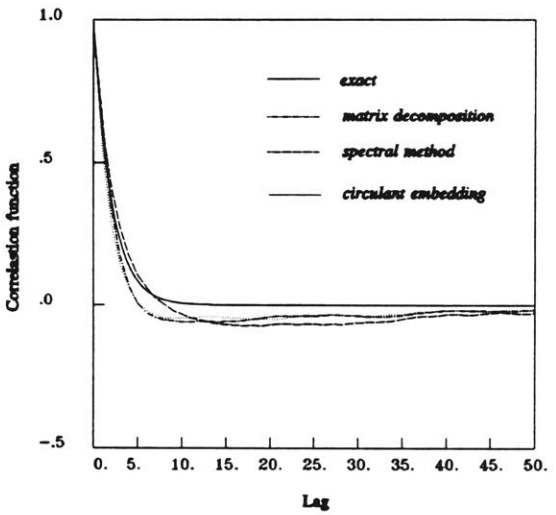

Figure 5.6 Exact and correlation function approximated using 1000 realizations of a stationary line process generated using various methods

The relative computational effort for generating the one-dimensional realizations using the spectral approach, matrix decomposition and circulant embedding approach are given in Table 5.1.

Table 5.1 Relative computational time required to generate 1000 realizations of a one-dimensional, 64 node random field

Method	Relative Computational Time (seconds)
spectral	8.2
matrix decomposition	1.0
circulant embedding approach	3.4

The matrix decomposition method like the circulant embedding approach are exact and there is no restriction on the covariance function that can be used. The circulant embedding approach required more than three times the computational effort than the matrix decomposition method. However, the matrix decomposition method is restricted to one-dimensional problems due to prohibitive storage requirements needed for higher dimensional problems. The use of the spectral method required more

the preferred method for generating the realizations required in the Monte Carlo simulation. This may not be the case for higher dimensional problems or problems with more random variables. The circulant embedding approach may be more appropriate in this case.

The first-order analysis was the most efficient method in this simple problem, followed by the point estimate method then followed by Monte Carlo simulation. A reason for this is that all the methods for generating the realizations required by the Monte Carlo simulation were greater than that required to calculate the backwater profile. Even though the point estimate method required more than twice the number of model evaluations than Monte Carlo simulation, it was also more efficient. Monte Carlo simulation may be more efficient than the point estimate method for more complicated hydrological or hydraulic models or problems with more random variables. However, it is unlikely that Monte Carlo simulation will be more efficient than first-order analysis.

The choice of reliability models depends on the accuracy and the type of results required. First-order analysis seems to be an accurate method for this problem. First-order analysis may not provide accurate results in highly nonlinear problems or problems where the variance of the random variables is large compared to their mean. Therefore, first-order analysis is the preferred method for relatively simple problems in one-dimension followed by the point estimate method. However, it would be prudent to verify the first-order analysis with one of the other reliability methods.

5.5 Generation of two-dimensional realizations

The circulant embedding approach, spectral method, matrix decomposition and turning bands have been used to generate a 16 × 16 random field with the two-dimensional correlation function

$$\rho(t_1,t_2) = exp\left(-(|x_1 - y_1|/l_1 + |x_2 - y_2|/l_2)\right) \qquad t_1 = (x_1,x_2),\ t_2 = (y_1,y_2) \in \mathbb{R}^2 \qquad (5.17)$$

and $\mu = 0$, $\sigma = 1$ and $l = 1$. This correlation function will always result in a non-negative circulant matrix. The random field produced using the circulant embedding approach with $m = 2^6$ is shown in Figure 5.7. The random field produced using the spectral method with N' is illustrated in Figure 5.8 and the random field generated using the matrix decomposition method is shown in Figure 5.9. Using $M = 20$ and $N' = 100$ in turning bands produced the random field shown in Figure 5.10.

The one-dimensional covariance function, given by equation (5.16) was calculated using the realizations generated by the spectral, matrix decomposition and circulant embedding methods. The one-dimensional correlation function was calculated for the 100 random fields generated by each method and the average correlation function was plotted against the exact correlation coefficient, given by $e^{-|x|/l}$ in Figure 5.11. Equation (5.17) corresponds to the simple correlation model $e^{-|x|/l}$ in one-dimension. The results in Figure 5.11 will confirm whether the random field generators have produced realizations with the desired correlation structure.

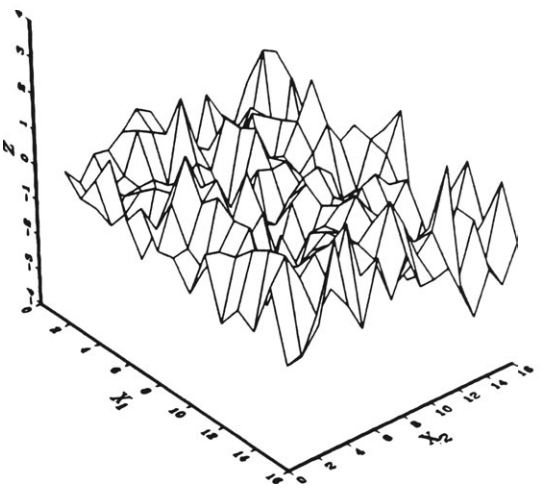

Figure 5.7 Realizations of a two-dimensional, 16×16 stationary process simulated using circulant embedding approach with $m = 2^6$

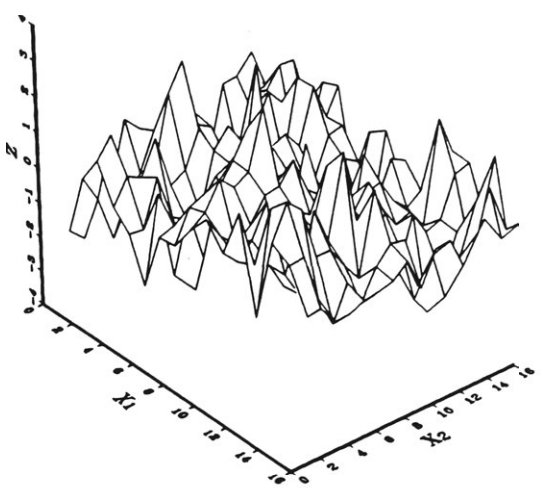

Figure 5.8 Realizations of a two-dimensional, 16×16 stationary process simulated using spectral method with $N' = 100$

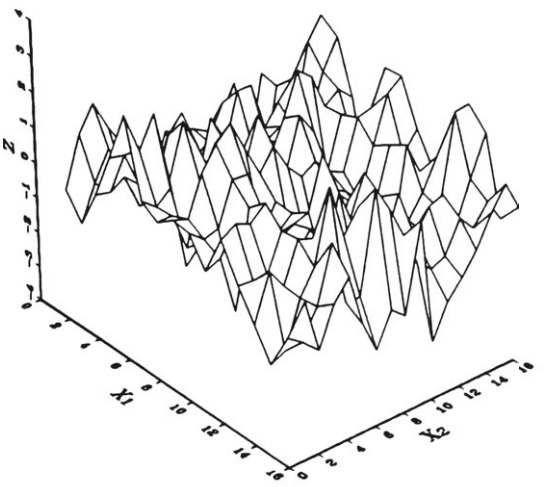

Figure 5.9 Realizations of a two-dimensional, 16×16 stationary process simulated using matrix decomposition method

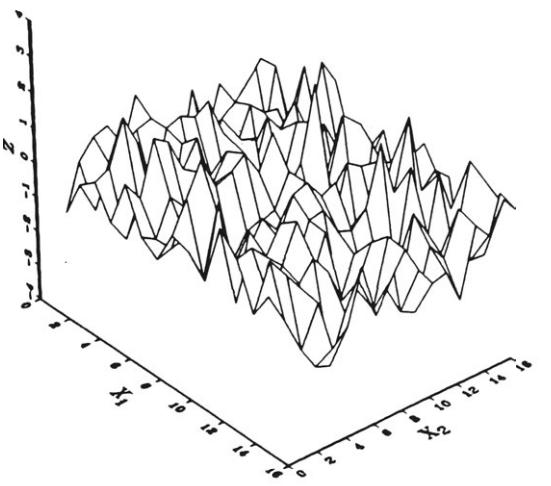

Figure 5.10 Realisations of a two-dimensional, 16×16 stationary process simulated using turning bands with $M = 20$ and $N' = 100$

Given the relative small sample size of 100 in this example, for practical purposes all the methods for producing spatial random fields have produced realizations that preserve the desired correlation structure.

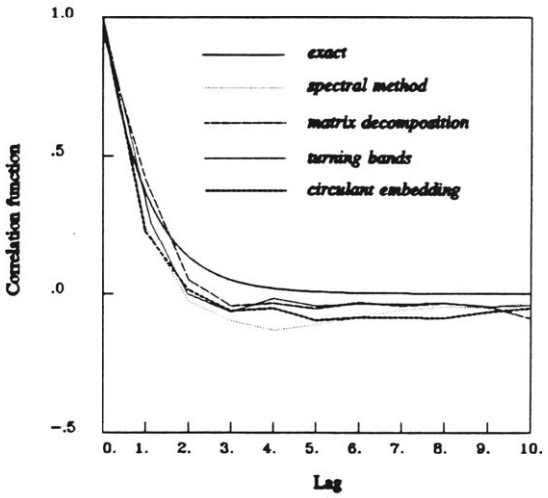

Figure 5.11 Exact and correlation function approximated using 100 realizations of a two-dimensional, 16×16 stationary process generated using various methods

The relative computational effort required by these methods to produce the 16 × 16 random field are given in Table 5.2.

Table 5.2 Relative computational time required to generate 100 realizations of a two-dimensional, 16×16 random field

Method	Relative Computational Time (seconds)
spectral	2.3
turning bands	66.0
matrix decomposition	1.0
circulant embedding approach	2.1

The spectral, matrix decomposition and the circulant embedding approach require similar computational effort compared to turning bands. The excessive computational time required by turning bands is not surprising in view of the computational effort required to generate the line realizations, see Table 5.1. The spectral, matrix decomposition and circulant embedding approach are relatively efficient. Although the circulant embedding approach is not as efficient as the matrix decomposition method, the computer resources required are modest when compared to the matrix decomposition method. It also has modest computing requirements when compared to the spectral or turning bands method. The computer resources required by the matrix decomposition method would be prohibitive for larger two-dimensional problems such as the freshwater lens problem.

This simple comparison does not establish the best method for generating random fields. Realistically a more thorough investigation should involve establishing the computational time required by each

method for numerous single and two-dimensional grid sizes. Plotting the execution time against the grid size for each method would give a quantitative indication of the relative efficiencies of these methods. The most cost effective method is that which has the smallest gradient. Unfortunately, such a comparison may not provide an accurate assessment of the performance of the various random field generators. A reason for this is that it depends on the competency of the programmer and the numerical algorithms that are required in some of the schemes may dramatically influence the efficiency of the overall scheme. For example, it may be more efficient to use fast Fourier transform or the circulant embedding approach rather than the spectral method for generating the line realizations in the turning band method (see, for example Cressie [1993]). There are however other compelling arguments for selecting one of the random field generators over others.

Black and Freyberg (1990) suggest that the use of arbitrary tests will not necessarily result in the choice of an appropriate generator. There may be instances in which parameter changes in these generators may improve results for one test but may have a detrimental impact in an application. Therefore, it is preferable to use the most accurate generator with the least number of parameters, which may not be the most efficient generator. Other factors that may influence the choice of a random field generator are the complexity of the model, the type of problem being considered and its general applicability.

The matrix decomposition method is simple to implement, exact and there is no restriction on the type of correlation function. Even though for this hypothetical problem this method seems to be the most efficient, modest grid sizes and storage requirements make this method computationally prohibitive.

The spectral method is an approximate method. It uses the central limit theorem, or for practical reasons it simplifies the correlation function.

Turning bands is also an approximate method. This method is limited by the forms of the correlation function. However, turning bands is the only method where realizations on a non-uniform grid can be generated.

From Table 3.2 there is a large range of measured permeabilities within a borehole and for different pumping tests at the same depth in a borehole. The variability in the measured permeability at each borehole excludes the use of conditional realizations for this problem. In addition, the computational grid used in the groundwater model is uniform, see Figure 3.6.

Brooker and Stewart (1993) compared the correlation function of data simulated using several two-dimensional random field generators for various square grids. Although they recommend the use of the turning band method, they found that for very small correlation distances the turning bands failed to produce a reasonable fit to the theoretical exponential covariance function. In their case, $M = 50$ line processes were used in the turning bands. Their comparison did not include the circulant embedding approach.

The circulant embedding approach is simple to implement and can be used to generate multi-dimensional realizations. It is exact if the circulant matrix is non-negative and there is no restriction on the form of the correlation function. It can also generate a large number of arrays of realizations efficiently. It is the preferred method for generating random fields in multi-dimensional problems.

Based on the above observations, the circulant embedding approach method will be used to generate the two-dimensional random field of permeabilities required by the sharp interface single aquifer model.

Chapter 6.

Statistical description of the data on Bonriki

Chidley and Lloyd (1977) found that the spatial variations in recharge and permeability are likely to be far more significant than temporal variations in recharge in determining the behaviour of the freshwater lens. Byers and Stephens (1983) and Gotway (1994) consider permeability as a critical parameter in modelling the behaviour of an aquifer. Therefore, the permeability will only be considered as a spatial random variable.

There have been 178 permeability measurements made on Bonriki in six boreholes at a number of depths and in some instances at the same depth (see Table 3.2). The permeability varies by an order of magnitude between 0 and 44 meters per day, which is not unusual. Byers and Stephens (1983) report that it may vary by several orders of magnitude. This data will be used to estimate the statistical moments and correlation structure of the permeability.

6.1 Mean and standard deviation

No assumption is made about the marginal probability density function of the random variables in the first-order and point estimate method. Only the statistical moments of the random variables are required. The measured permeabilities were treated as independent for the calculation of these statistical parameters. This increases the size of the data set and should provide a more reliable estimate of the marginal probability density function of the measured data. Using all the measured data the mean of the permeability $\mu_K = 12.1702$ metres per day, the standard deviation $\sigma_K = 8.4050$ metres per day, the skewness $\upsilon_K = 0.1040$ and the kurtosis $\varsigma_K = 0.0305$. The mean value for the permeability is only slightly different from the model calibrated value of $K = 14$ metres per day obtained by Falkland (1992) (see Section 3.3). The standard deviation of the permeability is large in comparison to its mean value. This violates the assumption made in the first-order analysis and may have a significant influence on the accuracy of its' estimate of the variance of the model response.

The random field generators however, assume that the marginal probability density function of the data is Gaussian. A histogram of the recorded permeability data shown in Figure 6.1 indicates that the data is highly skewed and does not resemble a Gaussian distribution. This can be confirmed using a simple diagnostic plot (see Ang and Tang [1984], p. 279). To test the validity of assuming that K is $N(\mu,\sigma)$ distributed, $F_N(K_i) = F_U(u_i) = u_i$ have been plotted in Figure 6.2, where u_i is a uniform distributed variable and F_X is the cumulative density function with probability density function X. A valid hypothesis will result in a uniform distribution. Figure 6.2 demonstrates that u_i is not uniformly distributed. Therefore, the permeabilities K is not normally distributed.

Many previous studies have found that the permeability of aquifers is highly skewed and that the normal distribution was not an appropriate description of the data. By transforming the data into the

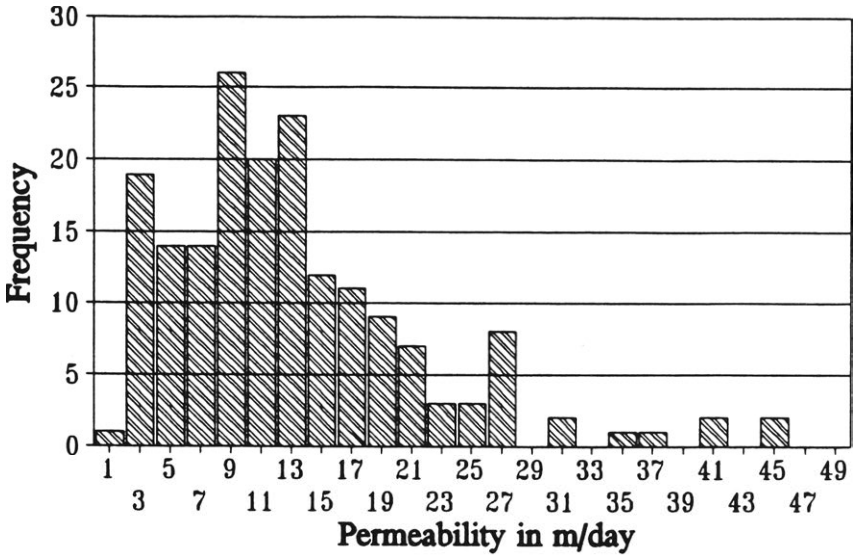

Figure 6.1 Histogram of measured permeability on Bonriki

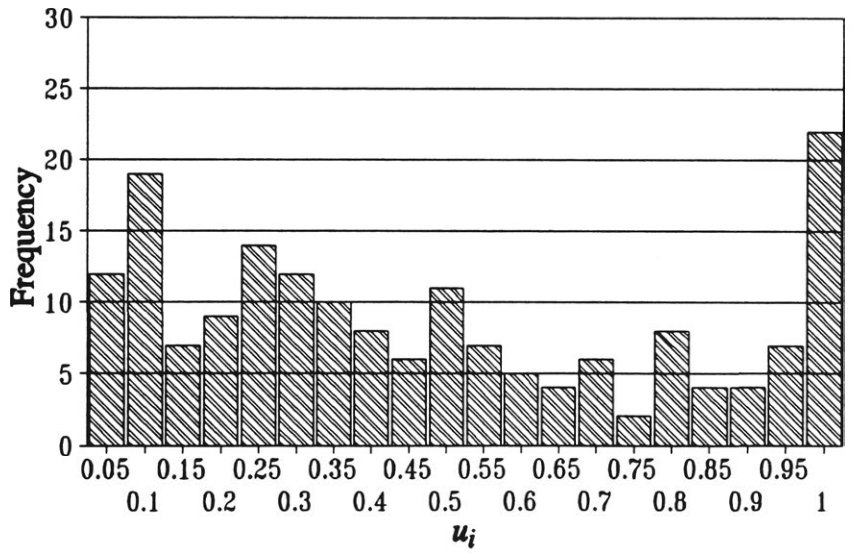

Figure 6.2 Transformation of measures values of K to uniform variates, u_i

natural logarithm (*ln*) or logarithm ($\log_{10}$) domain it was observed that the measured permeability fitted a normal distribution more accurately than the original data (Gotway [1994]). Byers and Stephens (1983) accept the hypothesis that $ln(K)$ is normally distributed in their measurements of K in fluvial sands in Socorro, New Mexico.

Assuming that $ln(K)$ is normally distributed, the following mean and variance of the *ln*-transformed permeabilities were obtained; $\mu_{ln(K)} = 2.2579$, $\sigma_{ln(K)} = 0.7535$ for $N = 177$. Although 178 permeability measurements were made, a value of zero was obtained at one site. This value was removed from the data set. Visual inspection of the histogram of $ln(K)$ illustrated in Figure 6.3 shows that these values resemble a Gaussian distribution more closely than the original data. However, the distribution is now skewed to the right. To assess the hypothesis that $ln(K)$ is normally distributed, the histogram of $u_i = U[0,1] = F_N(ln(K_i))$ is plotted in Figure 6.4, where F_N is the cumulative normal probability density function. The histogram of u_i will not be uniformly distributed for the null hypothesis. Neither the measured values or the *ln*-transformed values from the results shown in Figure 6.2 and 6.4, satisfy the normality assumption. Similar results were observed by Sudicky (1986) for the measured permeability in a sand aquifer at Borden, Ontario. Gotway (1994) found that the permeability measured from Culebra dolomite in eastern New Mexico was not $\log_{10}$-normally distributed. Logarithms to the base 10 were used because the permeabilities vary by eight orders of magnitude, which is claimed by Gotway (1994) to be typical of permeabilities of aquifers. Alternative transformations such as the Box-Cox transformation could be used (Box and Cox [1964]). Kernel filtering estimators could also be used to transform the data.

Kernel filtering estimators are fully non-parametric in that no assumption as to the underlying probability density is explicitly made.

Define

$$\hat{F}(x) = \frac{1}{n}\sum_{i=1}^{n} I(X_i \leq x) \tag{6.1}$$

which is simply the frequency curve of the raw data set containing n points. A continuous empirical distribution function can be estimated from n observations X_i using

$$\tilde{F}(x) = \frac{1}{nw}\sum_{i=1}^{n} \int_{-\infty}^{x} \kappa\{(y - X_i)/w\}\, dy \tag{6.2}$$

in which w is the window size, κ is a bounded compactly supported kernel function which satisfies

$$\int_{-\infty}^{\infty} \kappa(x)\, dx = 1 \quad \text{and} \quad \int_{-\infty}^{\infty} x\, \kappa(x)\, dx = 0.$$

This is essentially a smoother version $\hat{F}(x)$. $\tilde{F}(x)$ can approximate a different distribution by adjusting the window size w. The correct window size is established by testing the hypothesis that $\tilde{F}(x)$ has $U(0,1)$ distribution.

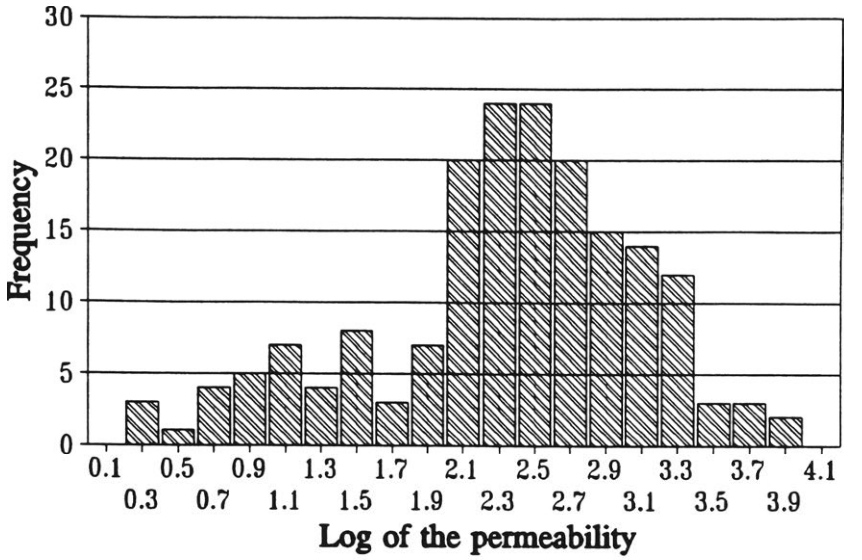

Figure 6.3 Histogram of the *ln*-transformed measured permeability on Bonriki

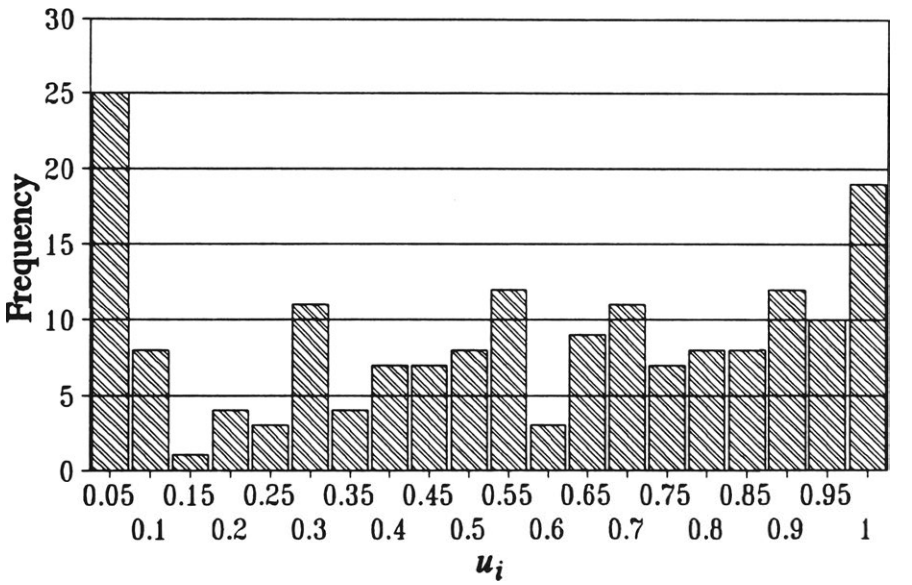

Figure 6.4 Transformation of $ln(K)$ to uniform variates, u_i

There are a number of kernel functions that can be used. For example, the triangular kernel is given by

$$\kappa(x) = \begin{cases} 1 - |x| & |x| \leq 1 \\ 0 & |x| > 1 \end{cases}$$

and the Epanechnikov kernel is given by

$$\kappa(x) = \begin{cases} 0.75(1 - x^2) & |x| < 1 \\ 0 & |x| \geq 1. \end{cases} \tag{6.3}$$

The rectangular kernel function is given by

$$\kappa(x) = \begin{cases} 0.5 & |x| < 1 \\ 0 & |x| \geq 1. \end{cases}$$

A family of kernels κ_α, which contain many of the kernels used in practice is (Härdle [1990])

$$\kappa_\alpha = C_\alpha(1 - x^2)^\alpha.$$

Table 6.1 contains values of α and C_α for the most common cases.

Table 6.1 Kernels from the family κ_α after Härdle (1990)

Kernel	α	C_α
Uniform (Rectangular)	0	1/2
Epanechnikov	1	3/4
Quartic (Bi-weight)	2	15/16
Tri-weight	3	35/32
Gaussian	∞	

The kernel estimate is sensitive to the choice of the bandwidth w. The bandwidth or smoothing parameter determines the roughness or smoothness of the estimated function. Smaller bandwidths result in fewer data points contributing to the estimate at any point and hence a rougher estimator is produced. Larger bandwidths however, allow averaging over a larger data space, resulting in a smoother estimator. As the bandwidth increases, bias increases and variance decreases. Moon and Lall (1994) suggest that the sensitivity to the bandwidth is perhaps an order of magnitude more important than the kernel choice. They used kernel estimators for flood frequency analysis.

The choice of kernels is generally based on the degree of differentiability required and the computational effort involved (Silverman [1986] and Härdle [1990, p. 137]). The Epanechikov kernel

has been used in this study.

Assuming that the measured permeabilities are independent, $\hat{F}(x)$ was estimated using equation (6.1). $\tilde{F}(x_i)$ was obtained using the Epanechnikov kernel in equation (6.2) for different values of the window w. Plots of $\hat{F}(x)$ and $\tilde{F}(x_i)$ are shown in Figures 6.5 and 6.6 for *ln*-transformed permeabilities and K using $w = 5/n$ and $w = 100/n$ respectively.

The simple diagnostic plots used above have been used to verify that the transformed data is normally distributed. Normality has been satisfied if $\tilde{F}(x_i) = F_U(u_i) = u_i$ are $U(0,1)$ distributed. Plots of u_i for the kernel filtered data shown in Figures 6.5 and 6.6 are shown in Figures 6.7 and 6.8 respectively. These figures indicate that the kernel filter chosen has produced uniformity in the results. These results were obtained using trial and error by adjusting w in the kernel function κ so that $\tilde{F}(x)$ approximates a uniform distribution.

The values of $\tilde{F}(x_i)$ shown in Figures 6.5 or 6.6 provide a convenient means of transforming the realizations produced from a Gaussian random field generator into realizations that have the desired covariance structure and the marginal probability distribution of the measured data. This is achieved by;

(*i*) estimating $\tilde{F}(x_i)$ using a suitable kernel function and window size w,

(*ii*) adjusting w until $\tilde{F}(x_i)$ approximates a uniform distribution,

(*iii*) generating a Gaussian random field with the desired covariance function and realizations having a marginal probability density function that is $N(0,1)$ distributed,

(*iv*) calculating $F_N(y_i) = F_U(u_i) = \tilde{F}(x_i)$ for each realization y_i in the random field and

(*v*) obtaining the realizations X_i, which have the same marginal probability density function and covariance structure of the measured data by performing the inverse transformation $X_i = \tilde{F}^{-1}(x_i) = \tilde{F}^{-1}(F_N(y_i))$.

Instead of numerically inverting equation (6.2) in step (*v*) above, tabulated values of $\tilde{F}(x_i)$ and X_i provide a simpler means of performing the inversion.

The empirical distribution function $\tilde{F}(x_i)$, for either K or $ln(K)$ filtered values could be used. Since the data indicates that permeability values of zero are possible, these values cannot be obtained using the *ln*-transformed data. Therefore, K filtered values were used in this study.

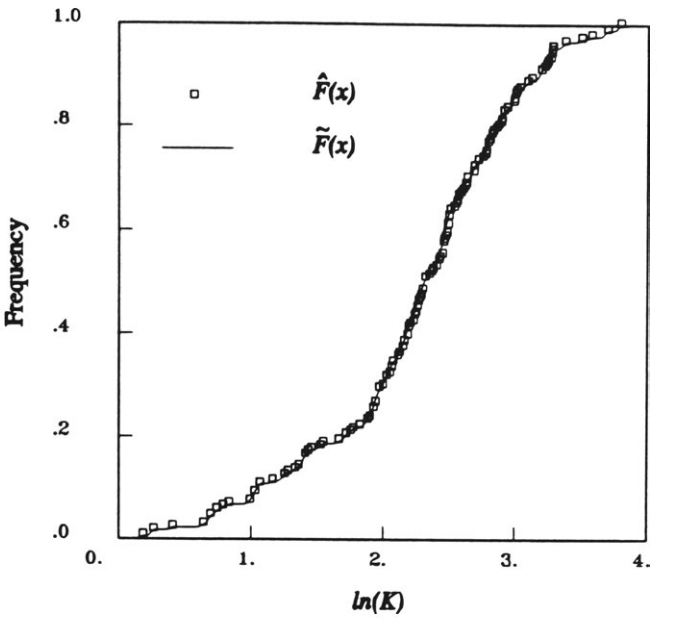

Figure 6.5 CDF of $ln(K)$ and filtered values of $ln(K)$ using $nw = 5$

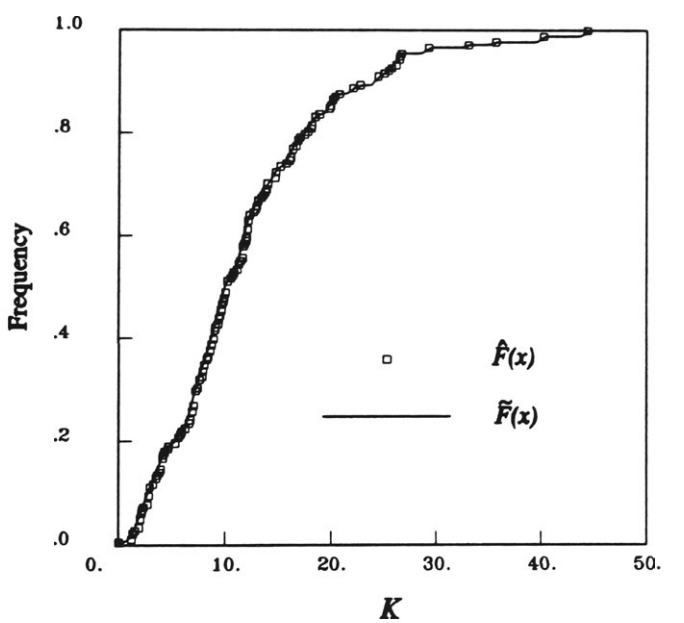

Figure 6.6 CDF of K and filtered values of K using $nw = 100$

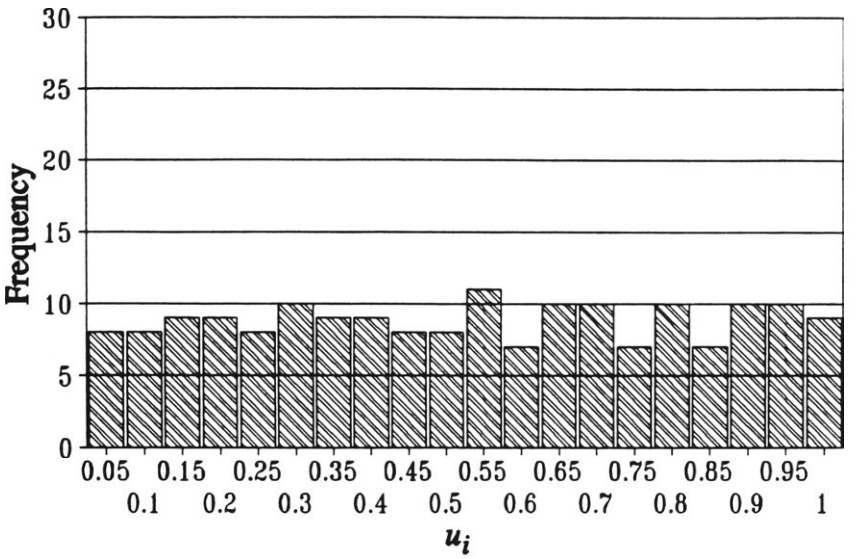

Figure 6.7 Transformation of filtered values of $ln(K)$ using $nw = 5$ to uniform variates, u_i

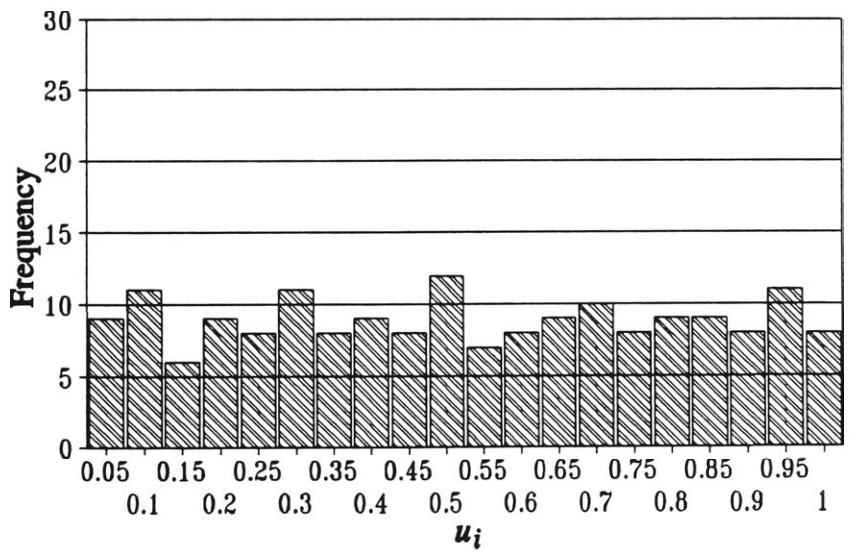

Figure 6.8 Transformation of filtered values of K using $nw = 100$ to uniform variates, u_i

6.2 Correlation structure of the permeability

Spatial random variables are not independent in practice. Random variables closer to each other tend to have similar properties when compared to those that are further apart. This is true for many spatial random variables encountered in water resource modelling.

Establishing the spatial correlation structure of the permeability data measured on Bonriki will be considered.

The sample size of the order of 10^3 is required for a two-dimensional correlation function. A more practical approach is to assume a separable correlation structure.

$$\rho(t_1,t_2) = \rho_x(t_1,t_2) \cdot \rho_y(t_1,t_2)$$

for the permeability where ρ_x and ρ_y are the correlation functions in the x and y co-ordinate directions respectively. With this correlation function structure, it is only necessary to estimate the correlation function in each principle direction separately using fewer samples. It has been suggested that a minimum of 20 to 50 samples are required to give a reliable estimate of the correlation function for a one-dimensional correlation function (see, for example Journel and Huijbregts [1978]). The problem can be further simplified by assuming that $\rho_x = \rho_y$. Therefore, only a single correlation function and integration scale needs to be estimated.

Rodrìguez-Iturbe *et al.* (1986) established the spatial correlation structure of rainfall data recorded in the Upper Guaire basin in Venuzuela. Forty-four storms were recorded at seven nonuniformly spaced rain gauges in their data set. The correlation structure of the data was estimated by calculating the correlation coefficient between the mean rainfall from the 44 storm events recorded concurrently at the seven rainfall gauges. This resulted in twenty-one values which were used to estimate the correlation structure of the data. This is a useful technique if the distance between sites is not regular and if at each site a number of regularly sampled values are known. Alternatively, the data is grouped into distance classes for sites that are not regularly spaced. The correlation distance is the mid-point of the class with each class having at least one data value. The correlation coefficient can be estimated from this regularly spaced data using equation (5.16). The major advantage of this approach is that this method utilizes all of the available information to estimate ρ.

A combination of both of these approaches was applied to the data measured on Bonriki, where the number of sites is small and the permeability at each site is not sampled at regular depth intervals (at the same frequency) at each site, see Table 3.2. This is not a criticism of the data collected on Bonriki. The monitoring program on Bonriki was developed to satisfy certain objectives, which did not include the estimation of the correlation structure of the permeability.

Using the data in Table 3.2, the average permeabilities were calculated for a number of depth intervals. These values and their corresponding depth intervals are given in Table 6.2 for the six monitoring boreholes. The correlation coefficient was calculated between pairs of boreholes which had at least three or more values at corresponding depth intervals. This excluded the use of the permeabilities at borehole BN7, where only one value was available. Using the remaining data, a total of ten values of the correlation coefficient were obtained at the four remaining boreholes. The correlation distance is equal to the distance between each pair of boreholes. The distance between each pair of boreholes given in Table 6.3 were estimated using the data in Table 3.1.

Table 6.2 Average permeabilities at each borehole for various depth ranges

Depth interval (metres)	Permeability in borehole (metres per day)					
	BN1	BN2	BN4	BN5	BN7	BN9
5-6	8.5	2.1	3.8			11.7
8-9	11.7	3.9	4.5	10.1	25.0	8.4
10-12						8.1
12-15	10.4	9.7	13.7	14.4		
20-21	18.1			12.1		25.2
>21		6.5	13.5	22.0		38.6

Table 6.3 Distances between boreholes in metres

Borehole	BN2	BN4	BN5	BN7	BN9
BN1	153	422	694	93	355
BN2		269	541	55	202
BN4			272	324	67
BN5				596	339
BN7					257

This provided an estimate of the correlation structure of the permeability over a distance of 67 to 694 metres.

The above approach is strictly not valid for aquifer properties. It is expected that there would also be a correlation structure with depth. The approach used by Rodrìguez-Iturbe *et al.* (1986) assumes that each storm events are independent and stationary with time. This is not the case for permeability. It would be reasonable to expect that the permeability is correlated with depth as well as space. Therefore, the stationarity with depth is violated. This is complicated by the possibility that the vertical correlation structure may be more complex than the horizontal structure. Byers and Stephens (1983) found that there is a greater variability in permeability in the vertical than the horizontal direction. Permeability showed a less easily interpreted spatial structure, with different correlation lengths and more complex functional forms of the correlation in the vertical than in the horizontal direction.

The ten estimated correlation values have been plotted in Figure 6.9 assuming that stationarity with depth exists.

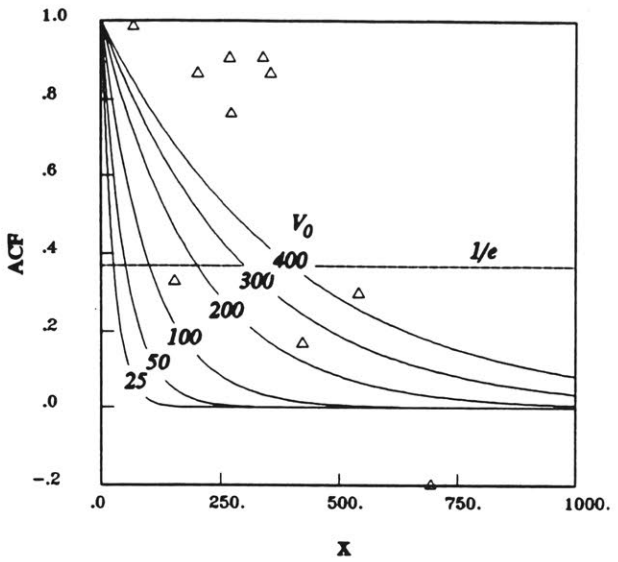

Figure 6.9 Variation of the exponential correlation function with correlation distance V_0 and correlation of the permeability data on Bonriki

There seems to be no discernable trend in the estimated correlation structure with distance. A negative correlation value was obtained between boreholes BN1 and BN5. Therefore, there is insufficient data to establish the correlation structure of the permeability using the data measured on Bonriki.

A suitable monitoring strategy for estimating the spatial correlation structure of the data can be suggested based on the difficulties encountered in estimating the correlation structure of the data measured on Bonriki. The monitoring boreholes should be drilled on a uniform grid and the number of boreholes should be significantly increased. The permeability should be measured at the same frequency and depth in each bore.

Since it is not possible to obtain an estimate of the correlation structure of the permeability of the aquifer on Bonriki, the correlation structure will be assumed.

Several correlation functions that have been used in water resources modelling have been used to describe the correlation structure of permeability in an aquifer. Amongst these are; (see, Table 6.4) (*i*) *Exponential function*, (*ii*) *Quadratic exponential or Gaussian function*, (*iii*) *Whittle or Bessel function*, (*iv*) *Power model*, (*v*) *Spherical model* and (*vi*) *Hole-effect model*. Bras and Rodrìguez-Iturbe (1976b) recommend the use of the Bessel type or single exponential type correlation functions and caution the use of the quadratic exponential correlation function.

The simple exponential correlation function

$$\rho(V) = exp\left[\frac{-|V|}{V_0}\right]$$

has also been adopted in this study and was based on previous studies on atolls where the covariance of the permeability has been established from measured data or assumed, see Table 6.4,

The integration scale, V_0 is also required to define the correlation function. The correlation distance should be chosen to reflect the relationship between values of the random variable along the channel. A large value of V_0 implies that the random variable is correlated over a large spatial extent, resulting in a smooth variation in property. Conversely, a small correlation distance implies a rapid spatial fluctuation. As $V_0 \rightarrow \infty$, the random variable becomes perfectly correlated $\rho = 1$, and the random field model degenerates into the single-random-variable approach. If the correlation function is assumed to be exponential in form, the integral scale or correlation scale may be determined graphically as the lag value that corresponds to a correlation equal to the inverse exponential decay constant, $1/e \approx 0.368$ (Byers and Stephens [1983]). For alternative correlation functions, values of ρ can be plotted on a graph similar to that shown in Figure 6.9 for the exponential correlation function. For a given or assumed correlation function, the value of integration scale V_0, can be determined from the graph which best fits the data.

Since there is insufficient data to establish the form of the correlation structure of the permeability data, it is also not possible to estimate the correlation distance. Previous studies do not provide any insight into typical values for the correlation distance, see Table 6.4. However, it is unrealistic to assume that the permeability should be treated as an independent random variable so that $\rho = 0$, or as a perfectly correlated random where $\rho = 1$. Without any other convincing argument, it is assumed that the correlation distance is 100 metres. This corresponds to the grid spacing used in the model so that $V_0 = \Delta x = \Delta y$.

Table 6.4 Correlation functions and correlation scale used to characterized permeabilities in aquifers in previous studies

Aquifer	Source	Correlation Function	Correlation Scale (m)	Soil Type
Normandry Bathonian	*Delhomme* (1979)	spherical	different ranges	
Borden Ontario	*Sudicky* (1986)	exponential	2.8 horizontal 0.12 vertical	sands
Socorro New Mexico	*Byers and Stephens* (1983)	approx. exponential		fluvial sands
Bet Dagan Israel	*Russo and Bresler* (1981)	spherical	2-12	
Las Cruces New Mexico	*Sisson and Wierenga* (1981)	exponential	0.12	sands

Chapter 7.

Reliability analysis of the freshwater lens

The behaviour of the freshwater lens for various management strategies can be examined using the sharp interface single aquifer model and the data described in the previous chapters. The various management strategies may involve different extraction rates and vegetation cover on the island. For example, the behaviour of the freshwater lens will be examined for the extraction rates 750, 1175 and 1500 cubic metres per day with 80%, existing, 40% and 20% vegetation cover. The consequences of various management strategies and the performance of different models and modelling approaches will be assessed using the predicted lens thickness at borehole BN4 over the period 1955 to 1992.

7.1 Estimating the expected value and standard deviation of the model response

First-order analysis, Monte Carlo simulation and the point estimate method could be used to calculate the expected and standard deviation of the model response for a given extraction rate and vegetation cover. The performance and applicability of these techniques will be examined by estimating the expected value and standard deviation of the thickness of the freshwater lens at borehole BN4 for the existing vegetation cover and an extraction rate of 750 cubic metres per day.

Estimates of the permeability, which are considered as random variables, are required at each computational node in the sharp interface single aquifer model. Since there are (22)(15) = 330 computational nodes defining the aquifer, then there are 330 random variables for this problem.

Using central differences to estimate the partial derivatives in equation (4.1), 1 + 2(22)(15) = 661 model evaluations (or 331 for backward or forward differences) are required in first-order analysis.

A sample size of 1000 was used in the Monte Carlo simulation. An approximation of the probability density function of the model response is required in this problem. The problem encountered with the use of Monte Carlo simulation by Robinson and Maul (1991) is not appropriate to the problem considered here. Therefore, the size of the sample is not as critical as it would be if an estimate of the probability of failure of the system is required. Other sample sizes were also used. Larger sample sizes did not provide significant changes in the estimated probability density function of the model response that would justify the additional computational effort required.

The circulant embedding approach was used to generate the two-dimensional realizations of permeabilities required by the single aquifer model in Monte Carlo simulation. The dimension of the circulant matrix is $m = 2^6$ in the circulant embedding approach. The computational effort required to generate a single realization of the random field is only a fraction of the time required to solve the equations describing the behaviour of the freshwater lens. The solution of the unsteady groundwater flow model required 30 times the computational effort than that required by the circulant embedding approach to generate the random field of permeabilities required by the model. Therefore, the computational effort required by Monte Carlo simulation is approximately twice that required by first-

order analysis. However, it provides an approximation of the probability density function of the model response. First-order analysis and the point estimate method only provide estimates of the statistical moments of the model response. Curve fitting techniques are required to estimate the probability density function of the model response using these statistical moments.

In the point estimate method, $(418^2 + 3(418) + 2)/2 = 87990$ model evaluations are required. This is far in excess to the number of model evaluations that are required in Monte Carlo simulation or first-order analysis. The point estimate method requires considerable more computing resources than either the first-order analysis or Monte Carlo simulation. Therefore, the point estimate method is an inappropriate method for this problem because of the number of simulations required.

Only first-order analysis and Monte Carlo simulation are capable of providing estimates of the expected value and standard deviation of the model response efficiently. The expected lens thickness at borehole BN4 predicted by using first-order analysis and Monte Carlo simulation are shown Figure 7.1. First-order analysis estimates the variability about a single sample from the population. Monte Carlo simulation provides an approximation of the true expected value of the model response. However, the expected values predicted by both methods for practical purposes are very similar.

The variance of the model response estimated using first-order analysis and Monte Carlo simulation is shown in Figure 7.2. First-order analysis has significantly overestimated the variance of the model response for this problem. Accurate results for the variance are not unexpected using first-order analysis since the model response is not linear and the variance of the permeability is large in comparison to its mean.

Monte Carlo simulation provides an estimate of the probability density function of the model response which is based on a physical model. The probability density function of the model response is shown in Figure 7.3 and 7.4 for 1980 and 1990 respectively. These are typical of the histograms of the model response for other years. It is a symmetrical model response and all the predicted model responses are physically plausible.

First-order analysis has produced prediction limits of the lens thickness that are physically unrealistic. The expected model response plus or minus two or three estimated standard deviations of the model response, produces unrealistic values for the thickness of the freshwater lens. This is a major advantage of Monte Carlo simulation, where the groundwater model produces physically plausible results. This is another reason why first-order analysis is only valid when the coefficient of variation of the random variables is small. Estimating the variance of the model behaviour by extrapolating the model results that have been perturbed about the mean model response ignores physically unrealistic results. First-order analysis is not an appropriate method for estimating the confidence interval of the model response for this problem.

Based on the above observations, the predicted expected value and prediction limits of the lens thickness for various management strategies will be estimated using only Monte Carlo simulation. The circulant embedding approach will be used to generate the realizations of the permeability required by the sharp interface single aquifer model.

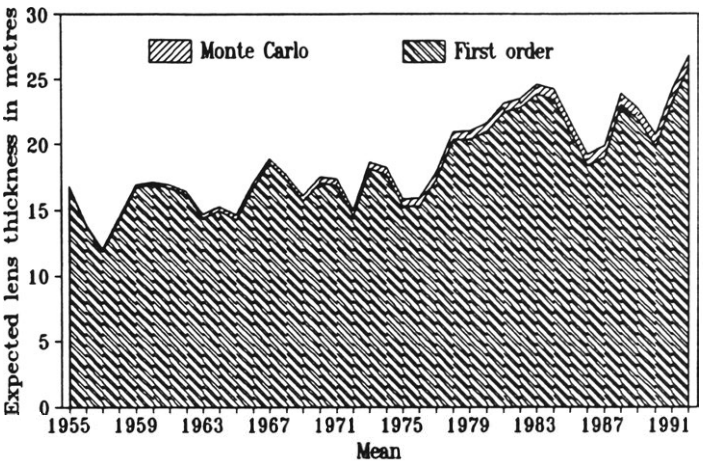

Figure 7.1 Estimated expected lens thickness using first-order analysis and Monte Carlo simulation for 80% vegetation cover and an extraction rate of 750 m^3/day

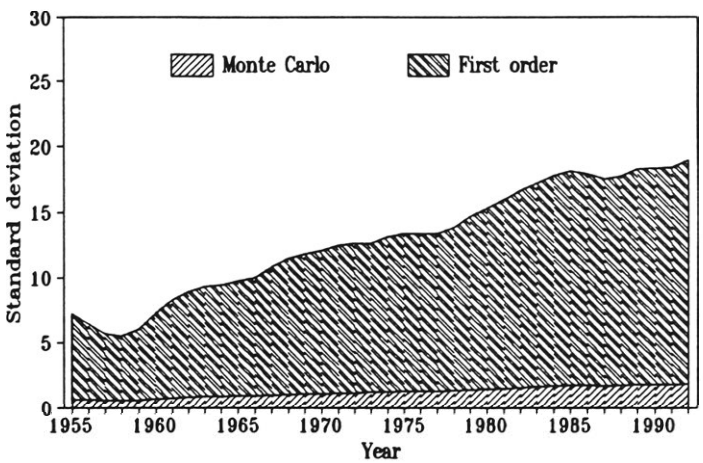

Figure 7.2 Estimated standard deviation of the lens thickness using first-order analysis and Monte Carlo simulation for 80% vegetation cover and an extraction rate of 750 m^3/day

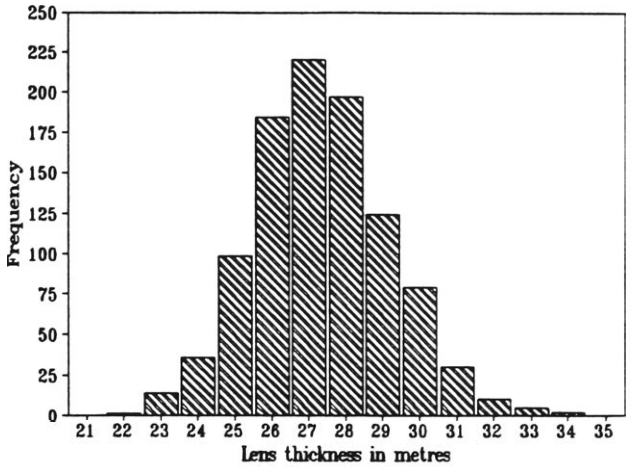

Figure 7.3 Frequency distribution of the predicted lens thickness at borehole BN4 during 1980 for an extraction rate of 750 m^3/day and 80% vegetation cover using Monte Carlo simulation

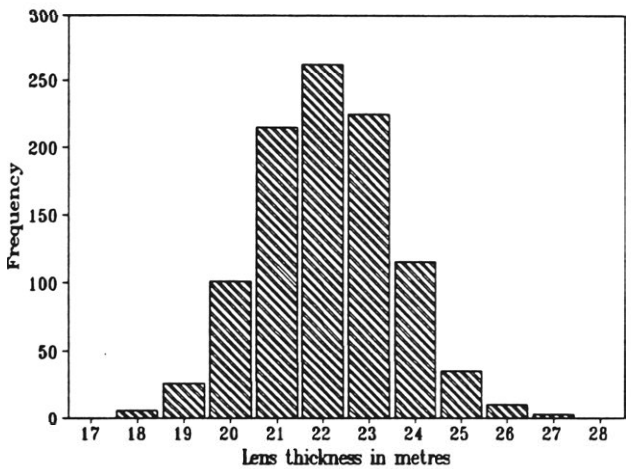

Figure 7.4 Frequency distribution of the predicted lens thickness at borehole BN4 during 1990 for an extraction rate of 750 m^3/day and 80% vegetation cover using Monte Carlo simulation

7.2 Sustainable yield from the freshwater lens

As indicated in Section 2.6, sustainable yield is a subjective quantity. Falkland (1994) defines it as the extraction rate that will not cause the thickness of the lens on Bonriki to fall below 5 metres. The thickness of the lens refers to the freshwater interface where the electrical conductivity of the water is 2500 μS per centimetre. An arbitrary limit on the thickness of 10 metres has been chosen in this study. This arbitrary criterion will be used to demonstrate how a numerical model can be used to assist in making sound management decisions. The sustainable yield will be defined as the extraction rate for which the predicted lens thickness does not fall below 10 metres at any time over the period of record. If the lens thickness falls below 10 metres, the long term sustainability of the freshwater lens is considered to have been compromised.

The behaviour of the freshwater lens can be predicted using either a deterministic or stochastic-deterministic approach. The implications of adopting these approaches will also be considered.

7.2.1 Deterministic modelling approach

The random variables are assumed to be known with certainty in a deterministic model. Usually the mean values for the random parameters are used in the model. This is equivalent to estimating the expected value of the model response using first-order analysis. As was shown in Figure 7.1, the expected value of the model response estimated using Monte Carlo simulation is very similar to the expected value estimated using first-order analysis. Therefore, the discussion regarding the deterministic modelling approach is based on the expected model response estimated using Monte Carlo simulation.

The estimated expected thickness of the freshwater lens for extraction rates of 750, 1175 and 1500 cubic metres per day with 20%, 40% and 80% vegetation cover are shown in Figures 7.5 to 7.7. There figures show that increasing the extraction rate and the vegetation cover reduces the thickness of the freshwater lens. An extraction rate of up to 1175 cubic metres per day is sustainable for the full range of vegetation cover considered when the subjective criterion that the sustainability of the freshwater lens is not compromised when the thickness of the freshwater lens falls below 10 metres is used.

Figure 7.7 illustrates that the lens thickness falls below 10 metres when the extraction rate is 1500 cubic metres per day with the existing vegetation cover. This extraction rate is sustainable if the vegetation cover is reduced. There is a tradeoff between increasing the extraction rate with the loss of production in coconut products due to the reduction in vegetation on the island.

The deterministic model provides managers with a tool to investigate the influence on the thickness of the freshwater lens of various management strategies. More informed decisions can be made by managers using this tool.

The results shown in Figures 7.5 to 7.7 assume that all model parameters are known with certainty and the model is exact. This is far from reality. The model response is not known exactly because the model parameters are not known with certainty. Figures 7.3 and 7.4 illustrate that there is a wide range of possible outcomes, with each outcome having a different probability of occurrence. The width of the probability density function of the model response is a reflection of the amount of uncertainty in the model parameters and the sensitivity of the model to these uncertainties. A wide range of possible outcomes may have an influence on the decision making process.

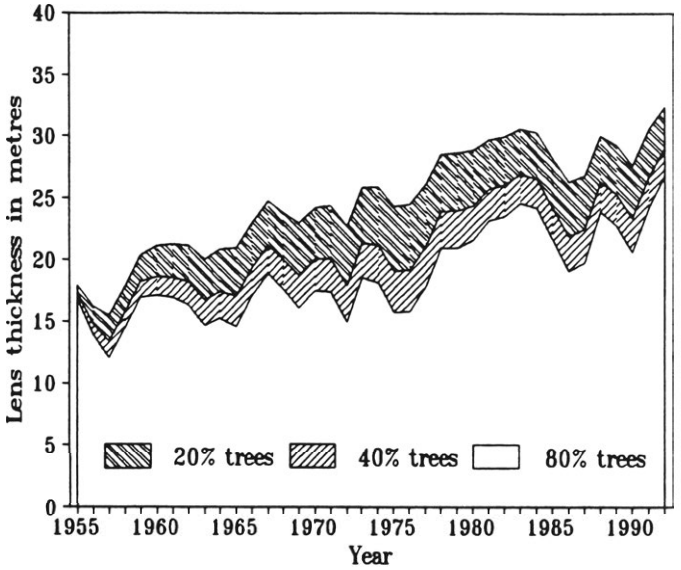

Figure 7.5 Predicted expected lens thickness for 20%, 40%, 80% tree cover and an extraction rate of 750 m^3/day using Monte Carlo simulation

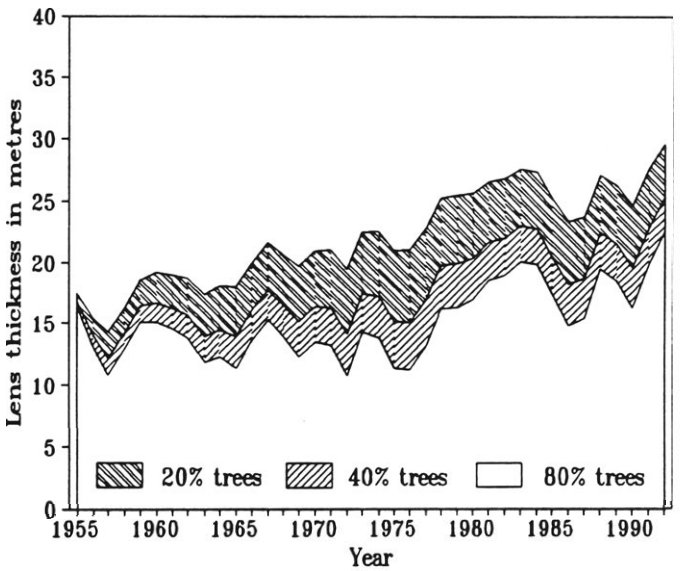

Figure 7.6 Predicted expected lens thickness for 20%, 40%, 80% tree cover and an extraction rate of 1175 m^3/day using Monte Carlo simulation

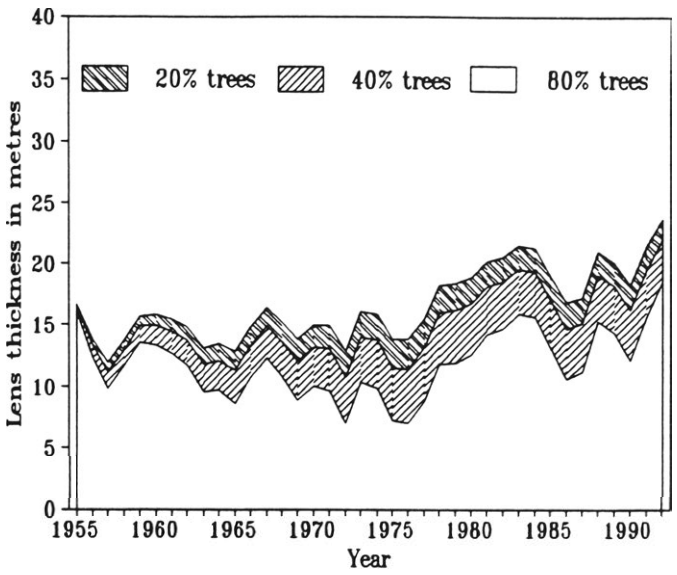

Figure 7.7 Predicted expected lens thickness for 20%, 40% and 80% tree cover and an extraction rate of 1500 m^3/day using Monte Carlo simulation

The stochastic-deterministic modelling approach will be used to incorporate the influence of uncertainties in the model parameters on the model response. The way these uncertainties may influence the decision making process is also considered.

7.2.2 Stochastic-deterministic approach

The 1, 50 and 99 percentiles of the lens thickness were obtained from the 1000 model simulations used in Monte Carlo simulation. These percentiles have been plotted in Figures 7.8 to 7.16 for different extraction rates and vegetation covers considered in this study.

The width of the prediction limit seems to increase with decreasing vegetation cover or increasing lens thickness. This suggests that the width of the confidence limit is proportional to the thickness of the freshwater lens. This was observed for all the considered extraction rates 750, 1175 and 1500 cubic metres per day.

It could be argued that the uncertainties in K might be considered as equivalent to the reduction in the vegetation on the island when the results in Figure 7.5 are compared with those obtained in Figure 7.9. For example, the results in Figure 7.9 suggest that the uncertainties in the permeabilities are equivalent to reducing the vegetation by between 40% to 20% of the surface of the island. Similar observations could be made for other extraction rates.

As with the deterministic modelling approach, the results in Figure 7.14 indicate that maintaining an extraction rate of 1500 cubic metres per day with 80% vegetation cover will compromise the viability of the freshwater lens. Therefore, this and larger extraction rates are not sustainable for the existing vegetation cover.

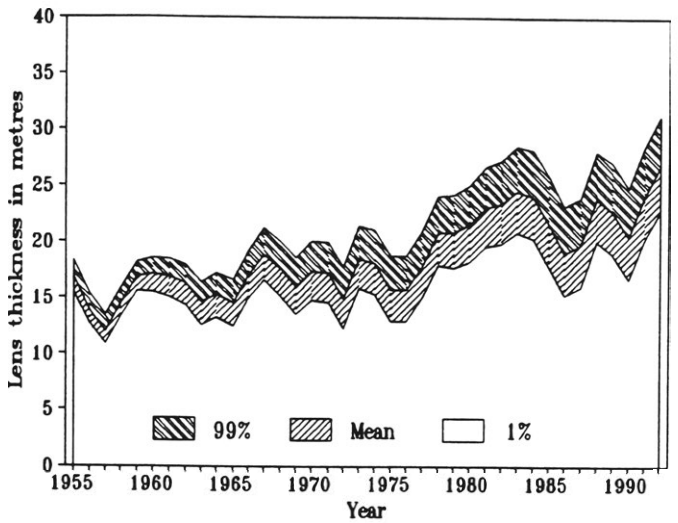

Figure 7.8 The expected, 1% and 99% prediction limits of the lens thickness using Monte Carlo simulation for an extraction rate of 750 m^3/day and 80% vegetation cover

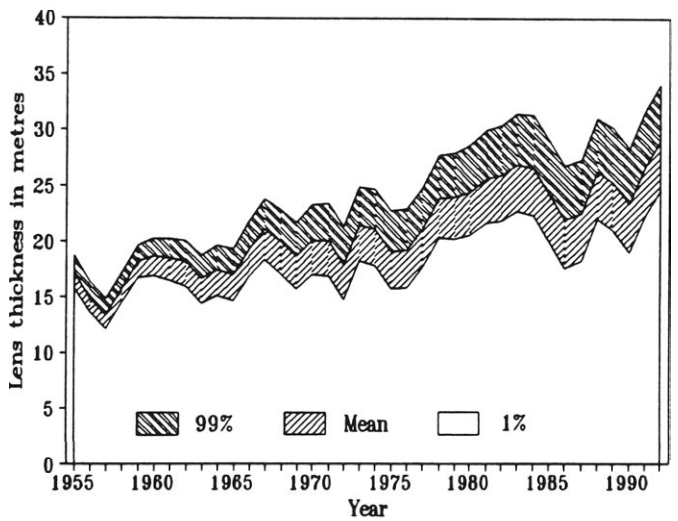

Figure 7.9 The expected, 1% and 99% prediction limits of the lens thickness using Monte Carlo simulation for an extraction rate of 750 m^3/day and 40% vegetation cover

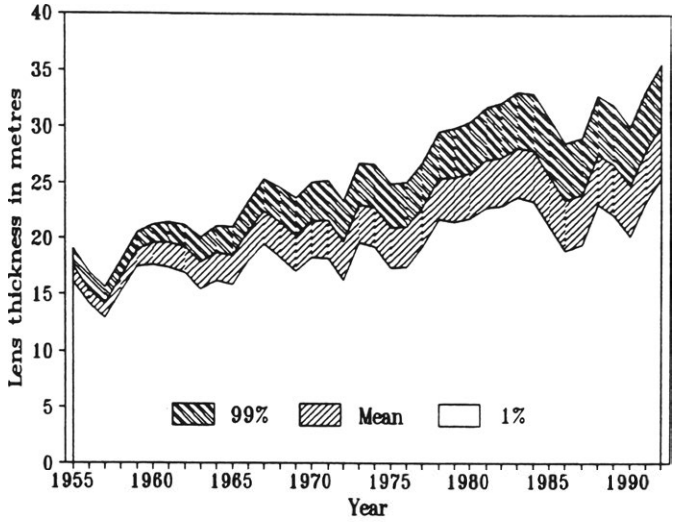

Figure 7.10 The expected, 1% and 99% prediction limits of the lens thickness using Monte Carlo simulation for an extraction rate of 750 m^3/day and 20% vegetation cover

Unlike the deterministic modelling approach shown in Figure 7.7, an extraction rate of 1500 cubic metres per day and 40% vegetation cover is not sustainable if uncertainties in the model parameters are considered. The stochastic-deterministic model results in Figure 7.15 suggests that there is a high probability that the lens thickness will fall below 10 metres, resulting in the freshwater lens being compromised. There is no doubt that from Figures 7.7 and 7.14 that an extraction rate of 1500 cubic metres per day with the existing vegetation cover is not sustainable. From the results obtained for the stochastic-deterministic model, shown in Figures 7.8 to 7.10 the conclusion drawn for the deterministic model results, shown in Figure 7.5 are also valid. An extraction rate of 750 cubic metres per day is sustainable for all vegetation covers. This is not the case for an extraction rate of 1175 cubic metres per day. The deterministic model implies that this extraction rate is sustainable for all vegetation covers. However, the results in Figure 7.11 and 7.12 suggest that this extraction rate is sustainable only if there is 40% or less vegetation cover on the island. The freshwater lens is compromised for 80% vegetation cover.

The situation improves by reducing the vegetation to 40% of the surface area of the island. However, based on the arbitrary criterion, an extraction rate of 1500 cubic metres per day is not sustainable. The extraction rate of 1500 cubic metres per day with 20% vegetation cover is sustainable.

There is a possibility that the freshwater lens may be compromised with 40% vegetation cover. A rational management decision can be made on whether the risks associated with compromising the security of the freshwater lens outweigh the benefits of the extraction rate of 1500 cubic metres per day with 40% vegetation cover. Alternatively, the vegetation could be further reduced to 20% of the surface area of the island. The freshwater lens in this case is never compromised. There is however a tradeoff in the extra security gained by requiring that the vegetation cover be reduced to 20%, that is there will be a loss in coconut production. There are also the additional costs associated with increasing the number of pumping galleries on the island. Currently there are 17 infiltration galleries each having a nominal pumping rate of 750 cubic metres per day. This provides a maximum yield of only 935 cubic metres per day. At least 22 galleries would be required for an extraction rate of 1175 cubic metres per day and 28 for 1500 cubic metres per day.

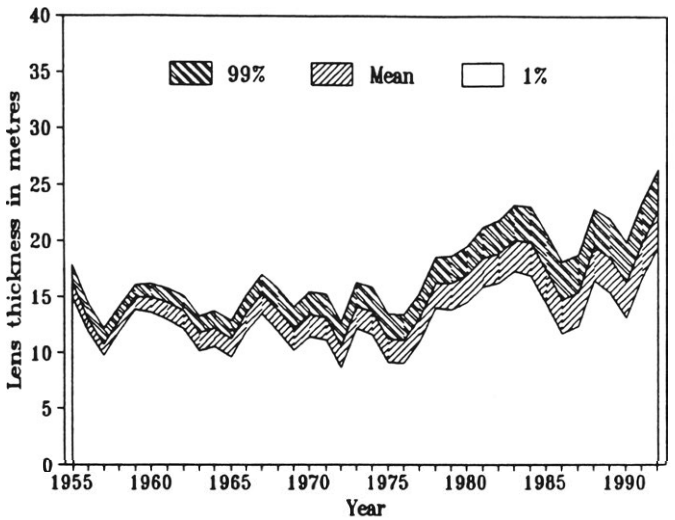

Figure 7.11 The expected, 1% and 99% prediction limits of the lens thickness using Monte Carlo simulation for an extraction rate of 1175 m^3/day and 80% vegetation cover

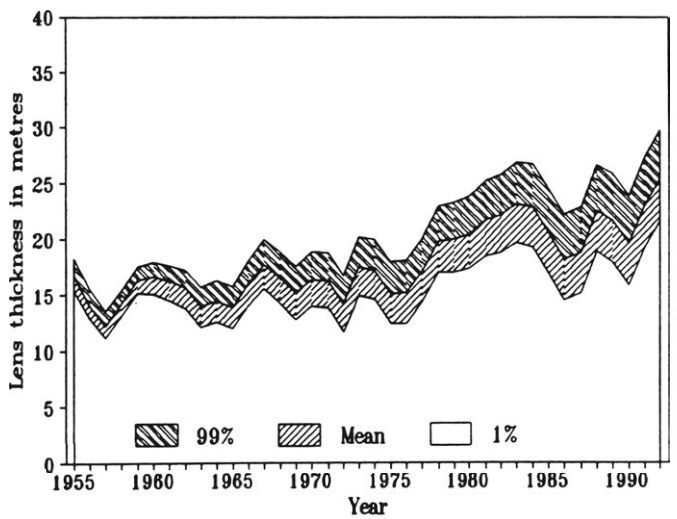

Figure 7.12 The expected, 1% and 99% prediction limits of the lens thickness using Monte Carlo simulation for an extraction rate of 1175 m^3/day and 40% vegetation cover

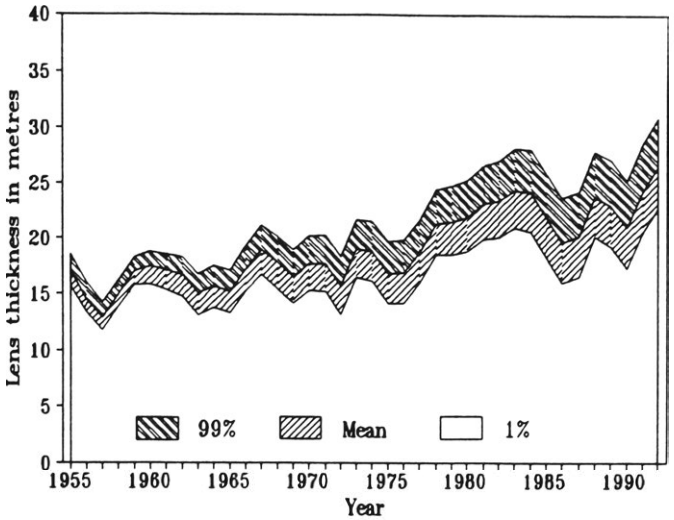

Figure 7.13 The expected, 1% and 99% prediction limits of the lens thickness using Monte Carlo simulation for an extraction rate of 1175 m^3/day and 20% vegetation cover

If the uncertainty in the permeability is ignored, the extraction rate of 1500 cubic metres per day with 80% vegetation cover only would be considered as not sustainable. This would be the conclusions drawn from a deterministic modelling approach which is the only modelling result generally available to managers. Uncertainties in the model parameters are not considered. Decision makers who base their decisions on these results alone may compromise the freshwater lens and jeopardize the survival of the inhabitants on Tarawa.

The decision making process can be refined by incorporating the uncertainties in the modelling process and placing prediction limits on the model response. The results from the stochastic-deterministic model suggests that the removal of the vegetation may not provide the additional yield anticipated. In addition, there is a high probability that the freshwater lens could be compromised because of the uncertainty in the model parameters.

These results illustrate the importance the influence of uncertainties in the model parameters have in the decision making process.

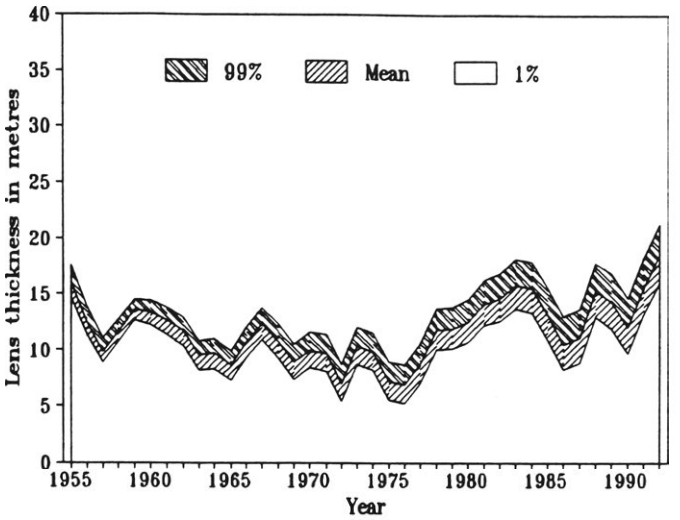

Figure 7.14 The expected, 1% and 99% prediction limits of the lens thickness using Monte Carlo simulation for an extraction rate of 1500 m^3/day and 80% vegetation cover

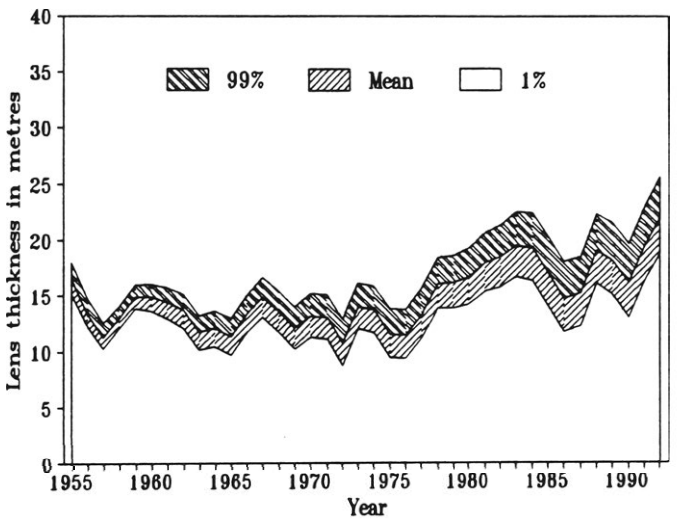

Figure 7.15 The expected, 1% and 99% prediction limits of the lens thickness using Monte Carlo simulation for an extraction rate of 1500 m^3/day and 40% vegetation cover

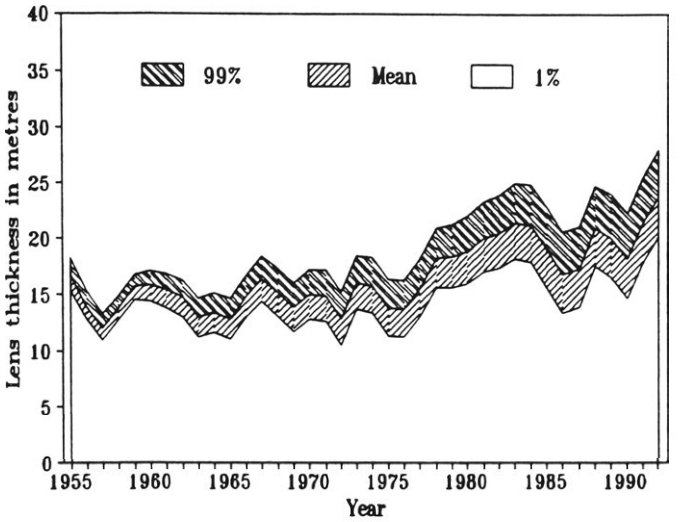

Figure 7.16 The expected, 1% and 99% prediction limits of the lens thickness using Monte Carlo simulation for an extraction rate of 1500 m^3/day and 20% vegetation cover

Chapter 8.

Conclusions and recommendations

A number of techniques for incorporating parameter uncertainty in a model's response have been examined using hypothetical examples and a case study. The consequences of ignoring these uncertainties on the decision making process has been demonstrated using a case study.

The importance of adopting a single-random-variable and the random field modelling approach for establishing the influence of spatially random variables on the response of a model has also been demonstrated. The random field model is the most appropriate for many water resources problems. The single-random-variable model overestimates the variability of the model response.

The reliability techniques that have been considered in this study include; (*i*) first-order analysis, (*ii*) point estimate method and (*iii*) Monte Carlo simulation.

First-order analysis is generally the simplest and involves significantly less computational effort than other reliability techniques involving correlated random variables. First-order analysis is exact if the model response is linear. If the model response is nonlinear then reasonably accurate results are obtained only when the coefficient of variation of the random variables is small.

The point estimate method is not as efficient as first-order analysis. With a moderate number of variables it is potentially more efficient than Monte Carlo simulation in many practical problems. It gives an exact expected value of a fourth-order multivariate polynomial, exact variance for a second-order polynomial and exact skewness and kurtosis for a linear function. There is no need to generate realizations for the random variables in the point estimate method and the correlation structure of the process is considered explicitly in the method. Very few assumption have been made about the distributions of the random variables in the point estimate method. It is applicable to both Gaussian and non-Gaussian random variables. The point estimate method is suitable for problems with a few random variables such as one-dimensional problems. For higher dimensional problems, the point estimate method is computationally expensive. In addition, the point estimate method may not provide accurate estimates of the higher-order statistical moments if the model response is highly nonlinear.

First-order analysis and the point estimate method only provide estimates of the statistical moments of the model response. If the prediction limits are required curve fitting techniques are required to estimate the probability density function of the model response using these statistical moments.

Monte Carlo simulation provides an approximation to the distribution of the model response. It is a powerful technique and intuitively appealing. It is a very flexible method that can be applied to solve a wide variety of problems. There are a number of techniques for generating the random field with the desired statistical properties required in Monte Carlo simulation if the random variables are spatially correlated. These include; (*i*) *matrix decomposition*, (*ii*) *spectral*, (*iii*) the *nearest neighborhood approach*, (*iv*) *turning bands* and (*v*) the *circulant embedding approach*.

Current approaches to generating random fields usually involve the generation of a stationary Gaussian process. The non-parametric Kernel filtering can be used with stationary Gaussian random field generators to produce realizations for any distribution. This was demonstrated using measured data in the case study.

Matrix decomposition via Cholesky factorization is exact and does not require stationarity. The prohibitively large storage requirements of matrix methods, for moderate number of random variables, prevent their generalized use. Even with a modest grid size the computational resources are very demanding. Multi-dimensional simulations are usually generated by alternative methods for this reason.

A major advantage of the spectral method is that it is not restricted to evenly spaced observations and it can be extended to multi-dimensional applications. However, the spectral method is approximate and is only asymptotically exact. The use of the spectral method requires careful analysis and fine tuning of parameters if spurious features in the resulting realizations are to be avoided. Furthermore, the method requires explicit knowledge of the spectral density function of the covariance function.

The nearest neighbor method may not produce a stationary process and it is difficult to specify a desired covariance structure *a priori*. Although it is possible to preserve the covariance structure in the principal directions of the grid, there is some doubt that it will be preserved on the diagonal.

The turning bands method for simulating isotropic Gaussian processes is also an approximate method because it depends on the application of the central limit theorem. Although it is only necessary to generate line processes in this method, it is restricted to particular forms of the covariance function.

The circulant embedding approach produces realizations with exactly the desired covariance structure. It can handle large problems efficiently and for practical problems there is no restriction on the covariance function that can be used. The only conditions required for this approach to be valid are; (*i*) the sampling grid is regular, (*ii*) the random field is stationary, and (*iii*) the embedding circulant matrix is non-negative definite.

Non-negativeness of the circulant matrix can often be achieved by making the matrix sufficiently large. Otherwise the method can approximate a stationary Gaussian field. The circulant matrix should be highly compact to achieve full efficiency of the fast Fourier transform.

For the one-dimensional backwater profile problem considered, the circulant embedding approach required more than three times the computational effort required by the matrix decomposition method. The spectral method is the most expensive means of generating the random fields. Therefore, for this and similar one-dimensional problems, the matrix decomposition method is the preferred method for generating the realizations required in the Monte Carlo simulation. This may not be the case for higher dimensional problems or problems with more random variables. The circulant embedding approach may be more appropriate in this case.

For simpler problems, where the model response seems to be linear, the point estimate method, first-order analysis and Monte Carlo simulation produce very similar results for the expected model response and for the 5% and 95% prediction limits.

Estimating the prediction limits of the thickness of a freshwater lens on Bonriki was chosen as the case study. The permeability of the aquifer, which is required by the groundwater model used to simulate the behaviour of the lens, was treated as a random variable.

Neither the measured permeabilities on Bonriki nor the *ln*-transformed values satisfy the normality assumption. The non-parametric Kernel filtering estimators were successfully used to obtain normality in the data.

Despite the amount of permeability data recorded on Bonriki, it was not possible to establish the correlation function or the correlation distance for the data. These were however, assumed.

Based on the difficulties encountered in estimating the correlation structure of the data measured on Bonriki, a suitable monitoring strategy for estimating the spatial correlation structure of the data has been suggested. The monitoring boreholes should be drilled on a uniform grid and the number of boreholes should be significantly increased. The permeability should be measured at the same frequency and depth in each bore.

First-order analysis, point estimate method and Monte Carlo simulation were used to estimate the prediction limits of the freshwater lens.

The circulant embedding approach was used to generate the two-dimensional realizations of permeabilities required by the sharp interface single aquifer model in Monte Carlo simulation. The computational effort required to generate a single realization of the random field is only a fraction of the time required to solve the equations describing the behaviour of the freshwater lens. The computational effort required by Monte Carlo simulation is approximately twice that required by first-order analysis.

The point estimate method requires considerable more computing resources than either first-order analysis or Monte Carlo simulation. Therefore, the point estimate method is an inappropriate method for this problem because of the number of simulations required.

Despite the fact that first-order analysis estimates the variability about a single sample from the population and Monte Carlo simulation provides an approximation of the true expected value of the model response, the expected values predicted by both methods for practical purposes are very similar. However, first-order analysis significantly overestimated the variance of the model response for this problem and has produced prediction limits of the lens thickness that are physically unrealistic. First-order analysis is not an appropriate method for estimating the confidence interval of the model response for this problem. Only Monte Carlo simulation produced physically plausible results.

The choice of reliability models depends on the accuracy and the type of results required. First-order analysis is the preferred method for relatively simple problems in one-dimension followed by the point estimate method. Both techniques are recommended for practical problems where the response of the model is approximately linear. However, it would be prudent to verify the first-order analysis with one of the other reliability methods. Monte Carlo simulation should be used for highly nonlinear problems.

The results of the case study suggest that Monte Carlo simulation is robust, efficient and provides results that are physically plausible. It should therefore be considered as the most reliable method for estimating the prediction limits of a model response.

Monte Carlo simulation only was used to estimate the prediction limits of the thickness of the freshwater lens for various management strategies. A management strategy for increasing the extraction rate of freshwater from the lens is to reduce the amount of vegetation on Bonriki. Increasing the extraction rate and the vegetation cover reduces the thickness of the freshwater lens. By using the

subjective criterion that the sustainability of the freshwater lens is not compromised when the thickness of the freshwater lens falls below 10 metres, an extraction rate of up to 1175 cubic metres per day is sustainable for the full range of vegetation cover considered. Both the deterministic and stochastic-deterministic modelling approach indicate that maintaining an extraction rate of 1500 cubic metres per day with 80% vegetation cover will compromise the viability of the freshwater lens. Therefore, this and larger extraction rates are not sustainable for the existing vegetation cover. The deterministic model indicates that the situation improves by reducing the vegetation to 40% of the surface area of the island. The extraction rate of 1500 cubic metres per day with 20% vegetation cover is sustainable.

Unlike the deterministic modelling approach, an extraction rate of 1500 cubic metres per day and 40% vegetation cover is not sustainable if uncertainties in the model parameters are considered. The stochastic-deterministic model results indicate that there is a high probability that the lens thickness will fall below 10 metres resulting in the freshwater lens being compromised. An extraction rate of 750 cubic metres per day is sustainable for all vegetation covers. This is not the case for an extraction rate of 1175 cubic metres per day. The deterministic model implies that this extraction rate is sustainable for all vegetation covers. However, the results from the stochastic-deterministic model suggest that this extraction rate is sustainable only if there is 40% or less vegetation cover on the island. The freshwater lens is compromised for 80% vegetation cover.

If the uncertainty in the permeability is ignored, the extraction rate of 1500 cubic metres per day with 80% vegetation cover only would be considered as not sustainable. This would be the conclusion drawn from a deterministic modelling approach, which is the only modelling result usually available to managers. Uncertainties in the model parameters are not considered. The decision making process can be refined by incorporating the uncertainties in the modelling process and placing prediction limits on the model response. The results from the stochastic-deterministic model suggests that the removal of the vegetation may not provide the additional yield anticipated. In addition, there is a high probability that the freshwater lens could be compromised because of the uncertainty in the model parameters. Decision makers who base their decisions on deterministic models alone may compromise the freshwater lens and jeopardize the survival of the inhabitants on Tarawa.

The results for the case study illustrate the importance uncertainties in the model parameters have in influencing the decision making process.

Future work should involve including uncertainties from other model parameters such as rainfall and porosity in the analysis and the use of more sophisticated groundwater models to predict the behaviour of the freshwater lens. Attempts should be made to obtain improved estimates of the covariance structure of the permeability.

Finally, a framework for the assessment of the influence of uncertainty in the modelling process has been demonstrated using hypothetical studies and a case study.

Chapter 9.

References

Ababou, R., (1991) 'Three-Dimensional Flow in Heterogeneous Geologic Media: High-Resolution Simulations', *International Hydrology and Water Resources Symposium, Institution of Engineers, Australia*, Publication No. 91/22, 725-731.

Anderson, M.P., (1976) 'Unsteady Groundwater Flow Beneath Strip Oceanic Islands', *Water Resources Research*, 12(4), 640-644.

Ang, A.H.S. and W.H. Tang, (1984) *Probability Concepts in Engineering Planning and Design, Vol. II-Decision, Risk and Reliability*, John Wiley and Sons, New York.

Anthony, S.S., (1987) 'Hydrogeochemistry of a Small Limestone Island: Laura, Majuro Atoll, Marshall Islands, Master's thesis, Department of Geology and Geophysics, *University of Hawaii at Manoa, Honolulu.*

Ayers, J.F. and H.L. Vacher, (1983) 'A Numerical Model Describing Unsteady Flow in a Fresh Water Lens', *Water Resources Bulletin, American Water Resources Association*, 19(5), 785-792.

Ayers, J.F. and H.L. Vacher, (1986) 'Hydrogeology of an Atoll Island: A Conceptual Model from Detailed Study of a Micronesia Example', *Ground Water*, 24(2), 185-198.

Bartlett, M.S., (1975) *The Statistical Analysis of Spatial Pattern*, Chapman and Hall, London.

Bellin, A., P. Salandin and A. Rinaldo, (1992) 'Simulation of Dispersion in Heterogeneous Porous Formulations: Statistics, First-Order Theories, Convergence of Computations', *Water Resources Research*, 28(9), 2211-2227.

Black, T.C. and D.L. Freyberg, (1990) 'Simulation of One-Dimensional Correlated Fields Using a Matrix-Factorization Moving Average Approach' *Mathematical Geology*, 22(1), 39-62.

Box, G.E.P. and D.R. Cox, (1964) 'An Analysis of Transformations', *Journal of the Royal Society*, 26, Series B, 211-246.

Box, G.E.P. and G.M. Jenkins, (1976) '*Time Series Analysis: Forecasting and Control*', Holden-Day, San Francisco.

Bras, R.L. and I. Rodríguez-Iturbe, (1976a) 'Rainfall Generation: A Nonstationary Time-Varying Multidimensional Model', *Water Resources Research*, 12(3), 450-456.

Bras, R.L. and I. Rodríguez-Iturbe, (1976b) 'Evaluation of Mean Square Error Involved in Approximating the Areal Average of a Rainfall Event by a Discrete Summation', *Water Resources Research*, 12(2), 181-184.

Bras, R.L. and I. Rodríguez-Iturbe, (1985) *Random Functions and Hydrology*, Addison-Wesley, Reading.

Brockwell, P.J. and R.A. Davis, (1991) *Time Series: Theory and Methods*, Springer-Verlag, Second Edition, New York.

Brooker, P.I., (1985) 'Two-Dimensional Simulation by Turning Bands', *Mathematical Geology*, 17(1), 81-90.

Brooker, P.I. and M.A. Stewart, (1993) 'Comparison of Methods of Simulation of Spatially Correlated Variables Obeying Exponential Covariance Structure in Two Dimensions', *International Congress on Modelling and Simulation*, Eds., M. McAleer and A. Jakeman, 3, 1259-1264.

Burges, S.J. and D.P. Lettenmaier, (1975) 'Probabilistic Methods in Stream Quality Management', *Water Resources Bulletin, American Water Resources Association*, 11(1), 115-130.

Burgess, S.M., (1987) 'The Climate and Weather of Western Kiribati', New Zealand Meteorological Service, Wellington, New Zealand, Report No. 188(7).

Byers, E. and D.B. Stephens, (1983) 'Statistical and Stochastic Analyses of Hydraulic Conductivity and Particle-Size in a Fluvial Sand', *Journal of the Soil Science Society of America*, 47(6), 1072-1081.

Cesare, M.A., (1991) 'First-Order Analysis of Open-Channel Flow', *Journal of Hydraulic Engineering, American Society of Civil Engineers*, Technical Note, 117(2), 242-247.

Chadderton, R.A., A.C. Miller and A.J. McDonnell, (1982) 'Uncertainty Analysis of Dissolved Oxygen Model', *Journal of the Environmental Engineering Division, American Society of Civil Engineers*, 108(EE5), 1003-1013.

Chan, G. and A.T.A. Wood, (1994) 'An Algorithm for Simulating Stationary Gaussian Random Fields', *Applied Satistics*, Series B, Submitted.

Chapman, T.G., (1985) 'The Use of Water Balances for Water Resources Estimation, with Special Reference to Small Islands', *Australian International Development Assistance Bureau*, Bulletin No. 4.

Chatfield, C., (1989) '*The Analysis of Time Series: An Introduction*', Fourth Edition, Chapman and Hall, London.

Chidley, T.R.E. and J.W. Lloyd, (1977) 'A Mathematical Model Study of Fresh-Water Lenses', *Ground Water*, 15(3), 215-222.

Chidley, T.R.E. and J.W. Lloyd, (1979) 'The Hydrogeological Assessment of Freshwater Lenses in Oceanic Islands', *Proceedings of the Third International Hydrology Symposium in Theoretical and Applied Hydrology*, Fort Collins, Colorado, 232-245.

Cressie, N.A.C., (1993) *Statistics for Spatial Data*, John Wiley and Sons, New York.

Daniell, T.M., (1983) 'Investigations Employed for Determining Yield of the Groundwater Resources of Tarawa Atoll, Kiribati', *Proceedings of the Meeting on Water Resources Development in the South*

Pacific, United Nations, Water Resources Series No. 57, Chapter IV, 108-120.

Davies, R.B. and D.S. Harte, (1987) 'Tests for Hurst Effect', *Biometrika*, 74(1), 95-101.

Davis, M.W., (1987) 'Generating Large Stochastic Simulations-The Matrix Polynomial Approximation Method', *Mathematical Geology*, 19(2), 99-107.

Delhomme, J.P., (1979) 'Spatial Variability and Uncertainty in Groundwater Flow Parameters: A Geostatistical Approach', *Water Resources Research*, 15(2), 269-280.

Dettinger, M.D. and J.L. Wilson, (1981) 'First Order Analysis of Uncertainty in Numerical Models of Groundwater Flow Part 1. Mathematical Development', *Water Resources Research*, 17(1), 149-161.

DHC (1982) 'Kiribati-Tarawa Water Resources: Pre-Design Study', *Australian Government, Department of Housing and Construction*, Unpublished Report.

Dietrich, C.R., (1993) 'Computationally Efficient Cholesky Factorization of a Covariance Matrix with Block Toeplitz Structure', *Journal of Statistics Computation and Simulation*, 45(3/4), 203-218.

Dietrich, C.R. and G.N. Newsam, (1993) 'A Fast and Exact Method for Multidimensional Gaussian Stochastic Simulations', *Water Resources Research*, 29(8), 2861-2869.

Epstein, B., (1948) 'Some Applications of the Mellin Transform in Statistics', *The Annals of Mathematical Statistics*, 19(2), 370-379.

Essaid, H.I., (1990) 'The Computer Model SHARP, A Quasi-Three-Dimensional Finite-Difference Model to Simulate Freshwater and Saltwater Flow in Layered Coastal Aquifer Systems', *U.S. Geological Survey*, Water Resources Investigations, Report No. 90-4130.

Evans, D.H., (1967) 'An Application of Numerical Integration Techniques to Statistical Tolerancing', *Technometrics*, 9(3), 441-456.

Evans, D.H., (1972) 'An Application of Numerical Integration Techniques to Statistical Tolerancing, III-General Distributions', *Technometrics*, 14(1), 23-35.

Falkland, A.C., (1983) 'Christmas Island (Kiritimati) Water resources Study, Volume 1, General Report', *The Australian Department of Housing and Construction*, Vol. 1, Unpublished Report.

Falkland, A.C., (1991) 'Water Resources Development and Management in Small Islands', Chapter 5, *Hydrology and Water Resources of Small Islands: A Practical Guide, UNECSO*, A.C. Falkland, Ed., 201-317.

Falkland, A.C., (1992) 'Review of Tarawa Freshwater Lenses', *Australian Capital Territory Electricity and Water, Hydrology and Water Resources Branch*, Unpublished Report.

Falkland, A.C., (1994) 'Management of Freshwater Lenses on Small Coral Islands', *Institution of Engineers, Australian*, Water DownUnder '94, Report No. NCP 94/10, 417-422.

Fishman, G.S., (1978) *Principles of Discrete Event Simulation*, John Wiley and Sons, New York.

Freeze, R.A., (1975) 'A Stochastic-Conceptual Analysis of One-Dimensional Groundwater Flow in Nonuniform Homogeneous Media', *Water Resources Research*, 11(5), 725-741.

Garen, D.C. and S.J. Burges, (1981) 'Approximate Error Bounds for Simulated Hydrographs', *Journal of the Hydraulics Division, American Society of Civil Engineers*, 107(HY11), 1519-1534.

George, A. and J.W.H. Liu, (1981) *Computer Solution of Large Sparse Positive Definite Systems*, Prentice-Hall, Ingelwood, New Jersey.

Ghassemi, F., (1994) Personel communication.

Ghassemi, F., A.J. Jakeman and G. Jacobson, (1990) 'Mathematical Modelling of Sea Water Intrusion, Nauru Island', *Hydrological Processes*, 4(3), 269-281.

Ghyben, W.B., (1888) 'Nota in Verband Met de Voorgenomen Putboring Nabij Amsterdam (Notes on the Probable Results of the Propsed Well Drilling Near Amsterdam)', *Tijdschrift van Let Koninklijk Instituut van Ingenieurs*, The Hague, 8-22.

Gotway, C.A., (1994) 'The Use of Conditional Simulation in Nuclear-Waste-Site Performance Assessment', *Technometrics*, 36(2), 129-141.

Griggs, J.E. and F.L. Peterson, (1989) 'Groundwater Flow and Development Alternatives: A Numerical Simulation of Laura, Majuro Atoll, Marshall Islands', *Water Resources Research Center, University of Hawaii*, Manoa, Honolulu, Technical Report No. 183.

Hahn, G.J., and S.S. Shapiro, (1967) *Statistical models in engineering*, John Wiley and Sons, New York.

Härdle, W., (1990) *Applied Nonparametric Regression*, Cambridge University Press, Cambridge.

Harr, M.E., (1989) 'Probabilistic Estimates for Multivariate Analysis', *Applied Mathematical Modelling*, 13(5), 313-318.

Hasofer, A.M., (1993) 'Simulation of Random Fields', *Proceedings of the Conference on Probabilistic Methods in Geotechnical Engineering*, K.S. Li. and S-C.R. Lo., Eds., A.A. Balkema, Rotterdam, 45-48.

Henderson, F.M., (1966) *Open Channel Flow*, McMillan Co., New York.

Herman, M.E., R.W. Buddemeier and S.W. Wheatcraft, (1986) 'A Layered Aquifer Model of Atoll Island Hydrology: Validation of a Computer Simulation', *Journal of Hydrology*, 84(3/4), 303-322.

Herzberg, B., (1901) 'Die Wasserversorgung Einiger Nordseebader (The Water Supply on Parts of the North Sea Coast in Germany)', *Journal, Gasbeleuchtung und Wasserversorgung*, Munich, 44, 815-819.

Hill, I.D., R. Hill and R.L. Holder, (1976) 'Algorithm AS 99 Fitting Johnson Curves by Moments', *Applied Statistics*, 25(2), 180-189.

Huang, K.Z., (1986) 'Reliability Analysis on Hydraulic Design of Open Channel', *Stochastic and Risk*

Analysis in Hydraulic Engineering, Water Resources Publication, B.C. Yen Ed., 59-65.

Hunt, B., (1979) 'An Analysis of the Groundwater Resources of Tongatapu Island, Kingdom of Tonga, *Journal of Hydrology*, 40(1/2), 185-196.

Hunt, C.D. and F.L. Peterson, (1980) 'Groundwater Resources of Kwajalein Island, Marshall Islands', *Water Resources Research Centre, University of Hawaii*, Manoa, Honolulu, Technical Report No. 126.

Jacobson, G., (1976) 'The Freshwater Lens on Home Island in the Cocos (Keeling) Islands', Bureau of Mineral Resources, *Journal Australian Geology and Geophysics*, 1(4), 335-343.

Jaffe, P.R. and F.L. Parker, (1984) 'Uncertainty Analysis of First-Order Decay Model', *Journal of the Environmental Engineering, American Society of Civil Engineers*, 110(1), 131-140.

Johnson, N.L., (1949) 'Systems of Frequency Curves Generated by Methods of Translation', *Biometrika*, 36(1/2), 149-176.

Jones, L. (1990) 'Explicit Monte Carlo Simulation Head Moment Estimates for Stochastic Confined Groundwater Flow', *Water Resources Research*, 26(6), 1145-1153.

Journel, A.G. and Ch.J. Huijbregts, (1978) *Mining Geostatistics*, Academic Press, London.

Kendall, M., A. Stuart and J.K. Ord, (1987) *Kendall's Advanced Theory of Statistics, Volume 1: Distribution Theory*, Fifth Edition, Charles Griffin and Co., London.

King, P.R. and P.J. Smith, (1988) 'Generation of Correlated Properties in Heterogeneous Porous Media', *Mathematical Geology*, 20(7), 863-877.

Kipp, K.L., (1987) 'HST 3D: A Computer Code for Simulation of Heat and Solute Transport in Three Dimensional Ground-Water Flow Systems', *United States Geological Survey*, Water Resources Investigations, Report No. 86-4095.

Larson, H.J., (1973) *Introduction to the Theory of Statistics*, John Wiley and Sons, New York.

Leduc, R., T.E. Unny and E.A. McBean, (1986) 'Stochastic Model of First-order BOD Kinetics', *Water Research*, 20(5), 625-632.

Leduc, R., T.E. Unny and E.A. McBean, (1988) 'Stochastic Models for First-order Kinetics of Biochemical Oxygen Demand with Random Initial Conditions, Inputs, and Coefficients', *Applied Mathematical Modelling*, 12(6), 565-572.

Li, K.S., (1991) 'A Point Estimate Method for Calculating Statistical Moments', *University College, Australian Defence Force Academy, The University of New South Wales*, Research Report No. R93.

Li, K.S., (1992) 'Point-Estimate Method for Calculating Statistical Moments', *Journal of Engineering Mechanics, American Society of Civil Engineers*, 118(7), 1506-1511.

Li, K.S. and P. Lumb, (1985) 'Reliability Analysis by Numerical Integration and Curve Fitting',

Structural Safety, 3, 29-36.

Li, S.G. and D. McLaughlin, (1991) 'A Nonstationary Spectral Method for Solving Stochastic Groundwater Problems: Unconditional Analysis', *Water Resources Research*, 27(7), 1589-1605.

Lloyd, J.W., J.C. Miles, G.R. Chessman and S.F. Bugg, (1980) 'A Ground Water Resources Study of a Pacific Ocean Atoll-Tarawa, Gilbert Islands', *Water Resources Bulletin, American Water Resources Association*, 16(4), 646-653.

Malone, R., D.S. Bowles, M.P. Windham and W.J. Grenney, (1983) 'Comparison of Techniques for Assessing Effects of Loading Uncertainty Upon a Long Term Phosphorous Model', *Applied Mathematical Modelling*, 7(1), 11-18.

Mantoglou, A. and J.L. Wilson, (1982) 'The Turning Bands Method for Simulation of Random Fields Using Line Generation by a Spectral Method', *Water Resources Research*, 18(5), 1379-1394.

de Marsily, G., (1986) *Quantitative Hydrogeology: Groundwater Hydrology for Engineers*, Academic Press, San Diego.

Matheron, G., (1973) 'The Intrinsic Random Functions and their Applications', *Advances in Applied Probability*, 5, 439-468.

Mejía, J.M. and I. Rodríguez-Iturbe, (1974) 'On the Synthesis of Random Field Sampling from the Spectrum: An Application to the Generation of Hydrologic Spatial Processes', *Water Resources Research*, 10(4), 705-711.

Melching, C.S. and B.C. Yen, (1986) 'Slope Influence on Storm Sewer Risk', *Stochastic and Risk Analysis in Hydraulic Engineering*, Water Resources Publications, B.C. Yen, Ed., 79-89.

Melching, C.S., B.C. Yen and H.G. Wenzel, (1991) 'Output Reliability as Guide for Selection of Rainfall-Runoff Models', *Journal of Water Resources Planning and Management, American Society of Civil Engineers*, 117(3), 383-398.

Miller, S.M. and L.E. Borgman, (1985) 'Spectral-Type Simulation of Spatially Correlated Fracture Set Properties', *Mathematical Geology*, 17(1), 41-52.

Mink, J.F., (1976) 'Groundwater Resources of Guam: Occurrence and Development', *Water Resources Research Centre, University of Guam*, Technical Report No. 1.

Moon, Y.I. and U. Lall, (1994) 'Kernel Quantile Function Estimator for Flood Frequency Analysis', *Water Resources Research*, 30(11), 3095-3103.

Murphy, P., (1981) 'Tarawa Water Supply Investigation', *Department of Housing and Construction*, Central Investigation and Research Laboratory, Major Report No. 232.

Park, C.S., (1987) 'The Mellin Transform in Probabilistic Cash Flow Modeling', *The Engineering Economist*, 32(2), 115-134.

Prickett, T.A. and C.G. Lonnquist, (1971) 'Selected Digital Computer Techniques for Groundwater

Resource Evaluation', *Illinois State Water Survey*, Urbana, Bulletin 55.

Rice, S.O., (1954) 'Mathematical Analysis of Random Noise', *Selected Papers on Noise and Stochastic Processes*, N. Wax, Ed., Dover, New York, 133-294.

Robinson, P.C. and Maul P.R., (1991) 'Some Experience with the Numerical Inversion of Laplace Transforms', *Mathematical Engineering with Industrial Applications*, 3(2), 111-131.

Rodríguez-Iturbe, I., D.R. Cox, and P.S. Eagleson, (1986) 'Spatial Modelling of Total Storm Rainfall', *Proceedings of the Royal Society of London*, Mathematics and Physical Sciences, Series A, 403, 27-50.

Rosenblueth, E., (1975) 'Point Estimates for Probability Moments', *Proceedings, National Academy of Science and Mathematics*, 72(10), 3812-3814.

Rosenblueth, E., (1981) 'Point Estimates for Probability', *Applied Mathematical Modelling*, 5(5), 329-335.

Rubin, Y., G. Mavko and J. Harris, (1992) 'Mapping Permeability in Heterogeneous Aquifers Using Hydrologic and Seismic Data', *Water Resources Research*, 28(7), 1809-1816.

Russo, D. and E. Bresler, (1981) 'Soil Hydraulic Properties as Stochastic Processes: I. An Analysis of Field Spatial Variability', *Journal of the Soil Science Society of America*, 45(4), 682-687.

Sagar, B., (1978) 'Galerkin Finite Element Procedure for Analyzing Flow Through Random Media', *Water Resources Research*, 14(6), 1035-1044.

Satish, M.G. and J. Zhu, (1994) 'Stochastic Analysis of Ground-Water Flow in Semiconfined Aquifer', *Journal of Hydraulic Engineering, American Society of Civil Engineers*, 120(2), 147-168.

Scavia, D., W.F. Powers, R.P. Canale and J.L. Moody, (1981) 'Comparison of First-Order Error Analysis and Monte Carlo Simulation in Time-Dependent Lake Eutrophication Models', *Water Resources Research*, 17(4), 1051-1059.

Schweppe, F.C., (1973) *Uncertain Dynamic Systems*, Prentice-Hall, Englewood Cliffs, New Jersey.

Shinozuka, M., (1971) 'Simulation of Multivariate and Multi-dimensional Random Processes, *Journal of the Acoustical Society of America*, 49(1), 357-367.

Shinozuka, M. and C.M. Jan, (1972) 'Digital Simulation of Random Processes and Its Applications', *Journal of Sound and Vibration*, 25(1), 111-128.

Silverman, B.W., (1986) *Density Estimation for Statistics and Data Analysis*, Chapman and Hall, London.

Sisson, J.B. and P.J. Wierenga, (1981) 'Spatial Variability of Steady-State Infiltration Rates as a Stochastic Process', *Journal of the Soil Science Society of America*, 45(4), 699-704.

Smith, L. and R.A. Freeze, (1979a) 'Stochastic Analysis of Steady State Groundwater Flow in a Bounded Domain 1. One-Dimensional Simulations', *Water Resources Research*, 15(3), 521-528.

Smith, L. and R.A. Freeze, (1979b) 'Stochastic Analysis of Steady State Groundwater Flow in a Bounded Domain 2. Two-Dimensional Simulations', *Water Resources Research*, 15(6), 1543-1559.

Smith, L. and F.W. Schwartz, (1981) 'Mass Transport 2. Analysis of Uncertainty in Prediction', *Water Resources Research*, 17(2), 351-369.

Solomon, H. and M.A. Stephens, (1978) 'Approximations to Density Functions Using Pearson Curves', *Journal, American Society of Statisticians*, 73(361), 153-160.

Sudicky, E.A., (1986) 'A Natural Gradient Experiment on Solute Transport in a Sand Aquifer: Spatial Variability of Hydraulic Conductivity and Its Role in the Dispersion Process', *Water Resources Research*, 22(13), 2069-2082.

Tang, W.H. and B.C Yen, (1972) 'Hydrologic and Hydraulic Design Under Uncertainties', *Proceedings of the International Symposium on Uncertainty in Hydrology and Water Resources Systems*, Tucson, Arizona, 2, 868-882.

Tang, W.H., L.W. Mays, and B.C. Yen, (1975) 'Optimal Risk Based Design of Storm Sewer Network' *Journal of the Environmental Engineering Division, American Society of Civil Engineers*, 101(EE3), 381-398.

Tompson, A.F.B., R. Ababou and L.W. Gelhar, (1989) 'Implementation of the Three-Dimensional Turning Bands Random Field Generator', *Water Resources Research*, 25(10), 2227-2243.

Touran, A. and E.P. Wiser, (1992) 'Monte Carlo Technique with Correlated Random Variables', *Journal of Construction Engineering and Management, American Society of Civil Engineers*, 118(2), 258-272.

Townley, L.R. and J.L. Wilson, (1985) 'Computationally Efficient Algorithms for Parameter Estimation and Uncertainty Propagation in Numerical Models of Groundwater Flow', *Water Resources Research*, 21(12), 1851-1860.

van Trease, H., (1993) 'Atoll Politics: The Republic of Kiribati', *Macmillan Brown Centre for Pacific Studies, University of Canterbury*, New Zealand.

Tumeo, M.A. and G.T. Orlob, (1989) 'An Analytic Technique for Stochastic Analysis in Environmental Models', *Water Resources Research*, 25(12), 2417-2422.

Tung, Y.K., (1987) 'Uncertainty Analysis of National Weather Service Rainfall Frequency Atlas', *Journal of Hydraulic Engineering, American Society of Civil Engineers*, 113(2), 179-189.

Tung, Y.K., (1988) 'Effects of Uncertainty on Optimal Risk-Based Design of Hydraulic Structures', *Journal of Water Resorces Planning and Management, American Society of Civil Engineers*, 113(5), 709-722.

Tung, Y.K., (1989) 'Uncertainty on Travel Time in Kinematic Wave Channel Routing', *Proceedings of the International Conference on Channel Flow and Catchment Runoff: Centennial of Manning's Formula and Kuichling's Rational Formula, American Society of Civil Engineers*, University of Virginia, B.C. Yen, Ed., 767-781.

Tung, Y.K., (1990) 'Mellin Transform Applied to Uncertainty Analysis in Hydrology/Hydraulics', *Journal of Hydraulic Engineering, American Society of Civil Engineers*, 116(5), 659-674.

Tung, Y.K. and L.W. Mays, (1980) 'Risk Analysis for Hydraulic Design', *Journal of the Hydraulics Division, American Society of Civil Engineers*, 106(HY5), 893-913.

Tung, Y.K. and L.W. Mays, (1981) 'Risk Models for Flood Levee Design', Water Resources Research, 17(4), 833-841.

Underwood, M.R., F.L. Peterson and C.I. Voss, (1992) 'Groundwater Lens Dynamics of Atoll Islands', *Water Resources Research*, 28(11), 2889-2902.

Ünlü, K., (1994) 'Assessing Risk of Ground-Water Pollution from Land-Disposed Wastes', *Journal of Environmental Engineering, American Society of Civil Engineers*, 120(6), 1578-1597.

Unny, T.E., (1984) 'Numerical Integration of Stochastic Differential Equations in Catchment Modeling', *Water Resources Research*, 20(3), 360-368.

Vacher, H.L., (1988) 'Dupuit-Ghyben-Herzberg Analysis of Strip-Island Lenses, *Bulletin, Geological Society of America*, 100(4), 580-591.

Vanmarcke, E.H. and M. Grigoriu, (1983) 'Stochastic Finite Element Analysis of Simple Beams', *Journal of Engineering Mechanics, American Society of Civil Engineers*, 109(5), 1203-1214.

Volker, R.E., M.A. Mariño and D.E. Rolston, (1985) 'Transition Zone Width in Ground Water on Ocean Atolls', *Journal of Hydraulic Engineering, American Society of Civil Engineers*, 111(4), 659-676.

Voss, C.I., (1984) 'SUTRA, Saturated-Unsaturated TRAnsport. A Finite-Element Simulation Model for Saturated-Unsaturated Fluid-Density-Dependent Groundwater Flow with Energy Transport or Chemically Reactive Single-Species Solute Transport', *United States Geological Survey*, Water Resources Investigations, Report No. 84-4369.

Wallis, J.R., N.C. Matalas and J.R. Slack, (1974) 'Just a Moment', *Water Resources Research*, 10(2), 211-219.

Wentworth, C.K., (1951) 'The Problem of Safe Yield in Insular Ghyben-Herzberg System' *Transactions, American Geophysical Union*, 32(5), 739-742.

Wheatcraft, S.W. and R.W. Buddemeier (1981) 'Atoll Island Hydrology', *Ground Water*, 19(3), 311-320.

Whittle, P., (1954) 'On Stationary Processes in the Plane', *Biometrika*, 41(3/4), 434-449.

WHO, (1971) 'International Standards for Drinking-Water', *World Health Organization*, Third Edition, Geneva, Switzerland.

Wood, E.F., (1976) 'An Analysis of the Effects of Parameter Uncertainty in Deterministic Hydrologic Models', *Water Resources Research*, 12(5), 925-932.

Wood, A.T.A. and G. Chan, (1993) 'Simulation of Stationary Gaussian Processes in $[0,1]^d$', *Centre for Mathematics and its Applications, Australian National University*, Research Report CMA-SR06-93.

Wood, A.T.A. and G. Chan, (1994) 'Simulation of Stationary Gaussian Processes in $[0,1]^d$', *Journal of Computational and Graphical Statistics*, 3(4), 409-432.

Woodroffe, C.D., (1989) 'Salt Water Intrusion into Groundwater; An Assessment of Effects on Small Island States Due to Rising Sea Levels', *Small States Conference on Sea Level Rise*, Republic of Maldives, 1-33.

Yen, B.C., S.T. Cheng and C.S. Melching, (1986) 'First Order Reliability Analysis', *Stochastic and Risk Analysis in Hydraulic Engineering*, Water Resources Publications, B.C. Yen, Ed., 1-36.

Yen, B.C., S.T. Cheng, and W.H. Tang, (1980) 'Reliability of Hydraulic Design of Culverts', Proceedings of the International Conference on Water Resources Development, *International Association for Hydraulic Research*, 2, 991-1001, Taipei, Taiwan.

Yen, B.C. and W.H. Tang, (1976) 'Risk-Safety Factor Relation for Storm Sewer Design', Technical Notes, *Journal of the Environmental Engineering Division, American Society of Civil Engineers*, 102(EE2), 509-516.

Yen, B.C. and W.H. Tang, (1977) 'Reliability of Flood Warning', *Stochastic Processes in Water Resources Engineering*, Water Resources Publications, Colorado, 333-347.

Yen, C.C. and G.L. Guymon, (1990) 'An Efficient Deterministic-Probabilistic Approach to Modelling Regional Groundwater Flow, 1: Theory', *Water Resources Research*, 26(7), 1559-15567.

Zielinski, P.A., (1988) 'Stochastic Dissolved Oxygen Model', *Journal of Environmental Engineering, American Society of Civil Engineering*, 114(1), 74-90.

Zoppou, C. and K.S. Li, (1992) 'Estimation of Uncertainty in Hydrology Using Reliability Theory', *University College, Australian Defence Force Academy, The University of New South Wales*, Research Report No. R127.

Zoppou, C. and K.S. Li, (1993) 'New Point Estimate Method for Water Resources Modeling', *Journal of Hydraulic Engineering, American Society of Civil Engineers*, 119(11), 1300-1307.

Zoppou, C. and K.S. Li, (1994) Discussion of 'Stochastic Analysis of Ground-Water Flow in Semiconfined Aquifer', by M.G. Satish and J. Zhu, *Journal of Hydraulic Engineering, American Society of Civil Engineers*, 121(3), 290-291.

Zoppou, C., A.A.T. Wood and A.C. Falkland (1994) 'Estimation of the Thickness of a Freshwater Lens Using an Exact Random Field Generator', *25th Congress of the International Association of Hydrogeologists*, 2, 149-154.

Zwillinger, D., (1989) *Handbook of Differential Equations*, Academic Press, Boston.